

Public reporting burden for this collection of information is estimated to average 1 hour per response, including the time for reviewing instructions, searching data sources, gathering and maintaining the data needed, and completing and reviewing the collection of information. Send comments regarding this burden estimate or any other aspect of this collection of information, including suggestions for reducing this burden to Washington Headquarters Service, Directorate for Information Operations and Reports, 1215 Jefferson Davis Highway, Suite 1204, Arlington, VA 22202-4302, and to the Office of Management and Budget, Paperwork Reduction Project (0704-0188) Washington, DC 20503.

PLEASE DO NOT RETURN YOUR FORM TO THE ABOVE ADDRESS.

1. REPORT DATE (DD-MM-YYYY)
15 Jan 2007

2. REPORT TYPE
Final Technical Report

3. DATES COVERED (From - To)
15 Jan 2007-Nov 30, 2009

4. TITLE AND SUBTITLE

Toward a Modular ionic Liquid Platform for the Custom Design of Energetic Materials: Understanding How the Dual nature of Ionic Liquids Relates Key Physical Properties to Target Structures

5a. CONTRACT NUMBER
FA9550-07-1-0117

5b. GRANT NUMBER

5c. PROGRAM ELEMENT NUMBER

5d. PROJECT NUMBER

5e. TASK NUMBER

5f. WORK UNIT NUMBER

6. AUTHOR(S)

Robin D. Rogers

7. PERFORMING ORGANIZATION NAME(S) AND ADDRESS(ES)

Robin D. Rogers
Center for Green Manufacturing and Department of Chemistry
The University of Alabama
Tuscaloosa, AL 35401

8. PERFORMING ORGANIZATION
REPORT NUMBER

9. SPONSORING/MONITORING AGENCY NAME(S) AND ADDRESS(ES)

USAF/AFRL
AFOSR
875 North Randolph Street
Arlington VA 22203

10. SPONSOR/MONITOR'S ACRONYM(S)
AFOSR

11. SPONSORING/MONITORING
AFRL-OSR-VA-TR-2013-1021

12. DISTRIBUTION AVAILABILITY STATEMENT

Distribution Statement A: Approved for public release. Distribution is unlimited.

13. SUPPLEMENTARY NOTES

14. ABSTRACT

The Air Force has pressing needs to develop new propellants for aircraft, rockets, and spacecraft. This work is part of the Air Force High Energy Density Matter program and it will help to develop new propellants that can make propulsion systems less expensive, safer, and more efficient. This will result in cost savings and improved mission capabilities for Air Force systems.

15. SUBJECT TERMS

16. SECURITY CLASSIFICATION OF:

a. REPORT	b. ABSTRACT	c. THIS PAGE
Unclassified	Unclassified	Unclassified

17. LIMITATION OF
ABSTRACT

Unclassified

18. NUMBER
OF PAGES
11

19a. NAME OF RESPONSIBLE PERSON

19b. TELEPHONE NUMBER (Include area code)
(703)

FINAL REPORT

Project Title:

Toward a Modular 'Ionic Liquid' Platform for the Custom Design of Energetic Materials:
Understanding How the Dual Nature of Ionic Liquids Relates Key
Physical Properties to Target Structures

Principal Investigator:

Robin D. Rogers
Center for Green Manufacturing and Department of Chemistry,
The University of Alabama, Tuscaloosa, AL 35401
Tel: (205) 348-4323, Fax: (205) 348-0823, Email: rdrogers@as.ua.edu

Reporting Period:

Jan. 15, 2007 – Nov. 30, 2009

Agreement Number: FA9550-07-1-0117

Report Prepared by: Robin D. Rogers, Marcin Smiglak, Julia Shamshina, and David M. Drab

20150504014

Table of Contents

TITLE PAGE	1
TABLE OF CONTENTS	2
I. OBJECTIVES	4
II. STATUS OF EFFORT	6
III. MAJOR ACHIEVEMENTS	7
IV. TECHNICAL SUMMARY OF THE WORK ACCOMPLISHED	8
1. Ionic Liquids Based on Azolate Anions	8
2. New Hydrogen Carbonate Precursors for Efficient and Byproduct-Free Syntheses of Ionic Liquids Based on 1,2,3-Trimethylimidazolium and N,N-Dimethylpyrrolidinium Cores	11
3. Ionic Liquid-Based Routes to Conversion or Reuse of Recycled Ammonium Perchlorate	13
4. Azolium azolates from reactions of neutral azoles with 1,3-dimethylimidazolium-2-carboxylate, 1,2,3-trimethylimidazolium hydrogen carbonate, and N,N-dimethylpyrrolidinium hydrogen carbonate	15
5. Synthesis of N-cyanoalkyl-substituted imidazolium halide and nitrate salts with variable N-alkyl and N-cyanoalkyl chain lengths, and the characterization of their structural and thermal properties as potential energetic ionic liquids	19
6. Synthesis of N-cyanoalkyl- and N,N-dicyanoalkyl-substituted imidazolium halide and dicyanamide salts with variable N-cyanoalkyl chain lengths, and the characterization of their structural and thermal properties as potential energetic ionic liquids	20
7. Introduction and initial demonstration of synthetic design platform for bridged multi-heterocycles with variable charge, structure, and symmetry options: Formation of 5-tetrazole-based products using a three step procedure of azole 'click' functionalization, 'click' synthesis of bi-heterocyclic precursors, and further product modification utilizing IL-based synthetic strategies	21
8. Click synthesis and thermal characterization of zinc-containing, alkyl-bridged imidazolium-tetrazolates with highly variable N-alkyl and alkyl bridge lengths as expansion of bridged multiheterocyclic design platform	22
9. Utilization of ionic liquid-based synthetic strategies for the targeting of properties via the multiheterocyclic design platform	24
10. Hypergolic Ionic Liquids for Monopropellant Applications	25
11. Eutectic mixtures of Ionic Liquids	29
V. PERSONNEL SUPPORTED	32
VI. PUBLICATIONS	32
VII. PRESENTATIONS	33
VIII. DISSERTATIONS	35
APPENDIX A (Synthesis)	36
APPENDIX A1	36
APPENDIX A2	42
APPENDIX A3	47
APPENDIX A4	51
APPENDIX A5	55
APPENDIX A6	59
APPENDIX A7	63
APPENDIX A8	68
APPENDIX A9	72
APPENDIX A10	74
APPENDIX A11	75
APPENDIX B (Analytical data)	76
APPENDIX B1	76
APPENDIX B2	79
APPENDIX B3	81
APPENDIX B4	86

<u>APPENDIX B5</u>	88
<u>APPENDIX B6</u>	90
<u>APPENDIX B7</u>	91
<u>APPENDIX B8</u>	92
<u>APPENDIX B9</u>	93
<u>APPENDIX B10</u>	94
<u>APPENDIX B11</u>	95
<u>APPENDIX C (Protocols and equipment)</u>	98
<u>APPENDIX D1 (NMR analysis)</u>	98
<u>APPENDIX D2 (TGA analysis)</u>	98
<u>APPENDIX D3 (DSC analysis)</u>	98
<u>APPENDIX D4 (powder AND single crystal X-ray diffraction)</u>	98
<u>APPENDIX D5 (FT-IR analysis)</u>	99
<u>APPENDIX D5 (Electrochemical analysis)</u>	99
<u>REFERENCES</u>	100

I. OBJECTIVES (as proposed)

The overall goal of this program is to develop an understanding of the dual-functional nature of ionic liquids (ILs) and their inherent design flexibility that will allow the custom synthesis of targeted structures tuned to exhibit the desirable chemical and physical attributes sought by the Air Force in energetic materials. The hypothesis for the proposed work is that a fundamental understanding of ILs and the interionic interactions responsible for IL behavior, will allow compartmentalized molecular level design of a wide range of new energetic materials, as well as, novel performance enhancement and delivery options. ILs, for example, may make a unique delivery system for energetic fluids: one ion can be fine tuned for its energy content, while the second ion can be independently fine tuned to provide oxygen balance and the optimal physical properties or vice-versa. In addition, IL strategies can take advantage of the dual nature of ILs to realize ready property enhancement or safe delivery options. Codification of the relationships between ionic structural features and the physical/chemical properties will allow the prediction of structures and functions. We, thus, propose the following objectives:

Objective 1: Modular design, synthesis, screening, and evaluation of IL components to create an IL toolbar for meeting each AF target criteria. Each AF target criteria (e.g., melting point depression, increase of density, vapor pressure depression, decrease of viscosity, long-term thermal stability, thermal stability enhancement, heat of formation, and improved combustion) will be investigated separately to allow for a better understanding of how introduction of a specific property in either ion affects the IL properties as a whole. The result will be an IL toolbar from which target EILs can be carefully designed and evaluated.

The specifications of desirable and explicit requirements for energetic IL materials suggested by the AF are shown in Table 1. Realizing the capability of EILs to address these current needs for advancement in energetic materials development, the task is, then, to learn how to incorporate all of the desirable features into a final material, develop fast and easy synthetic protocols, and enable safe and efficient delivery, handling and storage procedures.

Table 1. AF performance requirements for EILs.

<i>Physical Properties</i>		<i>Thermodynamic properties</i>	
Mp	< -40 °C	Heat of formation	as positive as possible
Viscosity	< 1 cPs at 0 °C	Heat of combustion	> 6 kcal g ⁻¹
Density	> 1.4 g/mL	<i>Thermal stability</i>	
Vapor pressure	~ 0 psi	TGA (75 °C, isothermal)	< 1% over 24 h
Surface tension	< 100 dyne cm ⁻¹	DSC (10 °C/min)	> 120 °C for T _{decomp}
<i>Hazard Sensitivity</i>		<i>Toxicology</i>	
Impact	> 50 kg cm	LD ₅₀	> 0.5 g kg ⁻¹
Friction	> 120 N	AMES	Negative
Detonation	class 1.3		
Electrostatic discharge	> 5000 V at 0.25 J		

The Modular Design will focus on careful selection and synthesis of target compounds (new and existing), that target each specific property needed in an iterative fashion. Each target property will be investigated separately to allow for a better understanding of how optimizing each target influences the global IL properties. This approach allows each design study to focus on a primary attribute (e.g., heat of formation or density), while secondary attributes (e.g., melting point, viscosity, etc.) can be optimized by either redesign of the ions (continuation of

Objective 1) or by performance enhancement (see **Objective 3**). The result will be an IL toolbar from which a variety of IL design options can be brought to bear on any synthetic scheme based on the desired set of final IL properties.

The design strategies will focus on the remarkable dual-functionality of ILs. The structural modifications of both ions will include: (i) substituent modification of alkyl chain length and composition (branched vs. linear, or saturated vs. unsaturated, unsubstituted alkyl chain vs. energetically substituted) directly appended to the heterocyclic rings, as well as, appended to core atoms; (ii) oxygen-balance; (iii) change in position on a heterocycle core; (iv) energetic functionality; and (v) other structure-dependent changes (ring strain, vinylogous functions, etc.). Each modification will be directed towards melting point depression, increase of density, vapor pressure depression, decrease of viscosity, long term thermal stability, thermal stability enhancement, heat of formation, and combustion improvement.

Target compounds will be prepared and evaluated using the established protocols developed at UA for assessing IL properties.¹ Key physical properties to be measured include: (i) melting point; (ii) stability and phase transitions; (iii) decomposition temperature and characteristics (exo- or endothermic); (iv) heat of formation; (v) heats of combustion; (vi) temperature of exothermic decomposition (using Acceleration Rate Calorimetry); (vii) density; (viii) viscosity; (ix) surface tension of IL materials; and (x) crystal structure studies as appropriate.

In the characterization of the material, the physical properties of the newly obtained salts will be compared with those of other examples in each examined series for detection of possible pattern agreements or digressions. It is at this crucial point where the design requires thorough evaluation: Was the intended product obtained? Does it meet the required specifications?

Each AF target property will be separately considered as the primary property, and all other target properties will be designated as secondary during any given iteration. This modular approach, which independently considers each property as primary at any given time, will allow for the construction of an IL toolbar containing utilities for each specified property. In the example provided below, the primary property was set to be heat of formation.

In this particular example, computational analyses and previously reported findings will be enabled as the specific tools for the prediction of the heats of formation of targeted structures. The synthetic protocols will then be chosen for the target molecule. The primary and secondary properties of the product will be screened with bomb calorimetry and ARC calorimetry measurements to obtain experimental values for heat of formation, heat of combustion, self-heating rate maximum, and character of decomposition process (exo- or endothermic, and rate of exothermal decomposition), which will be compared with the computationally predicted values. If the observed properties are in close agreement with the targeted specifications, the compound will be cleared for the next phase and the incorporated functionalities will be added to the IL toolbar.

At the point of our modular approach, where target EILs can be expected which exhibit the specified results, IL synthetic protocols (developed independently under **Objective 2**), will be implemented to improve the synthesis (e.g., halide-free or byproduct-free synthesis) and/or the delivery of the target functionality (e.g., the safe delivery of separately tuned modular units that may be combined and used on-site when needed). If the best available EIL does not meet all of the specified criteria – (i) the structure of the target compound will be redesigned following the structure modification step stated in **Objective 1**, or (ii) enhancement of performance will be considered through methods described in **Objective 3**.

Objective 2: New synthesis protocols and delivery of the materials. Utilizing present and past discoveries in IL synthetic methodology, we will develop new, halide- and metal-free, time- and cost-efficient, and more environmentally-benign synthetic protocols to target ions identified in **Objective 1**. We will also modify or develop protocols that allow for the safe transport of the reactive components and formation of desired product on-site when needed and with only benign byproduct formation (e.g. MeOH, CO₂).

Objective 3: Performance enhancement. We will utilize the ionic nature of ILs to enhance performance of selected 'near-miss' target materials by modification of the multi-component composition (not structural modifications). Such approaches will include multiple ion mixtures for depression of the melting point, density, and/or viscosity (eutectic mixtures), or the utilization of the unique solvent properties of ILs allowing dissolution of property modifiers.

Objective 4: Development of models to describe and predict performance properties. The current 'rules of thumb' methodologies used for IL design, particularly with relevance to this program, will be codified using QSPR models that relate the structure of the ions, as expressed by their connectivity, geometry, charge distribution, and quantum chemical parameters, to the observed physical and thermodynamic properties (melting points, decomposition temperatures, and other rheological data to be collected). The QSPR models will be used to understand and predict the way in which rational design strategies can be adopted.

II. STATUS OF EFFORT

Synthesis and characterization. To address **Objective 1** of the proposed work, the dual-functional nature of ILs has been exploited towards selective formation of new salts, where cation/anions are varied by structural modification and or ion exchange techniques. New classes of azolium azolate salts featuring ammonium, phosphonium, pyridinium, and imidazolium cations were obtained and isolated with a diverse group of azolate anions including nitro-substituted benzotriazolate, benzimidazolate, 1,2,4-triazolate, and imidazolate, as well as tetrazolate and nitrile-functionalized imidazolate.² Synthesis of candidate ILs was also achieved obtaining *N*-cyanoalkyl-functionalized imidazolium nitrate and dicyanamide salts.^{3,4} As electron-withdrawing groups (e.g., nitro, nitrile) directly appended to the azole core tend to deactivate the nucleophilicity of the ring for further substitution (e.g., *N*-alkylation to form quaternized azolium cation), the synthesis of ILs with either stable azolate anions or cations with energetic group appended to *N*-alkyl chains both represent strategies for EIL synthesis to circumvent synthetic obstacles.

In addition, novel synthetic protocols were developed for **Objective 2** that enable more efficient methods of EIL delivery, where the halide-free synthesis of hydrogen carbonate-based ILs via a methylcarbonate route serves as a demonstrated example.^{5,6,7} 1,2,3-trimethylimidazolium and N,N-dimethylimidazolium hydrogencarbonate salts from this protocol, then, provide easy access to chloride, nitrate, picrate, and perchlorate exchanged EILs by way of simple Brønsted acid-base chemistry. This work was advanced further, where the synthesis of azolium azolate salts was reported by the reaction of either hydrogen carbonate or 1,3-dimethylimidazolium-2-carboxylate with the generation of CO₂ and water as the only by-products. In another study, the utilization of ammonium perchlorate (AP) as a feedstock for the synthesis of new perchlorate-based salts (some ILs) was showcased through three distinct routes involving (i) reaction of AP with neutral amines with ammonia as by-product (ii) formation of perchlorate-based salts from Krapcho-type decarboxylation reaction with 1,3-

dimethylimidazolium-2-carboxylate and (iii) anion exchange of perchlorate with chloride-based phosphonium salts for the separation of phosphonium perchlorate ILs and recovery of NH_4Cl .⁸

Also within the scope of **Objective 2** was the successful effort to introduce and experimentally demonstrate a novel design platform for the general synthesis of bridged multi-heterocyclic compounds.⁹ For the initial demonstration, the synthesis of bi-heterocyclic, alkyl-bridged imidazolium-tetrazolate targets was achieved, where flexibility of structure, charge, and symmetry is shown in the conversion of a common 1-cyanomethylimidazolium chloride salt to (i) a Zn-coordinated 1-(5-tetrazolidyl)methyl-3-methylimidazolium zwitterion via Click chemistry, (ii) the removal of Zn to obtain 1-(5-1*H*-tetrazolyl)methyl-3-methylimidazolium chloride as the ‘cationic’ form of the material, and (iii) the removal of HCl from the structure to result in the free zwitterion 1(5-tetrazolidyl)methyl-3-methylimidazolium. Likewise, starting from a neutral precursor the ‘anionic’ form of Click cycloadducts may be accessed as was the case here with the synthesis of the sodium salt of 1-(5-tetrazolid-2-yl)ethyl-1,2,4-triazole from the Click reaction of 1-(2-cyanoethyl)-1,2,4-triazole. The fast and general scope of using *N*-cyanoalkyl-functionalized cations as Click precursors is shown with the synthesis and characterization of a homological series of Zn-containing 1-(5-tetrazolidyl)alkyl-3-alkylimidazolium zwitterions, where reaction rate information from an NMR study indicates that these products form very fast under ambient, aqueous conditions.¹⁰ Finally, the synthesis of tri-heterocyclic zwitterion 1-(2-(5-1*H*-tetrazolyl)ethyl)-3-(5-tetrazolidyl)methylimidazolium and its conversion into both room-temperature cationic or anionic ionic liquids by known IL-based strategies serves as proof-of-concept for the diversity available through this approach.

The **Objective 3** effort is embodied through our team’s study of methods to enhance the performance properties of IL-based systems. First, the initial discovery of hypergolic reactivity was established in hydroxyhydrazinium-based ILs, namely 2-hydroxyethylhydrazinium nitrate and dinitrate.¹¹ Each IL was found to self-ignite over a commercially available Shell 405 catalyst, which suggest potential replacement for the more volatile hydrazine that is in common use as a propellant. Second, the formation of IL eutectic mixtures to achieve desired performance parameters (e.g., melting point reduction) has been systematically examined, where neutral acidic azoles 4-nitro-1*H*-1,2,3-triazole and 4,5-dinitro-1*H*-imidazole are combined in calculated formulation with 1,3-dimethylimidazolium-2-carboxylate to react in Krapcho-type decarboxylation and result in a 3-component eutectic mixture.¹²

III. MAJOR ACCOMPLISHMENTS^{13,14}

1. Demonstration of how the dual-functional nature of ILs may be utilized to target and/or understand specific properties trends (e.g., melting point, thermal stability) through the modular synthesis of azolium azolates as well as *N*-cyanoalkyl-functionalized imidazolium nitrate and dicyanamide salts.
2. Reported are several new innovations for IL synthetic methodology. By the hydrogen carbonate approach, many new ILs become accessible via halide-free synthesis using simple acid-base chemistry. Also, ammonium perchlorate has been successfully employed as a feedstock for new IL synthesis with by-products of reduced negative environmental impact.
3. A new design platform for the synthesis of multi-heterocyclic compounds has been demonstrated and extended to show how IL-based materials (anionic or cation components) may be accessed selectively.
4. Demonstration of how materials performance may be enhanced by IL-based strategies has been demonstrated two-fold. First, discovering and characterizing the hypergolic reactivity

of HEH-based ILs has been achieved. In addition, the utilization of IL chemistry for the systematic formation of eutectic mixtures to targets specified properties (e.g., melting point) has been accomplished.

IV. TECHNICAL SUMMARY OF THE WORK ACCOMPLISHED.

1. Ionic Liquids Based on Azolate Anions

- 1. Ionic Liquids Based on Azolate Anions** Smiglak, M.; Hines, C. C.; Wilson, T. B.; Singh, S.; Vincek, A. S.; Kirichenko, K.; Katritzky, A. R.; Rogers, R. D. *Chem. Eur. J.* **2009**, *16*, 1572–1584, (accepted as VIP paper).

ILs containing azolate anions (imidazolate, triazolate, tetrazolate, benzimidazolate, or benzotriazolate) have received much less attention than those containing azolium cations, although more results are now starting to appear.¹⁵⁻²⁴ Over the past few years, our group has also investigated the possible use of azolate anions for the preparation of low melting energetic ionic liquids.²⁵ From our perspective, the use of such anions to form energetic salts, specifically with the addition of energetic substituents (nitro or cyano groups) to enhance their energetic capabilities is a very interesting approach. We recently reported a series of ILs containing substituted imidazolate, triazolate, tetrazolate anions paired with different cations and showed that salts of a wide range of heterocyclic azolate anions with 1-butyl-3-methylimidazolium cation gave several examples of room temperature ionic liquids.²⁵ In general it was found that these organic anion-based salts allowed for a similar degree of facile functionalization, due to structural similarity with the well-studied azolium cations.^{20,26,27}

In order to extend the scope of ILs, greater availability of organic anions providing the same, or similar, architectural flexibility as the commonly used organic cations (e.g., substituted imidazolium cations) needs to be achieved. Parallel to this, improvements in the basic understanding of the key physical and chemical properties of complex azolate-based ionic liquids must be obtained.

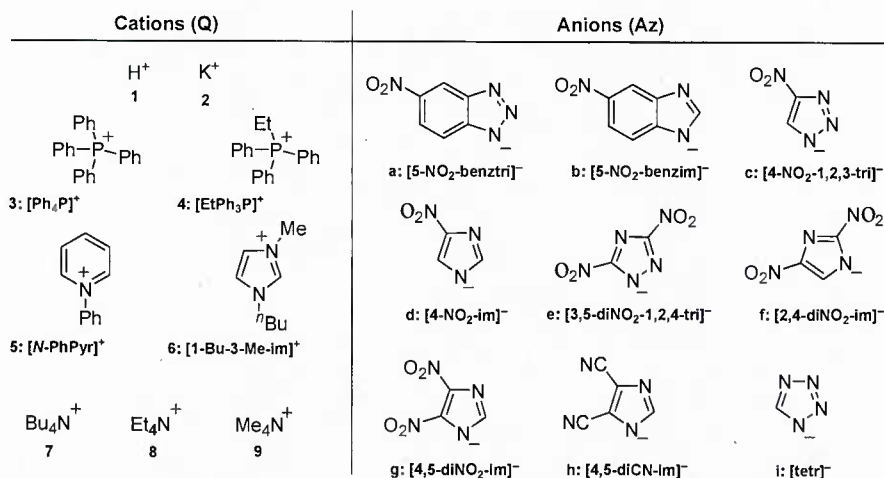


Figure 1.1 Cation and anion combinations explored in this work.

In continuing our previous study on new energetically substituted heterocyclic anions, we have expended our selection of used anions and cations in order to prepare even larger matrix of new salts and through their analysis gain better insight into the structure vs. properties relationship. More specifically, we have synthesized and characterized 31 novel organic salts based on tetraalkylammonium, 1,3-dialkylimidazolium, pyridinium, and phosphonium cations combined with energetically-substituted tetrazolate, triazolate, imidazolate, benzimidazolate, and benzotriazolate anions (Figure 1.1). Many of the neutral azoles used as precursors to the azolate anions, are energetic heterocyclic compounds which have been previously extensively studied as potential propellants and/or explosives.^{28,29} The ability to readily form azolate-based IL examples with enhanced stability relative to the starting heterocycles (controlled melting points, higher thermal decomposition temperatures, reduced volatility, etc.), and the generic observation that IL materials can be formed from a wide range of flat heterocyclic anions by modification or selection of the appropriate ions, sets out principles by which ILs containing this class of anions can be developed and exploited.

Electron withdrawing groups, such as nitro or nitrile, may act as destabilizing substituents on the aromatic core of many heterocyclic cations, as well as stabilizing substituents on many heterocyclic anions, and a wide range of azolate anion-based salts can thus be used to prepare EILs. The azolates have been found to not only introduce properties required for EILs, but also allow for the formation of low melting salts (Figure 1.2), and indeed in some cases ILs. They are surprisingly stable in the systems explored, and allow a degree of structural modification in a similar fashion to azolium cations.

Ionic liquids were obtained with all combinations of [1-Bu-3-Me-im]⁺ and the heterocyclic azolate anions studied, and with several combinations of [Bu₄N]⁺ or [Et₄N]⁺. The [1-Bu-3-Me-im]⁺ azolates were liquid at room temperature, forming glasses on cooling with transition temperatures in the range -53 to -82 °C (except for the [3,5-diNO₂-tri]⁻ salt, mp = 33 °C). Additionally, one of the most interesting findings was that the melting points and thermal stabilities of the [1-Bu-3-Me-im]⁺ salts allow for handling, operation, and usage over a wide liquidus range (Figure 1.2).

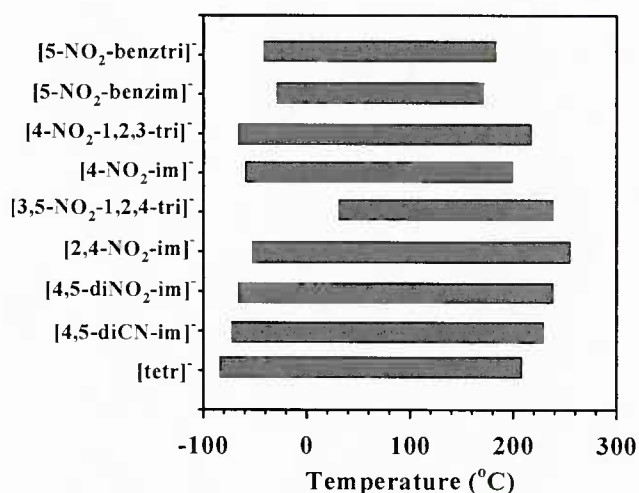
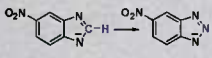
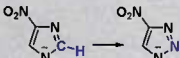
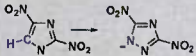
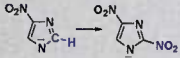
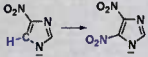
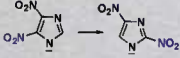
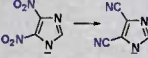
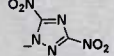


Figure 1.2 Liquidus ranges of the [1-Bu-3-Me-im]⁺ salts.

Taking into the account the specific properties analyzed (liquid range, thermal stability, oxygen balance) the most promising anion for the application in energetic ionic liquids seems to

be [3,5-diNO₂-tri]⁻. Other trends discovered (Table 1.1) include favorable structure property relationships when moving from 4- and 4,5-disubstituted anions to 3,5- and 2,4-disubstituted azolate anions. For example, it was found that the [2,4-diNO₂-im]⁻ anion contributes to low melting point, very good thermal stabilities, high oxygen balance, high nitrogen content, and high solid-state density for most of the analyzed salts. Overall, the development of ILs based on azolium azolate cores seems to be an attractive avenue for the future of not only energetic ionic liquids, but ILs in general.

Table 1.1. Summary of structure vs. property relationships.

Structure/Property Relationship	melting point	T_{dec}	Oxygen Balance (OB) [§]	Nitrogen Content ^{†30}	Solid Density
	Desired change in property				
	↓	↑	↑	↑	↑
	data inconclusive	↑	↑	↑	--
	↓	↑	↑	↑	↓
	↑	±29 °C ^[b]	↑	↑	↑
	±38 °C ^[a]	↑	↑	↓	↑
	↓	↑	↑	↓	=
	±50 °C ^[a]	↑	=	=	↑
	±36 °C ^[a]	±43 °C ^[b]	↓	↑	↓
	moderate 33-214 °C	high 205-368 °C	highest + 0	high 44.3%	high ^[††] 1.36 -1.55 g cm ⁻³

[§] The oxygen balance (OB) is calculated from the empirical formula of a compound in percentage of oxygen required for complete conversion of carbon to carbon dioxide, hydrogen to water, and metal to metal oxide; [†] Nitrogen content is defined as the amount of nitrogen in the molecule expressed in mass %; [††] The [3,5-diNO₂-tri]⁻ anion contributes to one of the higher densities among the analyzed family of salts. [a] maximum variation in temperature of melting point between salts of considered set of anions. [b] maximum variation in temperature of decomposition between salts of considered set of anions

2. New Hydrogen Carbonate Precursors for Efficient and Byproduct-Free Syntheses of Ionic Liquids Based on 1,2,3-Trimethylimidazolium and N,N-Dimethylpyrrolidinium Cores

1. **New hydrogen carbonate precursors for efficient and byproduct-free syntheses of ionic liquids based on 1,2,3-trimethylimidazolium and N,N-dimethylpyrrolidinium cores**, Smiglak, M.; Hines, C. C.; Rogers, R. D., *Green Chem.* **2010**, DOI: 10.1039/b920003g

One of the most challenging problems faced by researchers working with ILs, is difficulty in the reliable and reproducible preparation of pure compounds. Unfortunately, current methods for preparation of various ILs often involve multi-step synthesis, complex purification, and very often result in formation of undesirable and difficult to remove halide- or metal-containing species.³¹⁻³⁴ Thus, improved techniques for IL synthesis and purification would drive the end product cost down and provide higher purity materials and consistency between batches, even between different suppliers.

In this work, we have extended our research on the utility of dialkyl carbonates as alkylating agents to form new $[\text{HCO}_3]^-$ salt precursors for further halide free syntheses of other ILs. In order to obtain $[\text{MeCO}_3]^-$ -based salts, we targeted two amines as prototypes: (i) 1,2-dimethylimidazole, since the carboxylation reaction at the C2 carbon during the imidazole alkylation process is prevented due to methyl group substitution (the carboxylation at C4/C5 position requires higher temperatures and should not occur with appropriate reaction conditions), and (ii) *N*-methylpyrrolidine, which due to lack of aromaticity or other conjugation, is less likely to undergo any carboxylation reaction to form a zwitterionic compound.

We report (Figure 2.1) the formation of two new examples of $[\text{HCO}_3]^-$ IL precursors, 1,2,3-trimethylimidazolium hydrogen carbonate ($[1,2,3\text{-triMeIM}][\text{HCO}_3]$) and *N,N*-Dimethylpyrrolidinium Hydrogen Carbonate ($[N,N\text{-diMePyr}][\text{HCO}_3]$) where the $[\text{HCO}_3]^-$ anion is generated by conversion of the $[\text{MeCO}_3]^-$ anion in the presence of excess water, and $[1,2,3\text{-triMeIM}][\text{MeCO}_3]$. The crystallographic characterization of highly deliquescent crystals of $[1,2,3\text{-triMeIM}][\text{HCO}_3] \cdot \text{H}_2\text{O}$ and $[N,N\text{-diMePyr}][\text{HCO}_3]$ was performed in order to further validate product formation of the three new IL precursors.

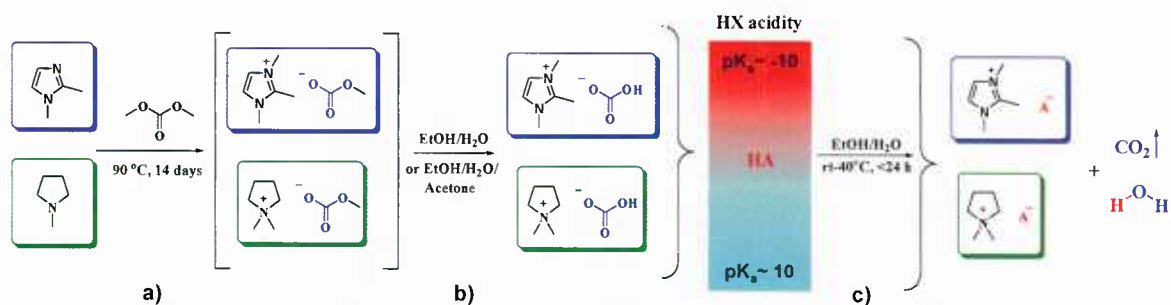


Figure 2.1 Efficient, three step synthesis of halide free imidazolium- and pyrrolidinium-based organic salts; a) alkylation reaction with formation of $[\text{MeCO}_3]^-$ salts; b) conversion of $[\text{MeCO}_3]^-$ into $[\text{HCO}_3]^-$; c) reaction of $[\text{HCO}_3]^-$ salt precursor with acid and formation of final product.

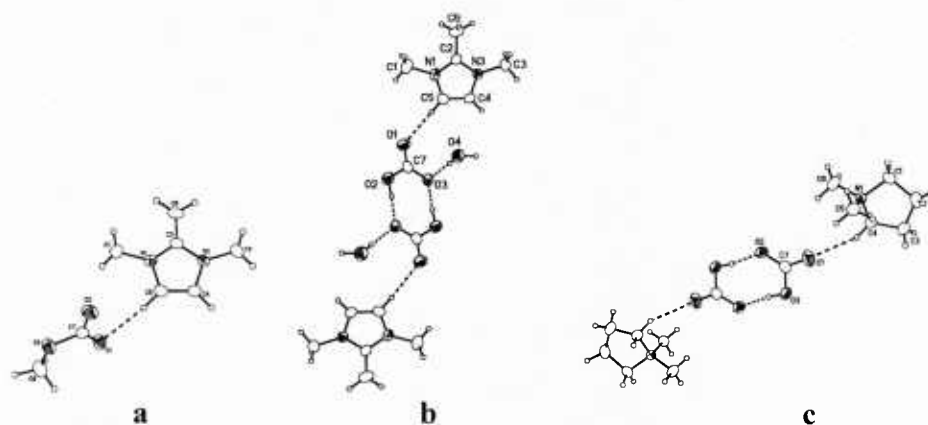


Figure 2.2 Crystal structures a) [1,2,3-triMeIM][MeCO₃]; b) [1,2,3-triMeIM][HCO₃] \cdot H₂O; c) [N,N-diMePyr][HCO₃] depicting the hydrogen bonded anion dimer and closest cation contact. Thermal ellipsoids are shown at the 50% probability level.

The new [HCO₃]⁻-based IL precursors were also used in reactions with several acids and [NH₄][ClO₄] to prove the potential of this family of salts for future applications in halide- and metal-free syntheses of ILs. As shown, it is possible to form virtually any salt from the [HCO₃]⁻ precursor when the pK_a of the acidic reagent is lower than that of H₂CO₃. Also, the use of ammonium salts results in formation of ammonia gas, which can be evacuated from the system, shifting the equilibrium towards product formation. The new organic salts with the chosen anions are formed with only gaseous byproducts (CO₂, H₂O, and in the case of [NH₄][ClO₄], NH₃) thus eliminating further purification steps. This reaction can be manipulated to accommodate a wide variety of anions by proper design of the reaction conditions.

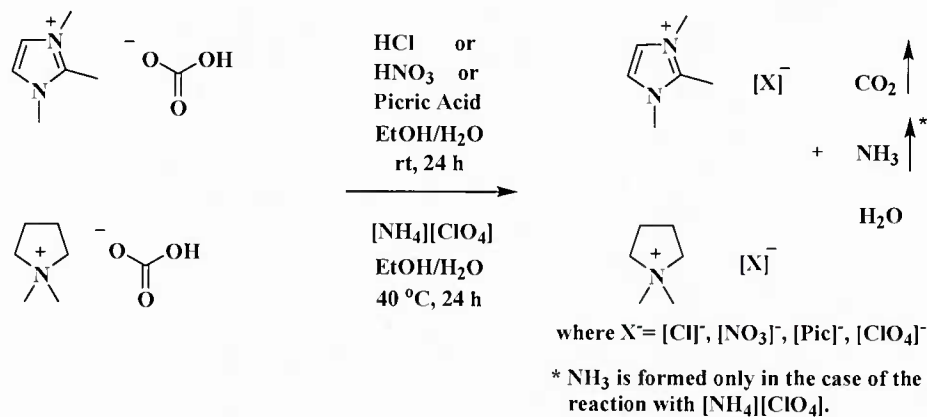


Figure 2.3 Reactions of [1,2,3-triMeIM][HCO₃] and [N,N-diMePyr][HCO₃] with hydrochloric, nitric, and picric acids, as well as ammonium perchlorate.

3. Ionic Liquid-Based Routes to Conversion or Reuse of Recycled Ammonium Perchlorate

- 1. Ionic Liquid-Based Routes to Conversion or Reuse of Recycled Ammonium Perchlorate**, Cordes, D. B.; Smiglak, M.; Hines, C. C.; Bridges, N. J.; Dilip, M.; Srinivasan, G.; Metlen, A.; Rogers, R. D. *Chem. Eur. J.* **2009**, *15*, 13441–13448.

Many modern energetic materials, even though highly advanced, and understood in terms of their performance and behavior, suffer from safety issues and environmental concerns.^{35,36} Organic salts are potential replacement energetic materials, and as such, interest in their synthesis has been growing rapidly in recent years.^{37,38} The reasons for this are manifold, but some of those most commonly expressed relate to their advantageous properties such as greater density and low or negligible vapor pressure under common operating conditions.

One of the most common oxidizers used, both in multi-component energetic systems³⁹ and in energetic salts, is the perchlorate anion. Moreover, one of the recent approaches to new liquid energetic salts has been to combine perchlorate with nitrogen-rich heterocyclic cations such as triazolium, tetrazolium, and more recently, bicyclic azolium salts.³⁸ Many of these salts use highly modified heterocyclic cations, with amino, nitro, and azo substitution of the heterocyclic ring that often results in the formation of products with melting points <100 °C, referred to as ionic liquids (ILs). By utilizing a common feature of ILs, *i.e.* their broad liquidus ranges, many of the problems associated with energetic materials may be overcome. Recent developments in energetic ionic liquids (EILs) research have been reviewed^{13,37c} and the initial results for many of these salts are promising as energetic materials.

A number of simpler heterocyclic perchlorate salts have also been prepared previously, with imidazolium,⁴⁰ 1-methylimidazolium,⁴¹ 1-butyl-3-methylimidazolium,⁴² 1,3-dibutylimidazolium,⁴³ and 1-hexyl-3-methylimidazolium cations.⁴⁴ The two predominant routes to such perchlorate-containing materials have been either through the protonation of a ring nitrogen using perchloric acid, resulting in the formation of thermally unstable, protonated salts, or by metathesis of an IL precursor with a perchlorate salt, most commonly AgClO₄. LiClO₄ also has been described as starting material for 1-butyl-3-methylimidazolium perchlorate.⁴⁵

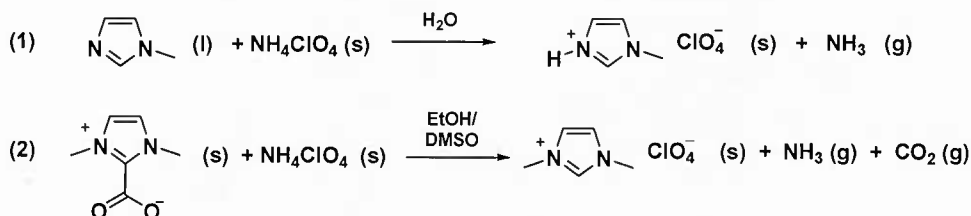
In order to effectively utilize AP in the synthesis of perchlorate-based energetic materials, new synthetic protocols for the formation of such products are required which allow for fast and benign (in terms of byproducts) synthesis of the target materials. Here we present three potential routes to incorporate the perchlorate anion into potentially energetic 1-methylimidazolium and phosphonium salts, using AP as the perchlorate source, including: 1) the reaction of a neutral amine (1-methylimidazole) with AP in aqueous solution, resulting in the formation of a protonated imidazolium perchlorate ([Hmim][ClO₄], **1**) and ammonia gas, 2) decarboxylation of 1,3-dimethylimidazolium-2-carboxylate⁴⁶ by reaction with AP to form 1,3-dimethylimidazolium perchlorate ([C₁mim][ClO₄], **2**), ammonia, and CO₂, and 3) the metathesis of 1-butyl-3-methylimidazolium chloride with AP in water, forming the insoluble 1-butyl-3-methylimidazolium perchlorate ([C₄mim][ClO₄], **3**) and water soluble NH₄Cl. Using this same metathesis methodology but with methanol as solvent, trihexyl(tetradecyl)phosphonium perchlorate ([P₆₆₆₁₄][ClO₄], **4**) was also prepared. Due to the relative hydrophobicity of these new salts, one could even envision recycle of aqueous perchlorate waste streams (for example from water washout of rocket engines) by forming an IL and separating the anhydrous IL phase.

The electrochemical remediation of perchlorate ions is one of the best ways of converting the toxic perchlorate to the non-toxic chloride ion efficiently. There are several reports on the electro-reduction of perchlorate at various electrodes. The literature in this area has recently been reviewed.⁴⁷ In most of the above papers, perchlorate reduction is carried out in aqueous systems, and to our knowledge, there are no reports on the electrochemical reduction of the perchlorate anion using an IL approach.

Given the wide exploration of ILs in electrochemistry, we felt it was appropriate to study the reduction of perchlorate in a medium which was both the reagent and the electrolyte. Using such a strategy, the perchlorate anion could be reduced to non-hazardous chloride, regenerating the starting salt which in return could be exchanged to a perchlorate anion again, thus creating a regenerative cycle for the remediation of perchlorate. The advantages of this approach would include the potentially improved electrochemical stability of ILs compared to water, no hydrogen/oxygen evolution during electrolysis if the IL is wisely chosen, good conductivity, and, most importantly, no requirement for volatile organic solvents and supporting electrolytes.

Using three different routes (Figure 3.1) and AP as the perchlorate source, we have prepared 1-methylimidazolium perchlorate, ([Hmim][ClO₄], **1**), 1,3-dimethylimidazolium perchlorate, ([C₁mim][ClO₄], **2**), 1-butyl-3-methylimidazolium perchlorate, ([C₄mim][ClO₄], **3**), and trihexyl(tetradecyl)phosphonium perchlorate, ([P₆₆₆₁₄][ClO₄], **4**). All four of these salts were formed in high yield, requiring little purification; **3** and **4** are ILs by definition, while **1** and **2** melt at temperatures above 100 °C.

Acid-base reaction:



Anion metathesis:

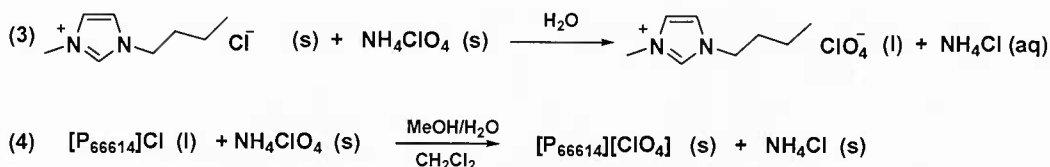


Figure 3.1 Synthetic routes to perchlorate ILs.

Three new routes have been shown for the synthesis of organic perchlorate salts of simple nitrogen heterocycles and a quaternary phosphonium compound, using AP as the source of perchlorate. Specifically, new preparative routes have been determined for the easy preparation of 1-methylimidazolium perchlorate, 1,3-dimethylimidazolium perchlorate, 1-butyl-3-methylimidazolium perchlorate, and trihexyl(tetradecyl)phosphonium perchlorate. The synthetic routes proceed in a single step from the chosen precursors, and produce the desired products in high yield and purity. Most importantly, the electrochemical remediation of the perchlorate ion from an ionic liquid leading to a potential perchlorate removal/remediation cycle was achieved. This could lead to a continuous process for converting perchlorate to chloride ions using a

strategy where an IL serves as both reagent and electrolyte. A few such strategies based on the results reported here are illustrated in Figure 3.2.

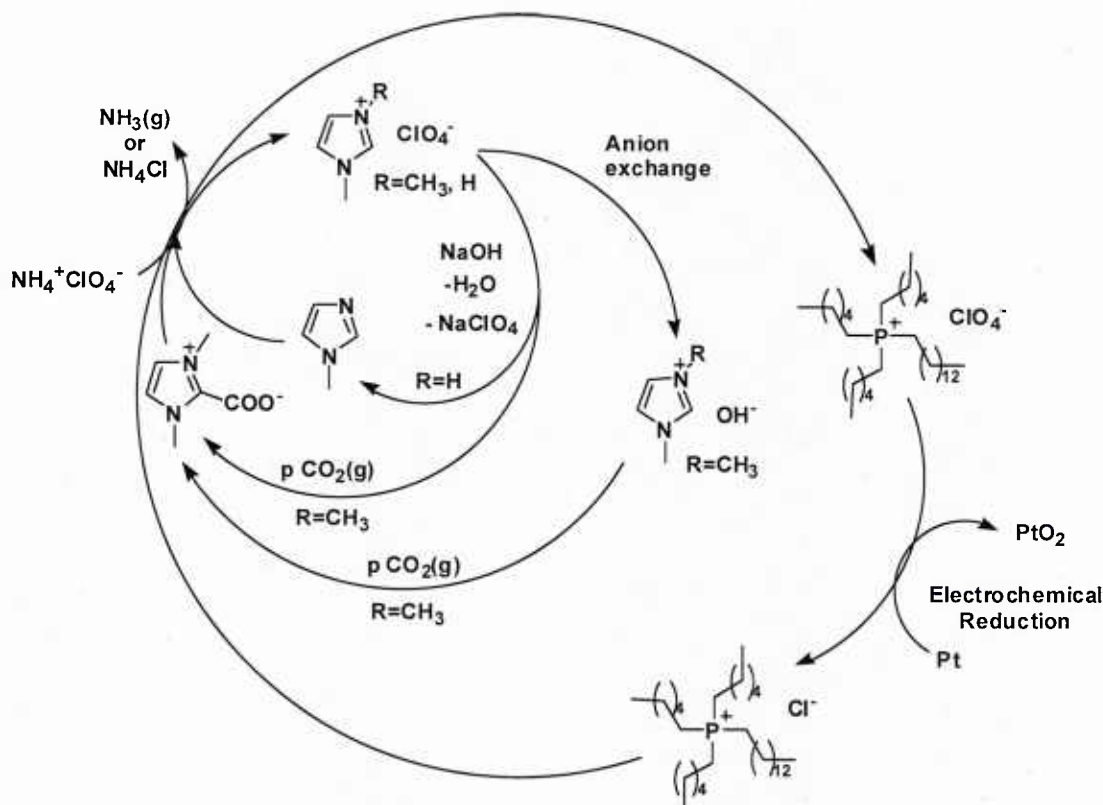


Figure 3.2 Possible AP IL reuse/remediation strategies.

4. Azolium azolates from reactions of neutral azoles with 1,3-dimethylimidazolium-2-carboxylate, 1,2,3-trimethylimidazolium hydrogen carbonate, and *N,N*-dimethylpyrrolidinium hydrogen carbonate

1. Azolium azolates from reactions of neutral azoles with 1,3-dimethylimidazolium-2-carboxylate, 1,2,3-trimethylimidazolium hydrogen carbonate, and *N,N*-dimethylpyrrolidinium hydrogen carbonate, Smiglak, M.; Hines, C. C.; Rogers, R. D.; 2010, *in preparation*.

A new group of organic azolate anions (e.g., imidazates, triazates, and tetrazates) was recently introduced into the field of ionic liquids (ILs), thus allowing for a similar degree of facile functionalization of anions, in a manner similar to the well-studied azolium cations.^{17,19,20,21,48-50} The first example using azolate anions in the synthesis of ILs was presented by Ohno *et al.*,¹⁷ who published the reaction of 1-ethyl-3-methylimidazolium hydroxide and either neutral 1,2,4-triazole or tetrazole. The formed salts, 1-ethyl-3-methylimidazolium 1,2,4-triazolate ($T_g = -76\text{ }^\circ\text{C}$) and 1-ethyl-3-methylimidazolium tetrazolate ($T_g = -89\text{ }^\circ\text{C}$), were the first reported azolium azolate-based ILs reported in the literature. Shortly after our group got interested in the topic of azolate base ILs and in our continuing work towards development of general design strategies for the formation of energetic ionic liquids (EILs), we have reported

formation of stable azolate anion-based salts by combination of such anions with variety of ionic liquid forming cations.^{2,25,50} That study concentrated on pairing the azolate anions (substituted imidazolate, triazolate, tetrazolate, benzimidazolate, and benztriazolate) with common quaternary ammonium, imidazolium, pyridinium, and phosphonium cations to allow for screening of the influence of the anion structure on the physical properties of the resulting salts. TGA analyses revealed that the azolate anions allow for the formation of highly stable salts with decomposition temperatures as high as 235 °C (for tetramethylammonium 3,5-dinitro-1,2,4-triazolate). The results suggested that the more substituted the azolate anion is with electron withdrawing groups, and the more nitrogen atoms are present in the heterocycle, the better is its anion charge delocalization and consequently its thermal stability.

In that earlier study, we found that combination of a common IL forming cation, 1-butyl-3-methylimidazolium [1-Bu-3-MeIM]⁺, with substituted azolate anions resulted in salts with very low melting points; the lowest melting salt being 1-butyl-3-methylimidazolium tetrazolate with only a glass transition at -82 °C. We recently reported the formation of two new examples of [HCO₃]⁻ IL precursors, 1,2,3-trimethylimidazolium hydrogen carbonate ([1,2,3-triMeIM][HCO₃]) and *N,N*-dimethylimidazolium hydrogen carbonate ([*N,N*-diMePyr][HCO₃]). The synthetic protocol for the formation of such IL precursors involves alkylation reactions of the chosen neutral amines with dimethyl carbonate, and later conversion of the formed [MeCO₃]⁻ salts to [HCO₃]⁻ salts in one step, at temperatures close to room temperature, and using only water. The salts ([1,3-diMIM-2-COO], [1,2,3-triMeIM][HCO₃], and [*N,N*-diMePyr][HCO₃]) were also used in reactions with several acids to prove their utility as IL precursors for the fast and efficient synthesis of imidazolium- and pyrrolidinium-based organic salts. The new organic salts were formed in quantitative yields with only gaseous byproducts (CO₂, H₂O, and in the case of [NH₄][ClO₄], NH₃) thus eliminating further purification steps.

Thus, combining the concepts developed during our previous studies (i) the utilization of azolate-based anions in the synthesis of ILs, (ii) the use of the zwitterionic 1,3-dimethylimidazolium-2-carboxylate IL precursor for the clean synthesis of 1,3-dimethylimidazolium salts, and (iii) the development of new [HCO₃]⁻ IL precursors ([1,2,3-triMeIM]⁺ and [*N,N*-diMePyr]⁺), it became possible to prepare a new family of azolate-based ILs in a fast and efficient fashion by reacting neutral azoles with the developed IL precursors. These routes would seem to provide a new alternative for the formation of azolate salts, overcoming the previously experienced limitations.

Here, the syntheses of 18 new azolate-based salts (Figure 1), containing either 1,3-dimethylimidazolium ([1,3-diMeIM-2-COO]), 1,2,3-trimethylimidazolium ([1,2,3-triMeIM]⁺), or *N,N*-dimethyl-pyrrolidinium ([*N,N*-diMePyr]⁺) cations is presented. The new salts include 12 examples of imidazolium azolates and 6 examples of pyrrolidinium azolate salts as a result of combinations of 3 cations and 6 anions (Figure 1). Even though the acidity of many of the neutral azoles utilized may seem to be too low for the reaction to be complete, these reactions can be driven toward product formation by simple evacuation of CO₂ as it is formed in the reaction.


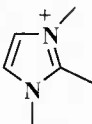
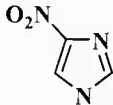
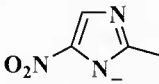
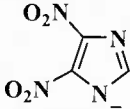
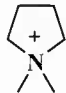
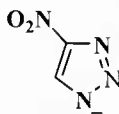
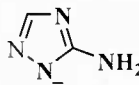
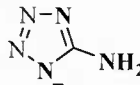
Cations	Anions			
				
[1,3-diMeIM] ⁺	[1,2,3-triMeIM] ⁺	[4-NO ₂ -IM] ⁻	[2-Me-5-NO ₂ -IM] ⁻	[4,5-diNO ₂ -IM] ⁻
				
[N,N-diMePyr] ⁺		[4-NO ₂ -1,2,3-tri] ⁻	[3-NH ₂ -1,2,4-tri] ⁻	[5-NH ₂ -tetr] ⁻

Figure 4.1 Cation and anion combinations explored along with their abbreviations.

Successful conversion of the IL precursors to the desired products was monitored using ¹³C NMR via simple analysis of the spectral region where presence of the [HCO₃]⁻ or carboxylate group of the zwitterion from the substrate would be expected in case of incomplete conversion. The absence of the relevant signal also served to indicate the completion of the reaction. None of the analyzed salts showed the presence of the carboxylate signal at ~160 ppm, indicating no residual substrate. In evaluating the ¹³C NMR results, it was concluded that all 18 new salts were formed approaching quantitative yield.

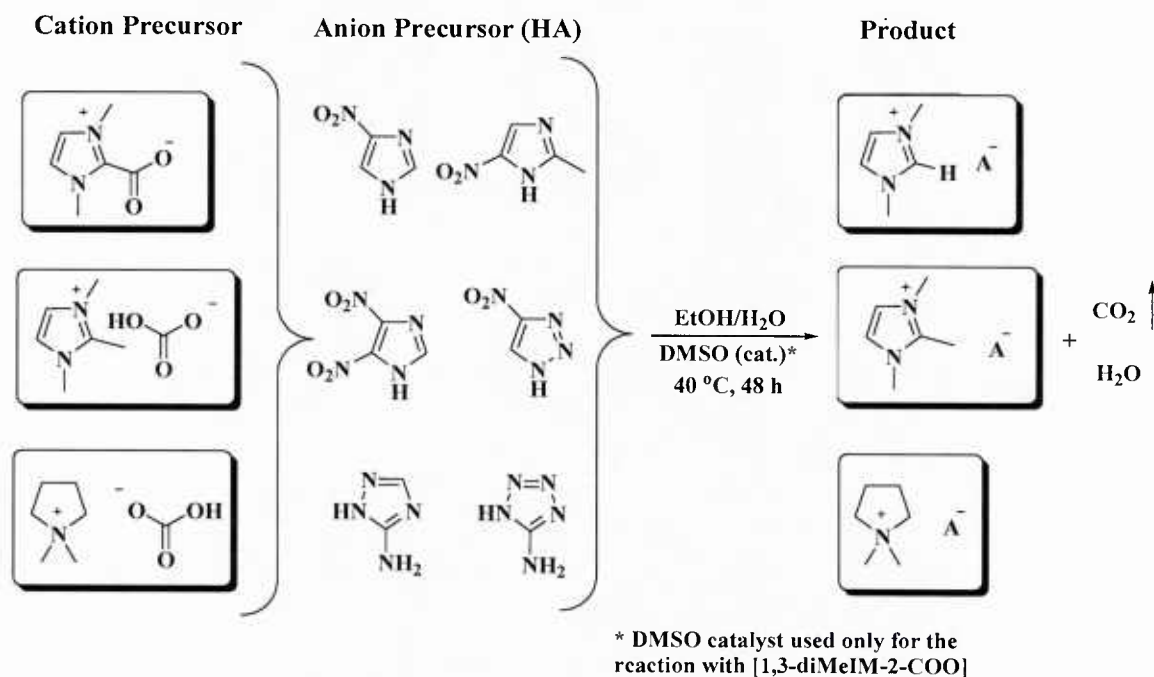


Figure 4.2 Reaction of [1,3-diMeIM-2-COO], [1,2,3-triMeIM][HCO₃], and [N,N-diMePyr][HCO₃] with neutral azole acids.

Even though the synthesized model compounds were composed of highly symmetrical cations ([1,3-diMeIM]⁺, [1,2,3-triMeIM]⁺, and [N,N-diMePyr]⁺), which usually results in the

5. Synthesis of *N*-cyanoalkyl-substituted imidazolium halide and nitrate salts with variable *N*-alkyl and *N*-cyanoalkyl chain lengths, and the characterization of their structural and thermal properties as potential energetic ionic liquids

- 1. Synthesis and thermal characterization of homologous *N*-cyanoalkyl-functionalized imidazolium nitrate salts as dual-functional energetic ionic liquids.** Drab, D. M.; Smiglak, M.; Hines, C. C.; Rogers, R. D., *in preparation*.

In order to address our first research goal, we invoked the dual-functional nature of ionic liquids for the design of new homologous series of *N*-cyanoalkyl-functionalized imidazolium nitrate salts. These targets are justified based upon evidence reported in the literature to suggest that each component contributes separately to a properties set relevant to the AFOSR target criterion. Specifically, it is believed that the *N*-alkyl-appended nitrile functionality may introduce desirable physicochemical contributions to the salt as tested, without the reduced nucleophilicity observed for imidazolium cores directly substituted with the $-C\equiv N$ group. Furthermore, the variation of both *N*-alkyl and *N*-cyanoalkyl chain lengths is expected to affect the thermal stability and melting point as is frequently the case for *N*-alkyl chain variation reported in the literature. Finally, the nitrate anion provides an oxidizing component that may be beneficial for the combustion of the ‘fuel-rich’ *N*-cyanoalkylated salt.

The 20 *N*-cyanoalkyl-functionalized imidazolium halide precursors and nitrate salts formed (Figure 5.1) were selected based upon homological differences in the *N*-alkyl and *N*-cyanoalkyl substituent length made commercially available from their haloalkylnitrile starting materials. The changes in cation structure were established early in the formation of the cation, and later the nitrate anion was introduced by resin supported anion exchange (synthesis of *N*-cyanoalkyl-functionalized imidazolium halides and nitrates as described in Appendix A5). This approach permitted the generation of cations with easy variation in *N*-alkyl and *N*-cyanoalkyl chain length, facile exchange for an energetic anion (e.g., NO_3^-), and their subsequent structural and thermal characterization to observe for trends based upon these modifications. The synthesis of all halide and nitrate salts is provided in Appendix A5. Details for the thermal analysis are provided in Appendix B5.

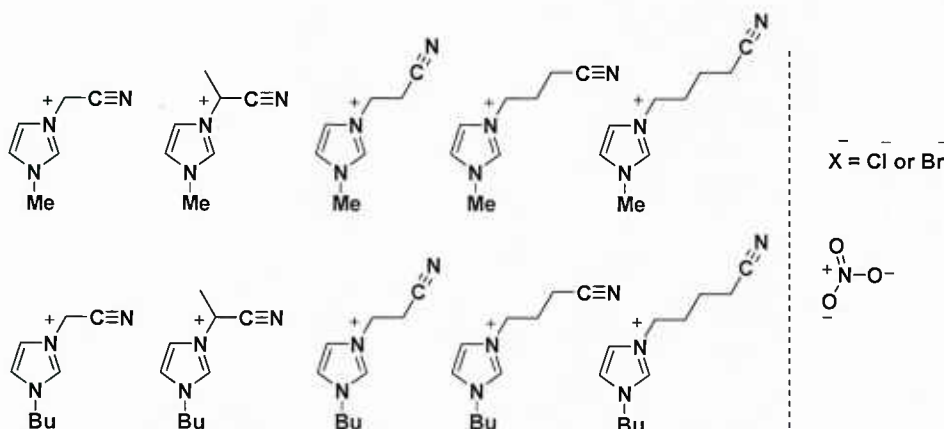


Figure 5.1 Investigated *N*-cyanoalkyl-functionalized imidazolium halides and nitrate analogs.

6. Synthesis of *N*-cyanoalkyl- and *N,N*-dicyanoalkyl-substituted imidazolium halide and dicyanamide salts with variable *N*-cyanoalkyl chain lengths, and the characterization of their structural and thermal properties as potential energetic ionic liquids

- 1. Synthesis and determination of thermal characteristics for a new, homologous series of *N*-cyanoalkyl and *N,N*-dicyanoalkyl-functionalized imidazolium dicyanamide ionic liquid salts.** Drab, D. M.; Smiglak, M.; Shamshina, J. L.; Schneider, S.; Hawkins, T. W.; Rogers, R. D., *in preparation*.

Ionic liquids (ILs) bearing the dicyanamide (dca) anion exhibit some of the lowest viscosities known for this class of organic salts. Furthermore, T. Hawkins and coworkers at Edwards Air Force Base have previously demonstrated that dca-based ILs may potentially react as hypergols. These are both properties of high interest targeted by the AFOSR for energetic applications, and here we report the synthesis and thermal characterization of 22 *N*-cyanoalkyl- and *N,N*-dicyanoalkyl-functionalized imidazolium halides and dicyanamide salts (Figure 6.1). Combining variable *N*-cyanoalkyl chain lengths with the known viscosity-reducing ability of the dca anion, it was hypothesized that EILs would exhibit ‘tunable’ thermal stability, low melting points, and a broad range of liquid behavior.

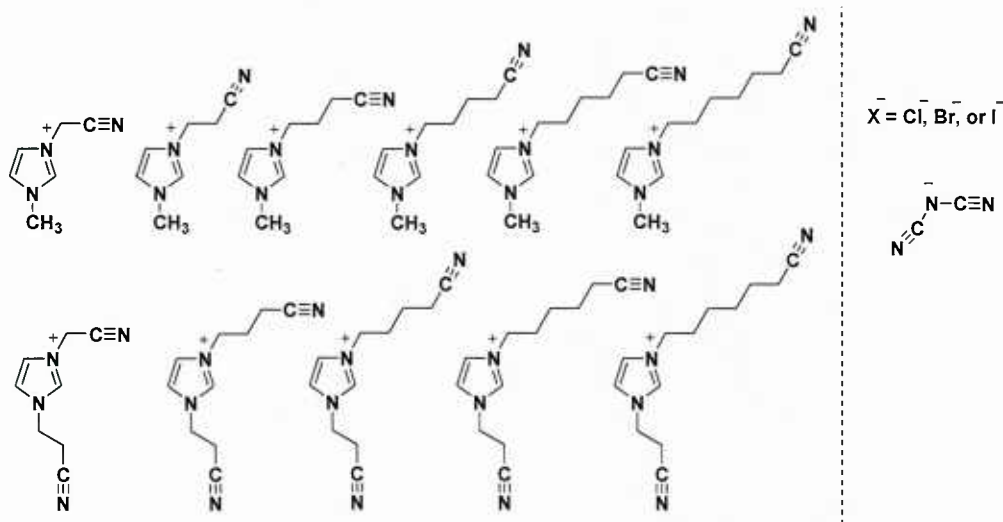


Figure 6.1 Investigated *N*-cyanoalkyl- and *N,N*-dicyanoalkyl-functionalized imidazolium halides and their dca analogs.

As with the case for the nitrates salts described previously, the dca study exploits the dual-functional nature of ILs to enable the synthesis of *N*-cyanoalkyl-functionalized imidazolium-based cations (either one or two *N*-cyanoalkyl functionalities, with variable chain length) as halide salts, followed by further exchange for the dca anion to arrive at the final product (Appendix A6). Details for the thermal analysis are provided in Appendix B6, where general trends include the observed lower thermal stability ($T_{5\% \text{decomp}}$) as the *N*-cyanoalkyl chain lengths are decreased. Additionally, the thermal stabilities for all *N*-(2-cyanoethyl)-functionalized salts were approximately the same, but this series of ILs were much more unstable in comparison with their mono-*N*-cyanoalkyl-functionalized analogues. Presumably, the loss of the *N*-(2-cyanoethyl) functionality as a leaving group to reform acrylonitrile by elimination may account for the observed trend. Also, DSC data shows that all of the dca salts are ionic liquids based

upon the measured melting points below 100 °C. Finally, after submitting all samples to our collaborators Dr. Tommy Hawkins' and his research team at Edwards AFB, impact sensitivity testing by drop-hammer determination showed that all the dca salts were very insensitive towards mechanical shock and, thus, indicate structural details that are potentially useful towards the design of EILs as insensitive liquid fuels.

7. Introduction and initial demonstration of synthetic design platform for bridged multi-heterocycles with variable charge, structure, and symmetry options: Formation of 5-tetrazole-based products using a three step procedure of azole 'click' functionalization, 'click' synthesis of bi-heterocyclic precursors, and further product modification utilizing IL-based synthetic strategies

- 1. A General Design Platform for Ionic Liquid Ions Based on Bridged Multi-Heterocycles with Flexible Symmetry and Charge.** Drab, D. M.; Shamshina, J. L.; Smiglak, M.; Hines, C. C.; Cordes, D. B.; Rogers, R. D., *Chem. Commun.* **2010**, *submitted*.

The development and implementation of IL-based methodology towards identifying new and improved synthetic protocols (e.g., halide-, solvent-, or metal-free; time/cost efficient, low impact on the environment) for the synthesis of targets of high interest to the AFOSR EIL directive remains a top priority. Previous work reported by D. Armstrong, J. Shreeve, T. Klapötke described the synthesis and highly variable properties possible with bridged multi-heterocycles. As both cationic and anionic structures are possible, this suggests a very general class of compounds (e.g., bridged multi-heterocycles) that might greatly benefit from the design options inherent to dual-functional ILs. Thus, in focusing on Objective 2, the results from efforts to conceptualize and initially demonstrate an unprecedented synthetic design platform for bridged multi-heterocyclic ionic liquids are described (Figure 7.1).

As an initial demonstration of how this design platform may be utilized towards EIL-related targets, 5-tetrazole-based structures were targeted. As the tetrazole moiety is frequently incorporated into EILs for high energy dense gas generators and their synthesis is readily accessible from well-known Click methods pioneered by K. B. Sharpless and coworkers, the synthesis of 5-tetrazole-based products from *N*-cyanoalkyl-functionalized cations and neutral molecules was the focus of the work completed for this study (Figure 7.2).

The syntheses of all products are described in Appendix A7, and all materials have been fully characterized by thermal analysis (Appendix B7). Whereas the metal-coordinated zwitterion, cation, and free zwitterion were all obtained sequentially from a common cationic precursor (1-cyanomethyl-3-methylimidazolium chloride), it was necessary to utilize a neutral substrate (1-(2-cyanoethyl)-1,2,4-triazole) in order to obtain the anionic salt as shown in Figure 7.2. Unfortunately, none of the products obtained were ILs by definition, as they were all found to have melting points > 100 °C. However, the synthetic flexibility to modify the charge, structure, and symmetry in the final product beckoned further investigation focusing on how IL-base synthetic strategies can be employed to expand the perceived design space.

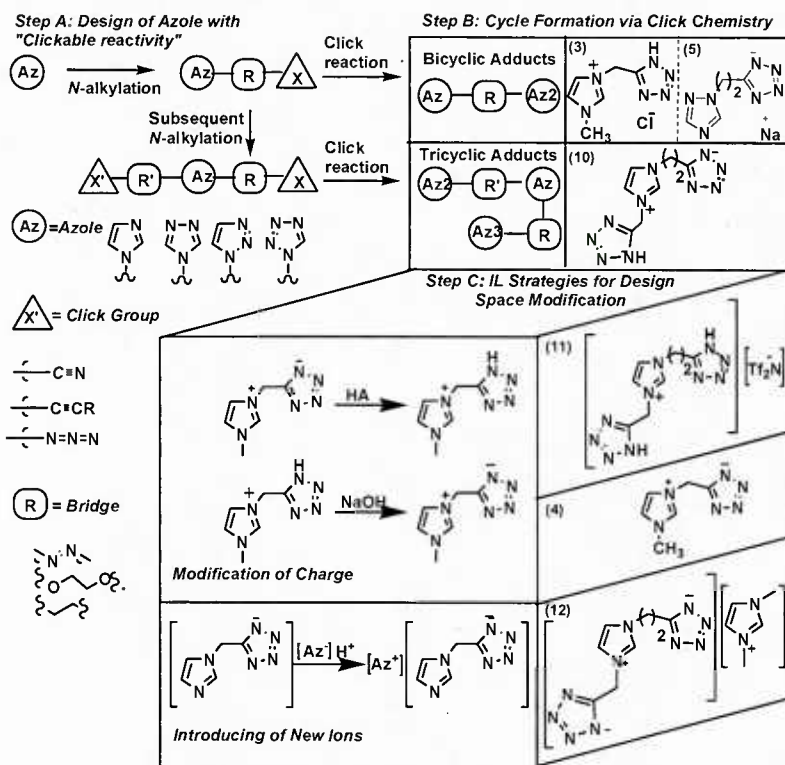


Figure 7.1 Synthetic design platform based upon design of 'clickable' azoles (Step A), Click synthesis of bridged multi-heterocycles (Step B), and formation of IL-based components with variable charge, structure and symmetry (Step C).

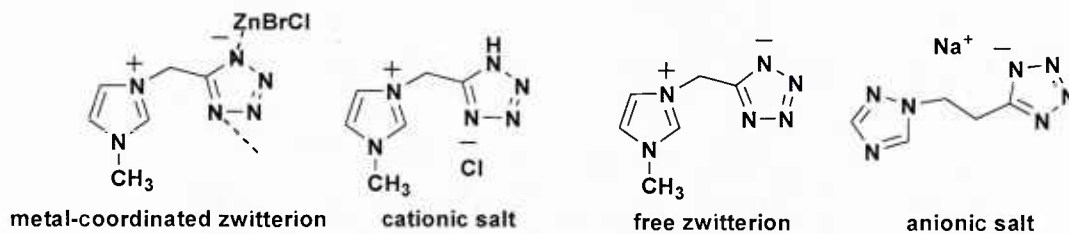


Figure 7.2 Bi-heterocyclic products obtained utilizing the multi-heterocyclic design approach, where variability in heterocyclic charge and type, metal coordination, as well as bridge length are all shown to be variable.

8. Click synthesis and thermal characterization of zinc-containing, alkyl-bridged imidazolium-tetrazolates with highly variable *N*-alkyl and alkyl bridge lengths as expansion of bridged multiheterocyclic design platform

1. Click synthesis and thermal characterization of zinc-containing, alkyl-bridged imidazolium-tetrazolates. Drab, D. M.; Smiglak, M.; Shamshina, J. L.; Rogers, R. D., *in preparation*.

The synthesis of 5-tetrazole based products from neutral aromatic nitriles and an azide source are well-known based upon methods pioneered by K. B. Sharpless and coworkers, as well as others. However, there appears to be limitations to this method when considering bridge lengths greater than 1 carbon, where harsh conditions and low synthetic yields are often the result. Due to the fast reaction times qualitatively observed for the cationic substrate in the initial demonstration of the design platform, further investigations to synthesize zwitterions of variable bridge length and *N*-alkyl substituent length were completed (Figure 8.1). It is hypothesized here that sufficient activation of the nitrile and azide anion are achieved when the substrate itself is a cation (e.g., formal positive charge on imidazolium to attract azide and maintain dipole for cycloaddition reaction), and that the formation of imidazolium-tetrazolate zwitterions is not limited to 1 carbon bridges or aromatic stabilization (as is often the case with neutral starting materials).

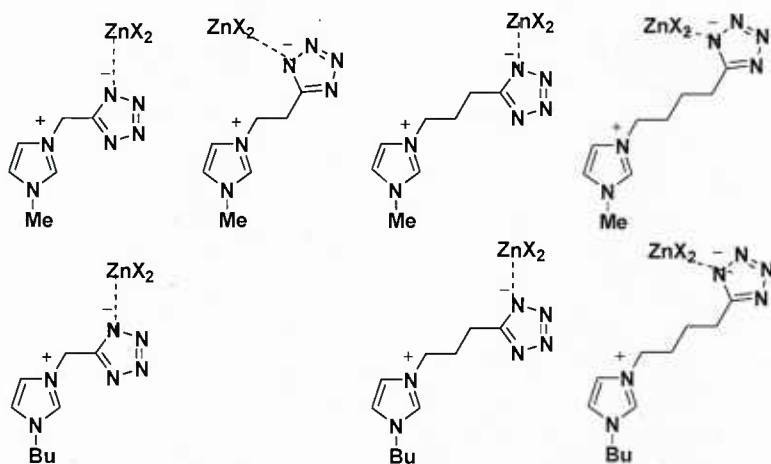
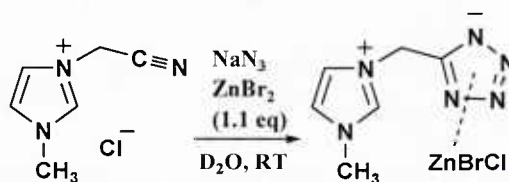


Figure 8.1 Alkyl-bridged imidazolium-tetrazolate zwitterionic products obtained as Zn-containing products

The synthesis of each product is described in Appendix A8, and the thermal properties are summarized in Appendix B8, where all products were very thermally stable and showed virtually no phase transitions. Finally, towards understanding how this reaction might be optimized in the future, the reaction of 1-cyanomethyl-3-methylimidazolium chloride with sodium azide in D₂O was observed in ¹H-NMR (Figure 8.2). Interestingly, the results from this study support that the cationic *N*-cyanoalkyl-functionalized imidazolium salts are more reactive under Sharpless Click conditions in comparison to many molecular substrates, where over 85 % conversion to Zn-containing Click product is observed in about 2.5 hours at room temperature.

Table 8.1 Study of reaction time for 1-cyanomethyl-3-methylimidazolium chloride as Click substrate



Time (min.)	Conc. s.m. [mol/L]	s.m. (%)	% Conv.
0	0.151	100	0
3	0.096	64	36
7	0.086	57	43
15	0.066	44	56
20	0.063	41	59
35	0.055	36	64
50	0.049	32	68
150	0.024	16	84

9. Utilization of ionic liquid-based synthetic strategies for the targeting of properties via the multiheterocyclic design platform

1. A General Design Platform for Ionic Liquid Ions Based on Bridged Multi-Heterocycles with Flexible Symmetry and Charge. Drab, D. M.; Shamshina, J. L.; Smiglak, M.; Hines, C. C.; Cordes, D. B.; Rogers, R. D., *Chem. Commun.* **2010**, submitted.

In the previous demonstration of the design platform for multi-heterocyclic synthesis, synthetic flexibility had been demonstrated by selective modification of (a) type of heterocycle included, (b) length of alkyl bridge and (c) overall charge of the final product (e.g., zwitterion, cation, anion). However, none of the products were ILs as tested, where to show how targeted properties of multi-heterocyclic systems (e.g., melting point) could be directed to fall within desired ranges (e.g., < 100 °C) was yet an unmet challenge. In the results presented here, tri-heterocyclic cationic and anionic components for new IL systems are synthesized from a common zwitterionic, tri-heterocyclic precursor (Figure 9.1).

The synthesis of each of these targets is described in detail in Appendix A9, where simple Brønsted acid-base chemistry, as well as IL formation by a decarboxylation protocol developed in our group is described. Thermal analysis data (TGA, Appendix B9) indicates that each of these ILs is equally or more stable than the zwitterionic precursor and that both the cationic and anionic IL forms can be used to make IL salts with melting points well below 100 °C (DSC).

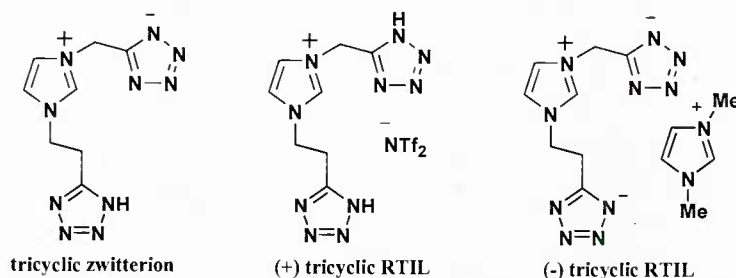


Figure 9.1 Synthetic tri-heterocyclic targets obtained to demonstrate IL-based strategies within the new design platform.

10. Hypergolic Ionic Liquids for Monopropellant Applications

- 1. Hypergolic Ionic Liquids for Monopropellant Applications**, Shamshina, J. L.; Smiglak, M.; Drab, D. M.; Dykes, Jr., W. H.; Reich, A. J.; Rogers, R. D. *Chem. Commun.* **2010**, in preparation.

Recently examples of ILs both hypergolic and catalytically ignited have been published,^{51,52} demonstrating that ILs might ignite when brought in contact with oxidants (red fuming nitric acid RFNA, nitrogen tetroxide NTO, etc.) or catalysts (Shell 405, S-405, Aerojet, KC-12 GA, etc.). Thus certain ILs can be a component of propellant fuels. While these results are promising, the need to use an oxidant (e.g., IRFNA, NTO) in order to initialize the ignition is required. There are a few known classes of propellants that ignite on catalyst,⁵³ though the current understanding does not yet allow one to predict which compounds will or will not be catalytically ignited.⁵⁴ Hydrazine, NH_2NH_2 , and its derivatives are the most popular examples due to their ready exothermic decomposition on alumina supported iridium catalysts (Shell-405, S-405).^{55,56} However, the acute toxicity of hydrazine, its sensitivity to impact, high vapor pressure, and small liquidus range ($\text{mp} = 1^\circ\text{C}$, $\text{bp} = 113.5^\circ\text{C}$)⁵⁷ are severe drawbacks that have prompted studies towards hydrazine substitutes.

Numerous hydrazine-derived ILs for propellant applications have been studied,⁵⁸⁻⁶¹ but many of these exhibit limited thermal stability.⁶² In contrast, 2-hydroxyethylhydrazinium (HEH) derivatives are thermally stable and possess substantially lower toxicity than that of other hydrazinium salts⁶³ and predicted high performance.⁶⁴ Nonetheless, the available literature is limited to the use of HEH salts with the addition of NTO or RFNA oxidants.⁶⁵ Given the suggested promising properties and the lack of available characterization data for nitrate salts of HEH, we chose this platform to test our hypothesis that a neutral propellant would be catalytically ignited when converted to an IL. Catalysts were chosen for study based on their use in the propellant field with particular emphasis on Shell 405, chosen for its ability to rapidly and reliably ignite and decompose hydrazine at relatively low temperature.⁶⁶⁻⁶⁸

2-Hydroxyethylhydrazinium nitrate (HEHN) and 2-hydroxyethylhydrazinium dinitrate (HEH2N) were prepared as reported by Drake. Their synthesis is provided in Appendix A10. and analyses (NMR, IR, DSC, TGA, long-term stability, water content) in Appendix B10. The initial screening for reactivity was conducted at ambient temperature and pressure.

Approximately 50 mg of HEHN or HEH2N was added to test tubes loaded with 10 mg of catalyst, which included Pd, Sm, Fe, Raney Ni, Pt foil, In foil, oxygen-free Cu (OFC), stainless steel, and Shell 405 (Ir on alumina 32%). Changes were visually monitored over a 3 h period and then examined again after 24 h. The only catalyst with observable activity (the formation of bubbles) was Shell 405.

Reactivity to Shell 405. Reactions of HEH, HEHN, and HEH2N with preheated Shell 405 (20-30 mesh, 32 wt. % Ir) were conducted by adding an exact amount of each to preweighted catalyst on a Fischer watch glass. Shell 405 was preheated in a sand bath at atmospheric pressure to temperatures of 50, 100, 150, or 200 °C. The HEH, HEHN, and HEH2N were preheated to the same temperatures as the catalyst and added dropwise to the preheated Shell 405 via Pauster pipettes. (HEH2N at 50 °C was added as a solid since this is below its melting point.) The First Drop Tests in Table 1 refer to addition of each compound to fresh Shell 405 and were followed by subsequent runs on the same catalyst at optimal temperature (150 °C).

First Drop (Clean Catalysts) Tests. At 50 °C, the reactions proceeded extremely slowly with only the formation of bubbles to indicate any reaction at all. Virtually all of the mass of sample added remained on the catalyst after ~4 h. The reactions were substantially faster at 100 °C and above where visible white smoke and in case of HEH2N flame was observable. The major differences observed between experiments included the time from addition of IL to the catalysts and the appearance of smoke; time between time from addition of IL to the catalysts and the flame, length of duration of the smoke; length of duration of the flame and the mass consumed in the reaction (measured as the residual mass left on the catalyst).

Upon the addition of the first drop of compound to catalyst, no observable smoke or loss of mass was observed at 50 °C for any of the compounds, while at 100 °C all three react, but with a delay between addition and gas evolution. Based on the delay time at 100 °C (Table 1), the order of initial reactivity is HEH2N > HEHN > HEH. When the reaction time is considered (measured as the total time of smoke evolution), the trend is the same HEH2N > HEHN >> HEH. Besides, HEH2N catalytically ignited at 100 °C. When the reaction temperatures are 150 °C and above, all three reactions are immediate with formation of a visible (but not measureable) caramel-like brown char.

Multiple Drop (Catalyst Recycle) Tests. For the 150 °C, approximately 10 min after each first drop test and after reheating each catalyst to the required temperature, a second portion of each IL was added and the results were noted. (This was repeated for the 3rd drop test using the same protocol.) In general, the qualitative results follow those reported above for the addition of the first drop at each temperature. However differences are apparent when considering the data in Table 1.

At 150 °C upon addition of the 2nd and 3rd drop, smoke appeared almost immediately for HEH, however, slight delay time was observed for HEHN. Contrarily, HEH2N reacted even faster than HEH. The delay times decreased in the order HEHN > HEH > HEH2N. In addition, the longevity of smoke evolution followed the order HEH2N > HEHN for salts. These results suggest that although the catalyst is still active after initial reaction, catalyst activity is decreased. This might be due to the interference of possible char, although in most cases no measurable char mass remained.

Table 10.1 Reactivity Data

<i>Comp.</i>		<i>50 °C</i>	<i>100 °C</i>	<i>150 °C</i>	<i>200 °C</i>
HEH <i>1st drop only</i>	Observations	No observable reaction	Smoke evolution after a short delay, no ignition observed	Smoke evolution after a short delay, no ignition observed	Smoke evolution after a short delay, no ignition observed, temperature is close to bp (219 oC)
	Delay of smoke		126 ms	48 ms	24 ms
	Smoke Longevity ^b		2904 ms	3012 ms	2838 ms
	Residue ^c	100%	0%	0%	0%
HEHN <i>1st drop</i>	Observations	No observable reaction	Smoke evolution after a short delay, no ignition observed	Smoke evolution after a short delay, then ignition	Smoke evolution after a short delay, then ignition
	Delay of smoke		1166 ms	90 ms	114 ms
	Smoke longevity		4538 ms	1826 ms	2556 ms
	Delay of flame		-	782 ms	958 ms
	Flame longevity		-	1826 ms	1064 ms
	Residue	100%	0%	0%	0%
<i>2nd drop</i>	Observations	No observable reaction		Smoke evolution after a short delay, then ignition	
	Delay of smoke			242 ms	
	Smoke longevity			2834 ms	
	Delay of flame			1898 ms	
	Flame longevity			1216 ms	
	Residue	100%		0% ^d	
<i>3rd drop</i>	Observations	No observable reaction		Smoke evolution after a short delay, then ignition	
	Delay of smoke			2594 ms	
	Smoke longevity			4042 ms	
	Delay of flame			4342 ms	
	Flame longevity			2294 ms	
	Residue	100%		0% ^d	
HEH2N <i>1st drop</i>	Observations	No observable reaction	Smoke evolution after a short delay, then ignition	Smoke evolution after a short delay, then ignition	Smoke evolution after a short delay, then ignition
	Delay of smoke		582 ms	28 ms	162 ms
	Smoke longevity		4690 ms	5614 ms	1242 ms
	Delay of flame		1158 ms	78 ms	966 ms
	Flame longevity		3652 ms	1716 ms	244 ms
	Residue	100%	0%	0%	0%
<i>2nd drop</i>	Observations	No observable reaction		Smoke evolution after a short delay, then ignition	
	Delay of smoke			312 ms	
	Smoke longevity			6180 ms	
	Delay of flame			2854 ms	
	Flame longevity			516 ms	
	Residue	100%		0%	
<i>3rd drop</i>	Observations	No observable reaction		Smoke evolution after a short delay, then ignition	
	Delay of smoke			688 ms	
	Smoke longevity			5920 ms	
	Delay of flame			1832 ms	
	Flame longevity			642 ms	
	Residue	100%		0%	

Catalytic Ignition. Catalytic ignition, with an observable flame, was noted for HEHN and HEH2N. HEH2N appeared the most reactive with catalytic ignition for all drops at 100 °C and above (although longer delay times were noted during each recycling run). HEHN was less reactive, but did demonstrate catalytic ignition at 200 °C with addition of the 1st and 2nd portions. In comparison, HEH showed no such reactivity toward Shell 405 at either temperature.



Figure 10.1 Ignition of HEHN on catalyst (preheated to 105°C) 782ms after the drop contacted the catalyst.

Two ILs, 2-hydroxyethylhydrazinium nitrate (a room temperature liquid, $T_g = -56.9$ °C) and hydroxyethylhydrazinium dinitrate (a white solid, $T_m = 67$ °C), catalytically decompose on Shell 405 catalyst, suggesting potential applications as hydrazine alternatives in propellant applications. Compared with the parent molecular liquid, hydroxyethylhydrazine, total reactivity increases in the order HEH2N > HEHN >> HEH. Catalytic ignition with an observable flame was noted for HEH2N at 100 °C and for HEHN at 150 °C, while HEH showed no such reactivity at either temperature. It was noted that the Shell 405 catalyst remains active after the initial reaction, although catalytic activity decreases. Use of ILs in propellant applications could possibly increase safety by reducing the hazards currently associated with handling of neutral, volatile forms of commonly used propellants. The ILs studied here possess relatively high thermal stabilities (>100 °C above the boiling point of hydrazine) and substantially decreased volatility, but certainly optimization of these salts and discovery of new catalytically ignited derivatives could produce even better results.

11. Eutectic mixtures of Ionic Liquids

1. **Direct, atom efficient, and halide free syntheses of azolium azolate energetic ionic liquids and their eutectic mixtures, and method for determining eutectic composition**
Smiglak, M.; Bridges, N. J.; Dilip, M.; Rogers, R. D. *Chem. Eur. J.* **2008**, *14*, 11314 – 11319.

It is well known, that in order for an organic salt to exhibit low melting or glass transition temperature, modifications to the structure of the cation or the anion must be made, usually to lower the symmetry and increase charge delocalization of the ions.⁶⁹ Unfortunately, in many cases this requires redesign of not only the individual ions, but also of the salt itself and its method of preparation since changes in ion structure may also change other important properties (e.g., viscosity, density, etc.). It is therefore interesting to note, that in the growing number of IL applications, the presence of a pure IL (one cation and one anion) may often not be necessary; one could merely use an entirely ionic fluid.

Specific applications such as liquid mirrors,⁷⁰ electrolytes,⁷¹ solvents for dissolution of biomass,⁷² and energetic materials, simply do not require a single cation and anion composition to perform at their best. One such example where the mixtures of quaternary ammonium salts with glycerol have been used to extract excess glycerol from biodiesel were recently presented by Abbott *et al.*⁷³ Moreover, we believe, that by formation of mixtures of ILs, multifunctional capabilities, possibly having synergistic effects, can be introduced by means of the combination of different properties brought together by different ion components in the mixture (Figure 11.1). More importantly, however, by proper selection of ions in the mixture, and their relative concentrations, eutectic mixtures can be envisioned which allow for further depression in the melting point and ready modification of the other physical properties. It is thus, surprising that the topic of eutectic mixtures composed entirely of multiple ILs has been relatively neglected in the IL field. (We note that eutectic mixtures of IL or similar salts with neutral solutes such as water, alcohols, hydrocarbons, etc, have been studied,⁷⁴⁻⁷⁷ but much of this work (for example Abbott's elegant work with deep eutectic solvents⁷⁸) tends to be excluded from the IL community, reputedly because of the presence of neutral 'molecules' in the system.)

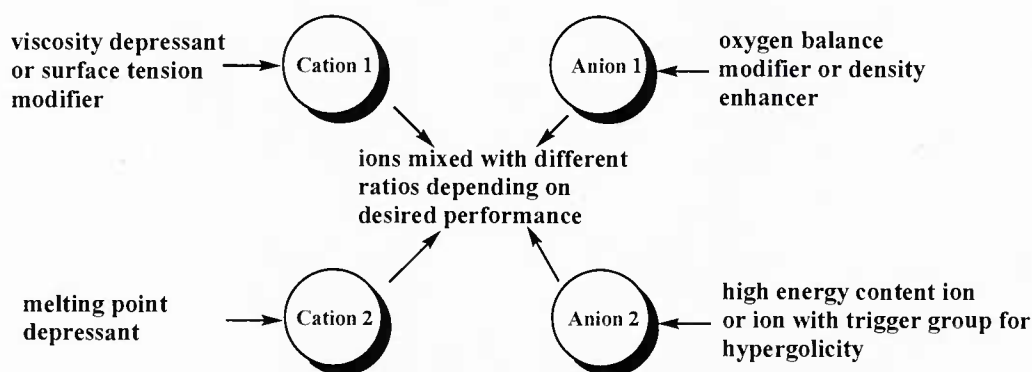


Figure 11.1 Synthetic strategy to form eutectic mixtures of ILs to tune bulk properties.

The investigation of the eutectic composition of [1,3-diMeIm][4,5-diNO₂-Im] and [1,3-diMeIm][4-NO₃-Tri] started with the careful preparation of mixtures of the salts for DSC experiments according to the protocol described in the experimental section where various mole fractions of each salt were prepared by addition of the latter. The data show significant melting point depression for the eutectic in comparison with the pure components ([1,3-diMeIm][4,5-

diNO₂-Im] mp = 98.5 °C, and [1,3-diMeIm][4-NO₂-Tri] mp = 85.7 °C). The intersection of the two linear equations constructed from the melting point of excess components in the mixture allowed determination of both the melting point for the eutectic mixture and the composition of this mixture. The melting point of the eutectic (T_E) was determined to be ~ 69.9 °C at a eutectic composition (X_E) of ~ 63 mol% of [1,3-diMeIm][4-NO₂-Tri] and 37 mol% of [1,3-diMeIm][4,5-diNO₂-Im].

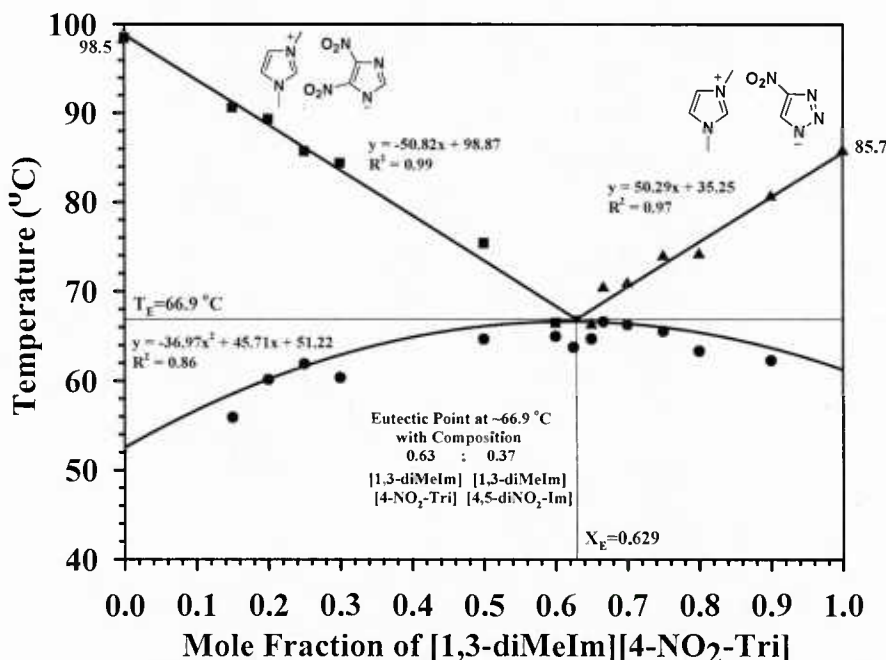


Figure 11.2 Two component phase diagram for the mixture [1,3-diMeIm][4,5-diNO₂-Im] and [1,3-diMeIm][4-NO₂-Tri]: (—●—) melting point of the eutectic mixture; (—■—) depressed melting point of [1,3-diMeIm][4,5-diNO₂-Im] when used in excess to the eutectic composition; (—▲—) depressed melting point of the [1,3-diMeIm][4-NO₂-Tri] when used in excess to the eutectic composition.

With the eutectic composition in hand, we attempted the direct synthesis of the eutectic using the one-step, halide free approach used to prepare the individual EILs. One equivalent of [1,3-diMeIm-2-COO] was reacted with 0.64 equivalents of 4-nitro-1,2,3-triazole and 0.36 equivalents of 4,5-dinitroimidazole, in a 9:1 solution of EtOH and DMSO (Figure 11.3). The eutectic mixture [1,3-diMeIm][4,5-diNO₂-Im]_{0.36}[4-NO₂-Tri]_{0.64} was obtained as yellow solid in quantitative yield. DSC analysis of the eutectic mixture of the salts gave a single melting point transition at 66.5 °C (Figure 11.4) which corresponds closely to the value expected from the binary phase diagram (66.9 °C).

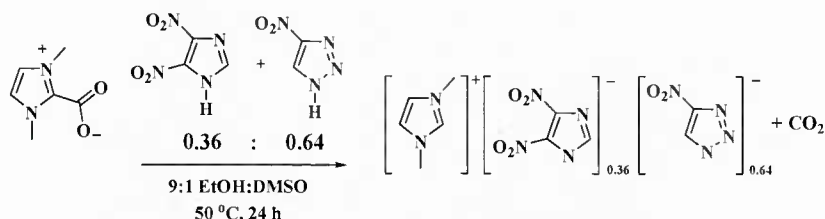


Figure 11.3 One-pot synthesis of the eutectic mixture
 $[\text{1,3-diMeIm}][\text{4,5-diNO}_2\text{-Im}]_{0.36}[\text{4-NO}_2\text{-Tri}]_{0.64}$.

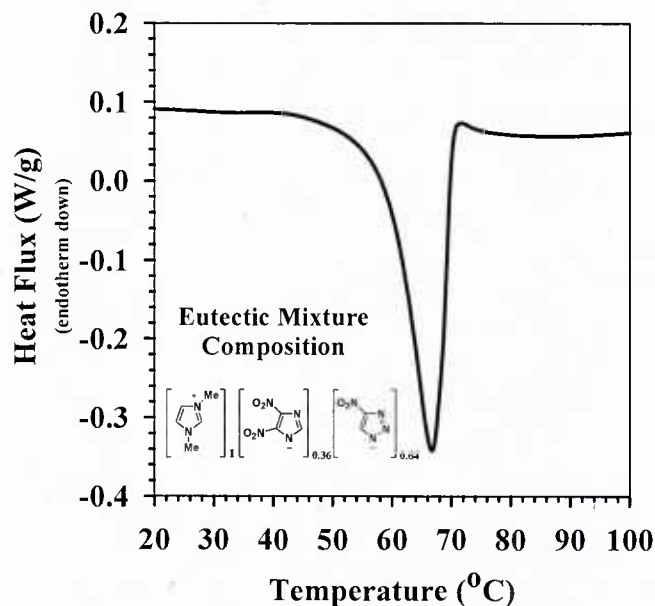


Figure 11.4 DSC analysis of the eutectic mixture.

We have demonstrated a synthetic protocol for halide free formation of pure 1,3-dialkylimidazolium salts which can also be utilized to directly prepare their eutectic mixtures. This easy to implement, synthetic protocol is applicable to a variety of imidazolium-based salts and can easily be extended to more complicated multiple ion systems. In order to determine the correct ion ratios for such multiple ion systems, we have also demonstrated a modified DSC technique for the determination of the eutectic composition which (i) is simple in operation, (ii) is quick, and (iii) requires very small sample sizes (ca. 200 mg of each IL for the entire study) which minimizes the hazards associated with the usage of high quantities of energetic materials.

We envision that the eutectic approach can be easily adapted to the modification of the melting points of many ILs when the targeted materials fall short of melting point (or other physical property) requirements and where the presence of multiple ions does not interfere with the specific application desired. The modified DSC protocol for the determination of the eutectic point can be used in high throughput screening of binary and ternary mixtures of ILs leading to the ready identification of additional useful eutectic mixtures.

V. PERSONNEL SUPPORTED

Prof. Robin D. Rogers (Principal Investigator)
Dr. Nicholas J. Bridges (Graduate Student)
Dr. Marcin Smiglak (Graduate Student/Post Doctoral Associate)
David M. Drab (Graduate Student)
Corey C. Hines (Graduate Student)
Gannon Parker (Undergraduate Student)

VI. PUBLICATIONS (BETWEEN FEB 1, 2007 – NOV 30, 2009)

(Published, Submitted and In Preparation)

1. Smiglak, M.; Hines, C. C.; Rogers, R. D., "Azolium azolates from reactions of neutral azoles with 1,3-dimethylimidazolium-2-carboxylate, 1,2,3-trimethylimidazolium hydrogen carbonate, and N,N dimethylpyrrolidinium hydrogen carbonate," **2010, in preparation.**
2. Drab, D. M.; Smiglak, M.; Hines, C. C.; Rogers, R. D., "Synthesis and thermal characterization of homologous N-cyanoalkyl-functionalized imidazolium nitrate salts as dual-functional energetic ionic liquids," **2010, in preparation.**
3. Drab, D. M.; Smiglak, M.; Shamshina, J. L.; Schneider, S.; Hawkins, T. W.; Rogers, R. D., "Synthesis and determination of thermal characteristics for a new, homologous series of N-cyanoalkyl and N,N-dicyanoalkyl-functionalized imidazolium dicyanamide ionic liquid salts," **2010, in preparation.**
4. Drab, D. M.; Smiglak, M.; Shamshina, J. L.; Rogers, R. D., "Click synthesis and thermal characterization of zinc-containing, alkyl-bridged imidazolium-tetrazolates," **2010, in preparation.**
5. Shamshina, J. L.; Smiglak, M.; Drab, D. M.; Dykes, Jr., W. H.; Reich, A. J.; Rogers, R. D., "Hypergolic Ionic Liquids for Monopropellant Applications," **2010, in preparation.**
6. Drab, D. M.; Shamshina, J. L.; Smiglak, M.; Hines, C. C.; Cordes, D. B.; Rogers, R. D., "A General Design Platform for Ionic Liquid Ions Based on Bridged Multi-Heterocycles with Flexible Symmetry and Charge," *Chem. Commun. submitted.*
7. Smiglak, M.; Hines, C. C.; Rogers, R. D. "New Hydrogen Carbonate Precursors for Efficient and Byproduct-Free Syntheses of Ionic Liquids Based on 1,2,3-Trimethylimidazolium and N,N-Dimethylpyrrolidinium Cores," *Green Chem.* **2009, accepted.**
8. Cordes, D. B.; Smiglak, M.; Hines, C. C.; Bridges, N. J.; Dilip, M.; Srinivasan, G.; Metlen, A.; Rogers, R. D. "Ionic Liquid-Based Routes to Conversion or Reuse of Recycled Ammonium Perchlorate," *Chem. Eur. J.* **2009, Early View**, DOI. 10.1002/chem.200901217.
9. Smiglak, M.; Hines, C. C.; Wilson, T. B.; Singh, S.; Vincek, A. S.; Kirichenko, K.; Katritzky, A. R.; Rogers, R. D. "Ionic Liquids Based on Azolate Anions," *Chem. Eur. J.* **2009, 16, 1572–1584. (accepted as VIP paper).**
10. Smiglak, M.; Bridges, N. J.; Dilip, M.; Rogers, R. D. "Direct, Atom Efficient, and Halide Free Syntheses of Azolium Azolate Energetic Ionic Liquids and Their Eutectic Mixtures, and Method for Determining Eutectic Composition," *Chem. Eur. J.* **2008, 36, 11314.**
11. Smiglak, M.; Metlen, A.; Rogers, R. D. "The Second Evolution of Ionic Liquids - From Solvents and Separations to Advanced Materials: Energetic Examples from the Ionic Liquid Cookbook" *Acc. Chem. Res.*, **2007, 40, 1182.**
12. Drab, D. M.; Smiglak, M.; Rogers, R. D. "Ionic liquids as a unique and versatile platform for the synthesis and delivery of energetic materials," In Proceedings for 54th JANNAF Propulsion Meeting, Denver, CO, (May 14-17, 2007), 62.

13. Bridges, N. J.; Hines, C. C.; Smiglak, M.; Rogers, R. D. "An intermediate for the clean synthesis of ionic liquids: Isolation and crystal structure of 1,3-dimethylimidazolium hydrogen carbonate monohydrate," *Chem. Eur. J.* **2007**, *13*, 5207.

VII. PRESENTATIONS (BETWEEN JAN. 15, 2007 – NOV. 30, 2009)

1. R. D. Rogers, "Approaches to the Understanding and Utilization of Unique Ionic Liquid Properties: Physical (Solvents), Chemical (Energetic Materials), and Biological (Pharmaceuticals)," Presented by R. D. Rogers before the 20th International Conference on Chemical Thermodynamics (2008), Warsaw, Poland, Abstract IL-In-1, p 181. (Invited Lecture)
2. M. Smiglak, R. D. Rogers, "Protocols for halide free synthesis of ionic liquids via hydrogen carbonate precursors." Presented by M. Smiglak before the 236th ACS National Meeting (2008), Philadelphia, PA, Abstract IEC-200.
3. R. D. Rogers, Marcin Smiglak, and David M. Drab "A Modular 'Ionic Liquid' Platform for the Custom Design of Energetic Materials," Presented by R. D. Rogers at the Energetic Ionic Liquids Workshop (2008), Colorado Springs, CO; no abstract. (Invited Presentation)
4. M. Smiglak, R. D. Rogers, "Protocols for Halide Free Synthesis of Ionic Liquids via Hydrogen Carbonate Precursors: Design of Ionic Liquid Energetic Materials" Presented by M. Smiglak before the 2nd Australasian Symposium on Ionic Liquids, Melbourne, Australia, May 11-12 2008.
5. R. D. Rogers, "Approaches to the Understanding and Utilization of Unique Ionic Liquid Properties: Physical (Solvents), Chemical (Energetic Materials), and Biological (Pharmaceuticals)," Presented by R. D. Rogers before the International Bunsen Discussion Meeting "Influence of Ionic Liquids on chemical and physicochemical reactions" (2008), Clausthal, Germany, Abstract Book p 63. (Invited Plenary).
6. R. D. Rogers, D. M. Drab, and M. Smiglak, "Ionic Liquids as a Unique and Versatile Platform for the Synthesis and Delivery of Energetic Materials," Presented by R. D. Rogers before the 54th Joint Army-Navy-NASA-Air Force (JANNAF) Propulsion Meeting (2007), Denver, CO, Program Booklet page 62.
7. R. D. Rogers, "The Evolution of Ionic Liquids - From Solvents and Separations to Advanced Materials and Pharmaceuticals: Examples from the Ionic Liquid Cookbook," Presented by R. D. Rogers before Current Status of Ionic Liquid Technology in Chemical Engineering Symposium; part of the Spring National Meeting of the Korean Institute of Chemical Engineering (2008), Jeju Island, Korea, Abstract C-2 p 82. (Invited presentation)
8. R. D. Rogers, "Ionic Liquids Beyond Solvents: Unprecedented Opportunities to Fine Tune Physical, Chemical, and Biological Properties," Presented by R. D. Rogers before the Gordon Research Conference on Organic Structures & Properties: Molecular Design & Supramolecular Assemblies (2008), Lucca (Barga), Italy, no abstract. (Invited Presentation)
9. R. D. Rogers, "The Evolution of Ionic Liquids - From Solvents and Separations to Advanced Materials and Pharmaceuticals: Examples from the Ionic Liquid Cookbook, Presented by R. D. Rogers before the 3rd Australian Symposium on Ionic Liquids (2008), Melbourne, Australia, Abstract Book. (Invited presentation)
10. S. Schneider, T. Hawkins, M. Rosander, R. D. Rogers, D. M. Drab, M. Smiglak, and A. Vij, "From halides to azides - Novel ionic liquid azides as energetic materials" Presented by A. Metlen, before the 2nd International Congress on Ionic Liquids (COIL-2), Yokohama, Japan, August 5-10, 2007, Abstract 2P03-043.

11. M. Smiglak, C. C. Hines, D. M. Drab, and R. D. Rogers, "Novel Energetic Ionic Liquid Materials Composed Solely of C, H, N, and O" Presented by M. Smiglak, before the 2nd International Congress on Ionic Liquids (COIL-2), Yokohama, Japan, August 5-10, 2007, Abstract 2P06-066.
12. M. Smiglak, C. C. Hines, N. J. Bridges, D. M. Drab, and R. D. Rogers, "New Precursors for the Halide Free Synthesis of Ionic Liquids Utilizing the Chemistry of Dimethylcarbonate" Presented by M. Smiglak, before the 2nd International Congress on Ionic Liquids (COIL-2), Yokohama, Japan, August 5-10, 2007, Abstract 1P03-047.
13. R. D. Rogers, M. Smiglak, W. L. Hough, A. Metlen, H. Rodríguez, R. P. Swatloski, S. K. Spear, D. T. Daly, J. Pernak, J. E. Grisel, R. D. Carliss, M. D. Soutullo, J. H. Davis, Jr., J. L. Scott, and D. R. MacFarlane, "The Evolution of Ionic Liquids - From Solvents and Separations to Advanced Materials to Pharmaceuticals: Energetic and API Examples from the Ionic Liquid Cookbook" Presented by R. D. Rogers, before the 2nd International Congress on Ionic Liquids (COIL-2), Yokohama, Japan, August 5-10, 2007, Abstract LMA1.
14. "The Past, Present, and Future of Ionic Liquids: From Designer Solvents to Advanced New Materials," Presented by R. D. Rogers to Lyondell Chemical Co., Newton Square, PA on 2/13/07.
15. "The Past, Present, and Future of Ionic Liquids: From Designer Solvents to Advanced New Materials," Presented by R. D. Rogers to Colgate-Palmolive, Piscataway, NJ on 9/10/07.
16. "Ionic Liquids as Transformational Technologies," Presented by R. D. Rogers to Nippon Chemical Industrial Company, Tokyo, Japan, on 4/21/08.
17. "The Evolution of Ionic Liquids – From Solvents and Separations to Advanced Materials and Pharmaceuticals: Examples from the Ionic Liquid Cookbook," Presented by R. D. Rogers at the Danish Technical University (2008), Copenhagen, Denmark, on 6/16/08.
18. "The Evolution of Ionic Liquids - From Solvents and Separations to Advanced Materials and Pharmaceuticals: Examples from the Ionic Liquid Cookbook," Presented by R. D. Rogers to Brookhaven National Laboratory, Upton, NY on 7/14/08.
19. "The Evolution of Ionic Liquids - From Solvents and Separations to Advanced Materials and Pharmaceuticals: Examples from the Ionic Liquid Cookbook," Presented by R. D. Rogers to Abbott, Waukegan, IL on 8/14/08.
20. "The Evolution of Ionic Liquids - From Solvents and Separations to Advanced Materials and Pharmaceuticals: Examples from the Ionic Liquid Cookbook," Presented by R. D. Rogers to the University of Alabama at Birmingham, Birmingham, AL on 9/8/08.
21. "The Evolution of Ionic Liquids - From Solvents and Separations to Advanced Materials and Pharmaceuticals: Examples from the Ionic Liquid Cookbook," Presented by R. D. Rogers to AMGEN, South San Francisco, CA on 9/10/08.
22. "The Evolution of Ionic Liquids - From Solvents and Separations to Advanced Materials and Pharmaceuticals: Examples for the Fragrance Industries," Presented by R. D. Rogers to Givaudan, Ashford, United Kingdom on 10/01/08.
23. "The Evolution of Ionic Liquids - From Solvents and Separations to Advanced Materials and Pharmaceuticals: Examples from the Ionic Liquid Cookbook," Presented by R. D. Rogers to The U.S. Army Research Office/U.S. Army Research Laboratory Ionic Liquids in Electroactive Devices MURI Annual Review, Philadelphia, PA on 12/16/08. (Invited Guest Speaker)
24. "The Evolution of Ionic Liquids - From Solvents and Separations to Advanced Materials and Pharmaceuticals: Examples from the Ionic Liquid Cookbook," Presented by R. D. Rogers to

Rutgers University, New Brunswick, NJ on 1/20/09. (Invited Colloquium Speaker)

25. "The Evolution of Ionic Liquids - From Solvents and Separations to Advanced Materials and Pharmaceuticals: Examples from the Ionic Liquid Cookbook," Presented by R. D. Rogers to Abbott, Waukegan, IL on 2/20/09. (Invited Abbott Seminar Series)
26. "Ionic Liquid Advances and Retreats as Solvents and Materials," Presented by R. D. Rogers to Colgate-Palmolive, Piscataway, NJ on 1/27/10.

VIII. DISSERTATIONS BETWEEN JAN. 15, 2007 – NOV. 30, 2009

1. Marcin Smiglak, Ph.D., A modular "ionic liquid" platform for the custom design of energetic materials, The University of Alabama, 2007, 327 pages; AAT 3313746
<http://libdata.lib.ua.edu:2048/login?url=http://proquest.umi.com/pqdlink?did=1541466881&sid=1&Fmt=2&clientId=31537&RQT=309&VName=PQD>
2. David M. Drab, Ph.D., A versatile design platform for multi-heterocyclic ionic liquids synthesis, The University of Alabama, *in preparation, to be submitted May 2010.*

Appendix A Synthesis of EILs

Appendix A1

Ionic Liquids Based on Azolate Anions

The preparation of azolate based salts. A diverse set of organic salts, combinations of cations **3-9** (**Q**) and anions **a-i** (**Az**) (Figure A1.1), were prepared by metathesis chemistry. Corresponding potassium azolates were combined with the corresponding ammonium or phosphonium halides in a solvent mixture of acetone:dichloromethane (DCM) (1:1), at 20–25 °C (Scheme A1.1). The cations included tetraphenylphosphonium **3** ($[\text{Ph}_4\text{P}]^+$), ethyltriphenylphosphonium ($[\text{EtPh}_3\text{P}]^+$) **4**, *N*-phenylpyridinium **5** ($[\text{N-PhPyr}]^+$), 1-butyl-3-methylimidazolium **6** ($[\text{1-Bu-3-Me-im}]^+$) (commonly known as $[\text{C}_4\text{mim}]^+$), tetrabutylammonium **7** ($[\text{Bu}_4\text{N}]^+$), tetraethylammonium **8** ($[\text{Et}_4\text{N}]^+$), and tetramethylammonium **9** ($[\text{Me}_4\text{N}]^+$). The anions included 5-nitrobenzotriazole **a** ($[\text{5-NO}_2\text{-benztri}]^-$), 5-nitrobenzimidazole **b** ($[\text{5-NO}_2\text{-benzim}]^-$), 4-nitro-1,2,3-triazolate **c** ($[\text{4-NO}_2\text{-1,2,3-tri}]^-$), 4-nitroimidazole **d** ($[\text{4-NO}_2\text{-im}]^-$), 3,5-dinitro-1,2,4-triazolate **e** ($[\text{3,5-diNO}_2\text{-1,2,4-tri}]^-$), 2,4-dinitroimidazole **f** ($[\text{2,4-diNO}_2\text{-im}]^-$), 4,5-dinitroimidazole **g** ($[\text{4,5-diNO}_2\text{-im}]^-$), 4,5-dicyanoimidazole **h** ($[\text{4,5-diCN-im}]^-$), and tetrazolate **i** ($[\text{tetr}]^-$).

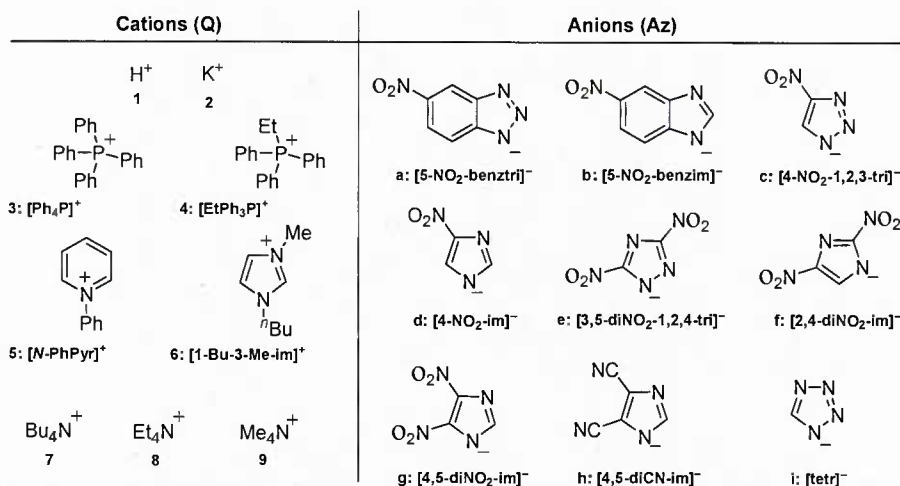
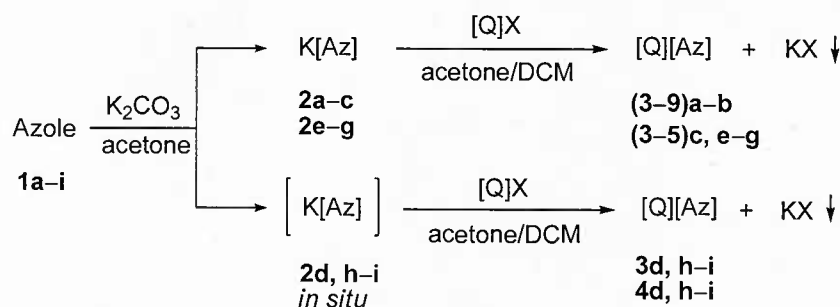


Figure A1.1. Cation and anion combinations explored in this work.



Scheme A1.1. Synthetic routes utilized to form azolate-based salts.

Potassium azolate salts **2a–c**, **e–g** were prepared by treatment of the corresponding azoles **1a–c**, **e–g** with potassium carbonate in acetone. The potassium azolates **2a–c**, **e–g** were reacted with equimolar amounts of halide salts of **3–9** and precipitated KX was filtered. Isolation of the corresponding azolates (**3–9**)**a–b** and (**3–5**)**c,e–g** was performed, *in vacuo* from the filtrate, in 88–99% yields. Difficult isolation of pure salts **2d**, **2h**, and **2i** was bypassed, by *in situ* generation with K₂CO₃, for the synthesis of 4-nitroimidazoles **3–4d**, 4,5-dicyanoimidazoles **3–4h**, and tetrazoles **3–4i**. Azoles **1d**, **h–i** were treated with *in situ* potassium carbonate and halide salts of **3–4** to give good yields of salts (**3–4**)**d, h–i** after removal of inorganic salts.

Structures of salts (**3–9**)**a–b** and (**3–5**)**c–i** were supported by ¹H and ¹³C NMR spectra, and elemental analyses (see Experimental Section). As presented in the experimental section, the crude products were mostly isolated as hydrates, supported by the elemental analyses. Most of the samples were recrystallized from alcohol prior to further thermal and crystallographic analysis. Eighteen of the salts were characterized by single crystal diffraction techniques. The family of [Ph₄P]⁺ salts are discussed in detail throughout the text, however cif files for all 19 salts are provided in the electronic supporting information.

Procedure for the Preparation of 4,5-Dinitroimidazole 1g. To 4-nitroimidazole (2.0 g, 18 mmol) dissolved in a minimum quantity of concentrated sulfuric acid was added a mixture of concentrated sulfuric acid (10 mL) and fuming nitric acid (90%, 8 mL, 0.17 mol). The mixture was heated under reflux for 5 h. After cooling, the mixture was poured into ice, and the pH was adjusted to 2 by the addition of sodium bicarbonate. The product was extracted with ethyl acetate. The extract was concentrated to give 4,5-dinitroimidazole as yellow crystals from water (1.55 g, 55%), mp 166–169 °C (lit. 188–189 °C); ¹H NMR ([D₆]DMSO) δ 12.37 (br s, 1H), 8.06 (s, 1H); ¹³C NMR ([D₆]DMSO) δ 135.5, 134.9.

General Procedure for the Preparation of Potassium Azolates 2a–c, e–g. Potassium carbonate (0.85 g, 6 mmol) was added to a solution of appropriate azole (4 mmol) in acetone (40 mL) (Scheme 1). The mixture was stirred at 20 °C for 6 h, filtered and the precipitate was washed with acetone. The solvent was evaporated and the residue was dried under vacuum to give potassium azolates **2a–c**, **e–g**.

General Procedure for the Preparation of Azolates (3–9)a–b and (3–5)c, e–g. A solution of appropriate tetraphenylphosphonium, ethyltriphenylphosphonium, *N*-phenylpyridinium, 1-butyl-3-methylimidazolium, or tetraalkylammonium halide (2 mmol) in dichloromethane (30 mL) was added to a solution of potassium azolate **2a–c**, **e–g** (2 mmol) in acetone (30 mL) at 20–25 °C. The reaction mixture was stirred for 3 h, but 24 h for the preparation of tetramethylammonium salts. The resultant potassium halide precipitate was removed by filtration and the solvent was evaporated under vacuum. The residue was dried under vacuum. The product was extracted with acetone, the extract was filtered, and the solvent was removed to give (**3–9**)**a–b** and (**3–5**)**c, e–g**.

General Procedure for the Preparation of Azolates (3–4)d, h–i. Anhydrous potassium carbonate (0.7 g, 5 mmol) was added to a solution of appropriate azole (2 mmol) in acetone (30 mL) and the mixture was stirred for 30 min at 20–25 °C. Then a solution of tetraphenylphosphonium, ethyltriphenylphosphonium, or *N*-phenylpyridinium halide (2 mmol) in dichloromethane (30 mL) was added and the reaction mixture was stirred for 3 h. The mixture was filtered and concentrated under vacuum. The product was extracted with acetone, the extract was filtered, and the solvent was removed to give (**3–4**)**d, h–i**.

Tetraphenylphosphonium 5-nitrobenzotriazolate (3a) monohydrate. Microcrystals from acetone (95%), mp 141–143 °C (DSC 2nd cycle mp 145 °C); ¹H NMR δ 7.46–7.53 (m, 8H),

7.65–7.74 (m, 9H), 7.77–7.86 (m, 5H), 8.67 (d, $J = 1.8$ Hz, 1H); ^{13}C NMR δ 114.5 (d, $J = 2.3$ Hz, 1C), 115.1, 116.0, 117.1 (d, $J = 89.9$ Hz, 4C), 130.5 (d, $J = 12.6$ Hz, 8C), 134.1 (d, $J = 10.3$ Hz, 8C), 135.6 (d, $J = 3.4$ Hz, 4C), 141.2, 144.4, 148.6. Anal. Calcd for $\text{C}_{30}\text{H}_{25}\text{N}_4\text{O}_3\text{P}$: C, 69.22; H, 4.84; N, 10.76. Found: C, 70.16; H, 4.47; N, 11.15.

Tetraphenylphosphonium 5-nitrobenzimidazolate (3b) monohydrate. Colorless oil (91%); DSC mp 55 °C; ^1H NMR δ 7.53–7.60 (m, 9H), 7.71–7.77 (m, 8H), 7.86–7.91 (m, 5H), 8.27 (s, 1H), 8.50 (d, $J = 1.6$ Hz, 1H); ^{13}C NMR δ 113.4, 114.8, 115.6, 117.1 (d, $J = 89.9$ Hz, 4C), 130.5 (d, $J = 13.2$ Hz, 8C), 134.0 (d, $J = 10.3$ Hz, 8C), 135.6 (d, $J = 2.9$ Hz, 4C), 140.9, 142.0, 146.9, 152.1. Anal. Calcd for $\text{C}_{31}\text{H}_{26}\text{N}_3\text{O}_3\text{P}$: C, 71.67; H, 5.04; N, 8.09. Found: C, 70.55; H, 4.78; N, 8.47.

Tetraphenylphosphonium 4-nitro-1,2,3-triazolate (3c) monohydrate. Light yellow microcrystals from acetone (95%), mp 157–159 °C (DSC 2nd cycle mp 155 °C); ^1H NMR δ 7.56–7.63 (m, 8H), 7.72–7.78 (m, 8H), 7.86–7.91 (m, 4H), 8.05 (s, 1H); ^{13}C NMR δ 117.1 (d, $J = 89.3$ Hz, 4C), 130.0, 130.5 (d, $J = 13.2$ Hz, 8C), 134.1 (d, $J = 11.3$ Hz, 8C), 135.6 (d, $J = 2.8$ Hz, 4C), 154.4. Anal. Calcd for $\text{C}_{26}\text{H}_{23}\text{N}_4\text{O}_3\text{P}$: C, 66.38; H, 4.93; N, 11.91. Found: C, 66.08; H, 4.36; N, 13.51.

Tetraphenylphosphonium 4-nitroimidazolate (3d). Microcrystals from acetone (94%), mp 162–165 °C (DSC 2nd cycle mp 171 °C); ^1H NMR δ 7.29 (s, 1H), 7.54–7.62 (m, 8H), 7.70–7.76 (m, 8H), 7.84–7.90 (m, 5H); ^{13}C NMR δ 117.2 (d, $J = 89.3$ Hz, 4C), 130.5 (d, $J = 12.6$ Hz, 8C), 132.1, 134.1 (d, $J = 10.3$ Hz, 8C), 135.6 (d, $J = 3.4$ Hz, 4C), 146.7, 146.7. Anal. Calcd for $\text{C}_{27}\text{H}_{22}\text{N}_3\text{O}_2\text{P}$: C, 71.83; H, 4.91; N, 9.31. Found: C, 71.01; H, 4.79; N, 9.24.

Tetraphenylphosphonium 3,5-dinitro-1,2,4-triazolate (3e). Microcrystals from acetone (99%), mp 175–178 °C (DSC 2nd cycle mp 171 °C); ^1H NMR δ 7.58–7.65 (m, 8H), 7.73–7.79 (m, 8H), 7.87–7.92 (m, 4H); ^{13}C NMR δ 117.2 (d, $J = 89.9$ Hz, 4C), 130.5 (d, $J = 13.1$ Hz, 8C), 134.2 (d, $J = 10.3$ Hz, 8C), 135.6 (d, $J = 2.9$ Hz, 4C), 163.2. Anal. Calcd for $\text{C}_{26}\text{H}_{20}\text{N}_5\text{O}_4\text{P}$: C, 62.78; H, 4.05; N, 14.08. Found: C, 62.65; H, 3.88; N, 14.26.

Tetraphenylphosphonium 2,4-dinitroimidazolate (3f). Microcrystals from acetone (90%), mp 195–197 °C (DSC 2nd cycle mp 191 °C); ^1H NMR δ 7.57–7.64 (m, 8H), 7.67 (s, 1H), 7.72–7.78 (m, 8H), 7.86–7.91 (m, 4H); ^{13}C NMR δ 117.2 (d, $J = 89.9$ Hz, 4C), 130.3, 130.5 (d, $J = 12.6$ Hz, 8C), 134.1 (d, $J = 10.9$ Hz, 8C), 135.6 (d, $J = 2.9$ Hz, 4C), 147.1, 154.2. Anal. Calcd for $\text{C}_{27}\text{H}_{21}\text{N}_4\text{O}_4\text{P}$: C, 65.32; H, 4.26; N, 11.29. Found: C, 64.48; H, 4.18; N, 11.26.

Tetraphenylphosphonium 4,5-dinitroimidazolate (3g). Microcrystals from acetone (92%), mp 159–162 °C (DSC 2nd cycle mp 145 °C); ^1H NMR δ 7.00 (s, 1H), 7.58–7.65 (m, 8H), 7.72–7.79 (m, 8H), 7.88–7.93 (m, 4H); ^{13}C NMR δ 116.9 (d, $J = 89.9$ Hz, 4C), 130.3 (d, $J = 12.6$ Hz, 8C), 133.9 (d, $J = 10.3$ Hz, 8C), 135.4 (d, $J = 2.8$ Hz, 4C), 139.5, 139.6, 140.3. Anal. Calcd for $\text{C}_{27}\text{H}_{21}\text{N}_4\text{O}_4\text{P}$: C, 65.32; H, 4.26; N, 11.29. Found: C, 64.37; H, 4.05; N, 11.37.

Tetraphenylphosphonium 4,5-dicyanoimidazolate (3h). Microcrystals from acetone (88%), mp 157–159 °C (DSC 2nd cycle mp 149 °C); ^1H NMR δ 7.37 (s, 1H), 7.56–7.64 (m, 8H), 7.71–7.78 (m, 8H), 7.87–7.92 (m, 4H); ^{13}C NMR δ 116.9, 117.2 (d, $J = 89.4$ Hz, 4C), 130.5 (d, $J = 13.2$ Hz, 8C), 134.1 (d, $J = 10.3$ Hz, 8C), 135.6 (d, $J = 3.4$ Hz, 4C), 148.9, 148.9. Anal. Calcd for $\text{C}_{29}\text{H}_{21}\text{N}_4\text{P}$: C, 76.30; H, 4.64; N, 12.27. Found: C, 75.42; H, 4.46; N, 12.74.

Tetraphenylphosphonium tetrazolate (3i) monohydrate. Microcrystals from acetone (85%), mp 308–311 °C (DSC mp at T_{dec} 290 °C); ^1H NMR δ 7.55–7.62 (m, 8H), 7.71–7.78 (m, 8H), 7.88–7.91 (m, 4H), 8.31 (s, 1H); ^{13}C NMR δ 117.1 (d, $J = 89.4$ Hz, 4C), 130.5 (d, $J = 13.2$ Hz,

8C), 134.0 (d, $J=10.3$ Hz, 8C), 135.5 (d, $J=3.4$ Hz, 4C), 149.6 (d, $J=2.9$ Hz, 1C). Anal. Calcd for $C_{25}H_{23}N_4OP$: C, 70.41; H, 5.44; N, 13.14. Found: C, 71.64; H, 5.04; N, 13.52.

Ethyltriphenylphosphonium 5-nitrobenzotriazolate (4a) monohydrate. Light brown microcrystals from acetone (99%); mp 120–122 °C (DSC 2nd cycle mp 131 °C); 1H NMR δ 1.29 (dt, $J = 19.8, 7.5$ Hz, 3H), 3.18–3.30 (m, 2H), 7.51–7.65 (m, 12H), 7.72–7.85 (m, 4H), 7.83 (dd, $J = 9.0, 2.2$ Hz, 1H), 8.65 (d, $J = 2.2$ Hz, 1H); ^{13}C NMR δ 6.6, 16.3 (d, $J = 52.7$ Hz, 1C), 114.3 (d, $J = 3.4$ Hz, 1C), 115.2, 115.9, 117.2 (d, $J = 86.4$ Hz, 3C), 130.3 (d, $J = 12.0$ Hz, 6C), 133.0 (d, $J = 9.8$ Hz, 6C), 135.1 (d, $J = 2.8$ Hz, 3C), 141.3, 144.3, 148.5. Anal. Calcd for $C_{26}H_{25}N_4O_3P$: C, 66.09; H, 5.33; N, 11.86. Found: C, 65.56; H, 4.89; N, 11.35.

Ethyltriphenylphosphonium 5-nitrobenzimidazolate (4b) monohydrate. Red oil (98%); DSC 1st cycle mp 88 °C; 1H NMR δ 1.28 (dt, $J=19.8$ & 7.4 Hz, 3H), 3.15 (dq, $J=12.6$ & 7.4 Hz, 2H), 7.50–7.58 (m, 7H), 7.61–7.68 (m, 6H), 7.76–7.81 (m, 3H), 7.89 (dd, $J=8.8$ & 2.2 Hz, 1H), 8.26 (s, 1H), 8.48 (d, $J=2.2$ Hz, 1H); ^{13}C NMR δ 6.4, 16.3 (d, $J = 52.1$ Hz, 1C), 113.5, 114.1, 115.2, 117.2 (d, $J = 85.9$ Hz, 3C), 130.3 (d, $J = 12.6$ Hz, 6C), 132.9 (d, $J = 9.7$ Hz, 6C), 135.1 (d, $J = 2.9$ Hz, 3C), 139.2, 144.8, 151.8, 158.1. Anal. Calcd for $C_{27}H_{26}N_3O_3P$: C, 68.78; H, 5.13; N, 8.91. Found: C, 67.43; H, 5.61; N, 7.94.

Ethyltriphenylphosphonium 4-nitro-1,2,3-triazolate (4c). Light yellow microcrystals from acetone (99%); mp 90–92 °C (DSC 2nd cycle mp 97 °C); 1H NMR δ 1.38 (dt, $J = 19.8, 7.4$ Hz, 3H), 3.44 (dq, $J = 12.8, 7.5$ Hz, 2H), 7.65–7.72 (m, 12H), 7.70–7.84 (m, 3H), 8.07 (s, 1H); ^{13}C NMR δ 6.6 (d, $J = 5.2$ Hz, 1C), 16.4 (d, $J = 52.7$ Hz, 1C), 117.4 (d, $J = 86.5$ Hz, 3C), 130.1, 130.4 (d, $J = 12.6$ Hz, 6C), 133.2 (d, $J = 9.7$ Hz, 6C), 135.1 (d, $J = 2.9$ Hz, 3C), 154.5. Anal. Calcd for $C_{22}H_{21}N_4O_2P$: C, 65.34; H, 5.23; N, 13.85. Found: C, 64.36; H, 5.13; N, 13.71.

Ethyltriphenylphosphonium 4-nitroimidazolate (4d) monohydrate. Light yellow microcrystals from acetone (98%); mp 89–91 °C (DSC 2nd cycle mp 100 °C); 1H NMR δ 1.35 (dt, $J = 19.8, 7.4$ Hz, 3H), 3.44 (dq, $J = 12.7, 7.5$ Hz, 2H), 7.28 (s, 1H), 7.60–7.72 (m, 12H), 7.78–7.84 (m, 3H), 7.89 (s, 1H); ^{13}C NMR δ 6.5 (d, $J = 5.2$ Hz, 1C), 16.3 (d, $J = 52.7$ Hz, 1C), 117.3 (d, $J = 86.2$ Hz, 3C), 130.4 (d, $J = 12.6$ Hz, 6C), 132.3, 133.1 (d, $J = 10.3$ Hz, 6C), 135.1 (d, $J = 2.9$ Hz, 3C), 146.7 (d, $J = 4.0$ Hz, 1C), 148.3. Anal. Calcd for $C_{23}H_{24}N_3O_3P$: C, 65.55; H, 5.74; N, 9.97. Found: C, 66.57; H, 5.40; N, 9.85.

Ethyltriphenylphosphonium 3,5-dinitro-1,2,4-triazolate (4e). Microcrystals from acetone (96%), mp 124–125 °C (DSC 2nd cycle mp 127 °C); 1H NMR δ 1.44 (dt, $J = 19.8, 7.6$ Hz, 3H), 3.38 (dq, $J = 12.6, 7.4$ Hz, 2H), 7.64–7.75 (m, 12H), 7.79–7.86 (m, 3H); ^{13}C NMR δ 6.6 (d, $J = 5.7$ Hz, 1C), 16.6 (d, $J = 53.3$ Hz, 1C), 117.2 (d, $J = 86.5$ Hz, 3C), 130.5 (d, $J = 12.6$ Hz, 6C), 133.2 (d, $J = 9.7$ Hz, 6C), 135.3 (d, $J = 3.5$ Hz, 3C), 163.2. Anal. Calcd for $C_{22}H_{20}N_5O_4P$: C, 58.80; H, 4.49; N, 15.58. Found: C, 58.63; H, 4.35; N, 15.19.

Ethyltriphenylphosphonium 2,4,-dinitroimidazolate (4f) monohydrate. Light yellow microcrystals from acetone (96%); mp 68–70 °C (DSC 1st cycle mp 70 °C); 1H NMR δ 1.41 (dt, $J=19.6, 7.4$ Hz, 3H), 3.39 (dq, $J=12.6, 7.4$ Hz, 2H), 7.63–7.74 (m, 13H), 7.78–7.86 (m, 3H); ^{13}C NMR δ 6.5, 16.4 (d, $J=53.3$ Hz, 1C), 117.1 (d, $J=85.9$ Hz, 3C), 130.3, 130.4 (d, $J=12.6$ Hz, 6C), 133.0 (d, $J=9.6$ Hz, 6C), 135.1 (d, $J=2.9$ Hz, 3C), 147.0, 154.1. Anal. Calcd for $C_{23}H_{23}N_4O_5P$: C, 59.23; H, 4.97; N, 12.01. Found: C, 60.29; H, 4.64; N, 11.40.

Ethyltriphenylphosphonium 4,5-dinitroimidazolate (4g). Yellow microcrystals from acetone (95%); mp 91–93 °C (DSC 1st cycle mp 97 °C); 1H NMR δ 1.39 (dt, $J = 19.8, 7.4$ Hz, 3H), 3.25 (dq, $J = 12.7, 7.5$ Hz, 2H), 7.00 (s, 1H), 7.59–7.73 (m, 12H), 7.79–7.85 (m, 3H); ^{13}C NMR δ 6.6, 16.6 (d, $J = 52.7$ Hz, 1C), 117.2 (d, $J = 86.4$ Hz, 3C), 130.5 (d, $J = 12.6$ Hz, 6C),

133.2 (d, $J = 9.7$ Hz, 6C), 135.3 (d, $J = 3.5$ Hz, 3C), 139.8 (d, $J = 5.7$ Hz, 1C), 140.6. Anal. Calcd for $C_{23}H_{21}N_4O_4P$: C, 61.61; H, 4.72; N, 12.49. Found: C, 61.33; H, 4.74; N, 12.36.

Ethyltriphenylphosphonium 4,5-dicyanoimidazolate (4h). Light yellow oil (96%); DSC 2nd cycle mp -29 °C; 1H NMR δ 1.40 (dt, $J = 19.5, 7.3$ Hz, 3H), 3.21 (dq, $J = 12.7, 7.4$ Hz, 2H), 7.39 (s, 1H), 7.59–7.66 (m, 6H), 7.68–7.74 (m, 6H), 7.81–7.86 (m, 3H); ^{13}C NMR δ 6.6, 16.6 (d, $J = 53.2$ Hz, 1C), 116.9, 117.1 (d, $J = 85.9$ Hz, 3C), 118.4, 130.5 (d, $J = 12.6$ Hz, 6C), 133.1 (d, $J = 9.7$ Hz, 6C), 135.4 (d, $J = 3.4$ Hz, 3C), 148.9 (d, $J = 8.0$ Hz, 1C). Anal. Calcd for $C_{25}H_{21}N_4P$: C, 73.52; H, 5.18; N, 13.72. Found: C, 72.87; H, 5.33; N, 13.44.

Ethyltriphenylphosphonium tetrazolate (4i) monohydrate. Light yellow microcrystals from acetone (89%); mp $83-85$ °C (DSC 1st cycle mp 51 °C); 1H NMR δ 1.32 (dt, $J = 20.0, 7.6$ Hz, 3H), 3.38 (dq, $J = 12.7, 7.8$ Hz, 2H), 7.62–7.72 (m, 12 H), 7.76–7.82 (m, 3H), 8.30 (s, 1H); ^{13}C NMR δ 6.4 (d, $J = 5.2$ Hz, 1C), 16.0 (d, $J = 52.7$ Hz, 1C), 117.5 (d, $J = 85.9$ Hz, 3C), 130.3 (d, $J = 12.6$ Hz, 6C), 133.1 (d, $J = 10.3$ Hz, 6C), 134.9 (d, $J = 2.9$ Hz, 3C), 149.6 (d, $J = 4.0$ Hz, 1C). Anal. Calcd for $C_{21}H_{23}N_4OP$: C, 66.65; H, 6.13; N, 14.81. Found: C, 66.87; H, 5.94; N, 14.57.

N-Phenylpyridinium 5-nitrobenzotriazolate (5a) monohydrate. Black microcrystals from acetone (96%); mp $79-81$ °C (DSC 1st cycle mp 75 °C); 1H NMR (DMSO- d_6) δ 7.73–7.76 (m, 4H), 7.83 (dd, $J = 9.0, 2.1$ Hz, 1H), 7.88–7.92 (m, 2H), 8.29–8.34 (m, 2H), 8.62 (d, $J = 2.0$ Hz, 1H), 8.79 (t, $J = 7.8$ Hz, 1H), 9.36 (d, $J = 5.6$ Hz, 2H); ^{13}C NMR (DMSO- d_6) δ 113.5 (d, $J = 3.4$ Hz, 1C), 115.0, 115.7, 124.7, 128.1, 130.2, 131.2, 140.7, 142.8, 143.8, 144.9, 146.6, 147.8. Anal. Calcd for $C_{17}H_{15}N_5O_3$: C, 60.53; H, 4.48; N, 20.76. Found: C, 59.92; H, 4.21; N, 21.11.

N-Phenylpyridinium 4-nitro-1,2,3-triazolate (5c). Microcrystals from acetone (94%); mp $129-131$ °C (DSC 2nd cycle mp 135 °C); 1H NMR (DMSO- d_6) δ 7.73–7.76 (m, 3H), 7.89–7.92 (m, 2H), 8.02 (s, 1H), 8.30–8.34 (m, 2H), 8.80 (t, $J = 7.8$ Hz, 1H), 9.36 (d, $J = 5.5$ Hz, 2H); ^{13}C NMR (DMSO- d_6) δ 124.7, 128.1, 129.5, 130.2, 131.2, 142.8, 144.9, 146.6, 154.1. Anal. Calcd for $C_{13}H_{11}N_5O_2$: C, 57.99; H, 4.12; N, 26.01. Found: C, 57.75; H, 3.95; N, 26.28.

N-Phenylpyridinium 3,5-dinitro-1,2,4-triazolate (5e). Microcrystals from acetone (88%); mp $158-160$ °C (DSC 2nd cycle mp 167 °C); 1H NMR (DMSO- d_6) δ 7.73–7.77 (m, 3H), 7.88–7.92 (m, 2H), 8.30–8.35 (m, 2H), 8.80 (t, $J = 7.8$ Hz, 1H), 9.36 (d, $J = 5.5$ Hz, 2H); ^{13}C NMR (DMSO- d_6) δ 124.7, 128.1, 130.2, 131.2, 142.8, 145.0, 146.6, 162.9. Anal. Calcd for $C_{13}H_{10}N_6O_4$: C, 49.69; H, 3.21; N, 26.74. Found: C, 49.53; H, 2.99; N, 26.27.

N-Phenylpyridinium 2,4-dinitroimidazolate (5f). Light yellow microcrystals from acetone (93%); mp $140-142$ °C (DSC 2nd cycle mp 143 °C); 1H NMR (DMSO- d_6) δ 7.71 (s, 1H), 7.74–7.77 (m, 3H), 7.89–7.92 (m, 2H), 8.30–8.35 (m, 2H), 8.80 (t, $J = 7.8$ Hz, 1H), 9.37 (d, $J = 5.7$ Hz, 2H); ^{13}C NMR (DMSO- d_6) δ 100.1, 124.8, 128.1, 130.2, 130.3, 131.2, 142.8, 145.0, 146.6, 146.8. Anal. Calcd. For $C_{14}H_{11}N_5O_4$: C, 53.68; H, 3.54; N, 22.36. Found: C, 53.99; H, 3.40; N, 22.29.

N-Phenylpyridinium 4,5-dinitroimidazolate (5g). Light brown microcrystals from acetone (91%); mp $129-132$ °C (DSC 2nd cycle mp 140 °C); 1H NMR (DMSO- d_6) δ 6.94 (s, 1H), 7.74–7.77 (m, 3H), 7.88–7.91 (m, 2H), 8.29–8.34 (m, 2H), 8.79 (t, $J = 7.8$ Hz, 1H), 9.36 (d, $J = 5.8$ Hz, 2H); ^{13}C NMR (DMSO- d_6) δ 124.7, 128.1, 130.2, 131.2, 139.3, 139.4, 142.8, 145.0, 146.5. Anal. Calcd. For $C_{14}H_{11}N_5O_4$: C, 53.68; H, 3.54; N, 22.36. Found: C, 53.45; H, 3.34; N, 22.29.

1-Butyl-3-methylimidazolium 5-nitrobenzotriazolate (6a). Colorless oil (94%); DSC 2nd cycle T_g -41 °C; 1H NMR δ 0.83 (t, $J = 7.3$ Hz, 3H), 1.15–1.28 (m, 2H), 1.66–1.76 (m, 2H), 3.92 (s, 3H), 4.09 (t, $J = 7.4$ Hz, 2H), 7.24 (t, $J = 1.8$ Hz, 1H), 7.28 (t, $J = 1.6$ Hz, 1H), 7.82 (d, $J = 8.9$ Hz, 1H), 7.94 (dd, $J = 8.9$ & 2.1 Hz, 1H), 8.78 (d, $J = 2.1$ Hz, 1H), 9.81 (s, 1H); ^{13}C NMR δ

13.1, 19.2, 31.7, 36.2, 49.7, 114.2, 116.0, 116.1, 121.8, 123.2, 137.2, 142.0, 144.2, 148.3. Anal. Calcd for $C_{14}H_{18}N_6O_2$: C, 55.62; H, 6.00; N, 27.80. Found: C, 54.65; H, 6.16; N, 27.00.

1-Butyl-3-methylimidazolium 5-nitrobenzimidazolate (6b) monohydrate. Colorless oil (98%); DSC 2nd cycle T_g -34 °C; 1H NMR δ 0.87 (t, J = 7.3 Hz, 3H), 1.16–1.29 (m, 2H), 1.64–1.74 (m, 2H), 3.79 (s, 3H), 3.99 (t, J = 7.3 Hz, 2H), 7.15–7.17 (m, 2H), 7.57 (d, J = 8.9 Hz, 1H), 7.93 (dd, J = 8.9 & 2.2 Hz, 1H), 8.29 (s, 1H), 8.50 (d, J = 2.2 Hz, 1H), 9.42 (s, 1H); ^{13}C NMR δ 13.1, 19.2, 31.7, 36.0, 49.5, 113.1, 115.2, 115.2, 121.8, 123.1, 136.5, 140.4, 143.0, 149.2, 154.7. Anal. Calcd for $C_{15}H_{21}N_5O_3$: C, 56.41; H, 6.63; N, 21.93. Found: C, 56.42; H, 6.62; N, 21.89.

Tetrabutylammonium 5-nitrobenzotriazolate (7a) monohydrate. Microcrystals from acetone (96%), mp 91–93 °C (DSC 2nd cycle mp 60 °C); 1H NMR δ 0.92 (t, J = 7.2 Hz, 12H), 1.32 (sextet, J = 7.2 Hz, 8H), 1.43–1.53 (m, 8H), 3.03–3.09 (m, 8H), 7.82 (d, J = 8.9 Hz, 1H), 7.94 (dd, J = 8.9 & 2.1 Hz, 1H), 8.80 (d, J = 2.1 Hz, 1H); ^{13}C NMR δ 13.4, 19.4, 23.6, 58.4, 114.3, 115.7, 116.0, 141.7, 144.1, 148.3. Anal. Calcd for $C_{22}H_{41}N_5O_3$: C, 62.38; H, 9.76; N, 16.53. Found: C, 61.97; H, 10.04; N, 15.98.

Tetrabutylammonium 5-nitrobenzimidazolate (7b). Microcrystals from acetone (99%), mp 99–101 °C (DSC 2nd cycle mp 81 °C); 1H NMR δ 0.94 (t, J = 7.0 Hz, 12H), 1.22–1.40 (m, 16H), 2.75–2.80 (m, 8H), 7.53 (d, J = 8.8 Hz, 1H), 7.89 (dd, J = 8.8 & 2.3 Hz, 1H), 8.21 (s, 1H), 8.51 (d, J = 2.3 Hz, 1H); ^{13}C NMR δ 13.5, 19.4, 23.5, 58.2, 113.6, 114.2, 115.5, 139.4, 144.9, 152.0, 158.4. Anal. Calcd for $C_{23}H_{40}N_4O_2$: C, 68.28; H, 9.96; N, 13.85. Found: C, 67.17; H, 10.42; N, 13.35.

Tetraethylammonium 5-nitrobenzotriazolate (8a). Colorless oil (98%); DSC 2nd cycle mp 64 °C; 1H NMR δ 1.15 (dt, J = 7.3 & 1.7 Hz, 12H), 3.08 (q, J = 7.3 Hz, 8H), 7.81 (d, J = 9.0 Hz, 1H), 7.93 (dd, J = 9.0 & 2.1 Hz, 1H), 8.78 (d, J = 2.1 Hz, 1H); ^{13}C NMR δ 7.3, 52.2 (t, J = 3.0 Hz, 4C), 114.1, 115.7, 116.0, 141.7, 144.2, 148.4. Anal. Calcd for $C_{14}H_{23}N_5O_2$: C, 57.32; H, 7.90; N, 23.87. Found: C, 56.01; H, 8.17; N, 22.58.

Tetraethylammonium 5-nitrobenzimidazolate (8b) monohydrate. Microcrystals from acetone (99%), mp 42–43 °C (DSC 2nd cycle mp 101 °C); 1H NMR δ 1.11 (tt, J = 7.3 & 1.6 Hz, 12H), 2.97 (q, J = 7.3 Hz, 8H), 7.59 (d, J = 8.8 Hz, 1H), 7.94 (dd, J = 8.8 & 2.3 Hz, 1H), 8.28 (s, 1H), 8.53 (d, J = 2.2 Hz, 1H); ^{13}C NMR δ 7.12, 52.1 (t, J = 2.9 Hz, 4C), 113.1, 115.0, 115.2, 140.3, 143.2, 149.4, 155.1. Anal. Calcd for $C_{15}H_{26}N_4O_3$: C, 58.04; H, 8.44; N, 18.05. Found: C, 58.80; H, 8.47; N, 17.88.

Tetramethylammonium 5-nitrobenzotriazolate (9a). Microcrystals from acetone (89%), mp 192–195 °C (DSC mp at T_{dec} 192 °C); 1H NMR (DMSO) δ 3.13 (s, 12H), 7.74 (d, J = 8.8 Hz, 1H), 7.82 (dd, J = 8.8 & 2.1 Hz, 1H), 8.62 (d, J = 2.1 Hz, 1H); ^{13}C NMR (DMSO) δ 54.3 (t, J = 4.4 Hz, 4C), 113.5, 114.6, 115.8, 140.5, 144.1, 148.4. Anal. Calcd for $C_{10}H_{15}N_5O_2$: C, 50.62; H, 6.37; N, 29.52. Found: C, 50.29; H, 6.73; N, 28.46.

Tetramethylammonium 5-nitrobenzimidazolate (9b) monohydrate. Microcrystals from acetone (93%), mp 66–68 °C (DSC 2nd cycle mp 119 °C); 1H NMR (DMSO) δ 3.10 (s, 12H), 7.37 (d, J = 8.8 Hz, 1H), 7.73 (dd, J = 8.8 & 2.3 Hz, 1H), 7.98 (s, 1H), 8.27 (d, J = 2.3 Hz, 1H); ^{13}C NMR (DMSO) δ 54.4, 112.5, 113.0, 115.0, 137.9, 145.4, 152.9, 158.8. Anal. Calcd for $C_{11}H_{18}N_4O_3$: C, 51.96; H, 7.13; N, 22.03. Found: C, 53.54; H, 6.45; N, 21.06.

Appendix A2

New Hydrogen Carbonate Precursors for Efficient and Byproduct-Free Syntheses of Ionic Liquids Based

Preparation of Hydrogen carbonate IL precursors. *Reactivity of 1,2,3-Trimethylimidazolium Methyl Carbonate ([1,2,3-triMeIM][MeCO₃]).* The salt 1,2,3-trimethylimidazolium methyl carbonate ([1,2,3-triMeIM][MeCO₃]) was synthesized by alkylation of 1,2-dimethylimidazole with dimethyl carbonate, at 70 °C for 10 days in a sealed pressure tube (Figure 3a). Because of the possible reaction outcomes (i.e., formation of the desired [1,2,3-triMeIM][MeCO₃] or the 1,2,3-trimethylimidazolium-4-carboxylate ([1,2,3-triMeIM-4-COO]) byproduct (Figure 4)), the correct NMR solvent had to be used in order to provide reliable proof for the structure of the final product. The pyrrolidinium core was chosen for study to represent non-aromatic amines that would not undergo bonding of the carbonate group to the pyrrolidinium core, and thus not form a zwitterionic species. Another benefit of working with this cation core is its wide electrochemical window, thus having potential for use in electrochemical applications.⁷⁹ It was anticipated that in the reaction of *N*-alkylpyrrolidine and dialkyl carbonate, only the *N,N*-dialkylpyrrolidinium alkyl carbonate would be formed. This could then undergo an anion conversion process, as described above, with clean formation of the [HCO₃]⁻-based salt and alcohol as the byproduct.

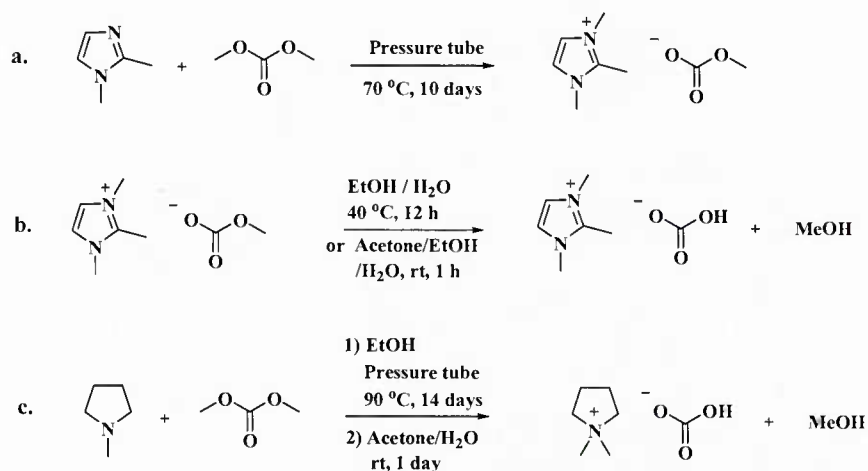


Figure A2.1. General protocol for the synthesis of a) 1,2,3-trimethylimidazolium methyl carbonate, b) 1,2,3-trimethylimidazolium hydrogen carbonate, and c) *N,N*-dimethylpyrrolidinium hydrogen carbonate.

Synthesis of 1,2,3-Trimethylimidazolium Methyl Carbonate ([1,2,3-triMeIM][MeCO₃]).

The synthesis of [1,2,3-triMeIM][MeCO₃] followed a previously published method for the synthesis of [1,3-diMeIM-2-COO] via an alkylation reaction of 1-methylimidazole with DMC. 4.8 g (50 mmol) of 1,2-dimethylimidazole and 9 g (100 mmol) of DMC were placed in a 20 mL thick-walled glass pressure tube. The tube was sealed, placed in an oven, and heated to 70 °C for 10 days (Figure 3a). The resulting yellow liquor was cooled to room temperature and unreacted substrates removed under high vacuum, at which time the product (7.44 g) crystallized in the form of slightly colored crystals.

1,2,3-Trimethylimidazolium Methyl Carbonate ([1,2,3-triMeIM][MeCO₃]): White solid, very hygroscopic, 80% yield, m.p. 79 °C, $T_{5\%dec} = 104$ °C; ¹H NMR (500 MHz, CDCl₃) δ = 2.74 (s, 3H, C2-CH₃), 3.45 (s, 3H, CH₃CO₃), 3.94 (s, 6H, N-CH₃), 7.74 (s, 2H, C4/C5-H); ¹³C NMR (125 MHz, CDCl₃) δ = 9.52 (C2-CH₃), 35.16 (N-CH₃), 52.02 (CH₃CO₃), 122.69 (C4/C5), 143.99 (C2), 157.98 (CH₃CO₃); ¹H NMR (500 MHz, [D₄] MeOH) δ = 2.50 (s, 3H; C2-CH₃), 3.23 (s, 3H; CH₃CO₃), 3.71 (s, 6H, N-CH₃), 7.35 (s, 2H, C4/C5-H); ¹³C NMR (125 MHz, [D₄] MeOH) δ = 9.34 (C2-CH₃), 35.42 (N-CH₃), 49.90 (CH₃CO₃), 123.35 (C4/C5), 146.52 (C2), 161.37 (CH₃CO₃). Single crystal X-ray diffraction analysis: colorless plates; C₈H₁₄N₂O₃; MW 186.21; T = 173 K; Monoclinic; $P2_1/n$; a = 6.8805(6) Å; b = 11.6254(10) Å; c = 11.9614(11) Å; β = 96.229(2)°; V = 951.13(15) Å³; Z = 4; D_{calc} = 1.300 g cm⁻³; R₁, wR₂ [I > 2 σ (I)] = 0.0428, 0.1044; R₁, wR₂ (all data) = 0.0510, 0.1087.

Synthesis of 1,2,3-Trimethylimidazolium Hydrogen Carbonate ([1,2,3-triMeIM][HCO₃]).
Via Reaction in EtOH/H₂O: 0.5 g (2.7 mmol) of [1,2,3-triMeIM][MeCO₃] was dissolved in 3 mL of EtOH and 1.5 mL (83 mmol) DI H₂O was added (Figure 3b). The reaction was stirred overnight at 40 °C, after which time the solvent was evaporated on the rotary evaporator, and the sample was analyzed by NMR. The NMR spectra confirmed the quantitative conversion to [1,2,3-triMeIM][HCO₃]. The slightly colored solid product (0.46 g) was obtained in 99% yield.

Via Reaction in EtOH/Acetone: 1.5 g (8.1 mmol) of [1,2,3-triMeIM][MeCO₃] was dissolved in a minimum amount of EtOH (2 mL) and heated to 40 °C to allow complete dissolution of the starting material. 10 mL of acetone, spiked with 0.3 mL (16.7 mmol) DI H₂O, was then added dropwise to the EtOH solution, producing a precipitate which was separated by centrifugation. The remaining solution was concentrated by partial evaporation of the solvent on a rotary evaporator at 40 °C, and another portion of acetone (10 mL) was added allowing for more precipitation. The process was repeated 2 more times until no precipitate was noticed. The combined solid was dried under high vacuum at 40 °C for 12 h. A white, hygroscopic solid (1.39 g), with a melting point at the decomposition temperature was obtained with a total yield of 91%.

1,2,3-Trimethylimidazolium Hydrogen Carbonate Monohydrate ([1,2,3-triMeIM][HCO₃].H₂O): White solid, very hygroscopic, 91% yield, m.p. at $T_{5\%dec}$, $T_{5\%dec} = 112$ °C; ¹H NMR (500 MHz, D₂O) δ = 2.57 (s, 3H; C2-CH₃), 3.78 (s, 6H, N-CH₃), 7.30 (s, 2H, C4/C5-H); ¹³C NMR (125 MHz, D₂O) δ = 9.41 (C2-CH₃), 35.32 (N-CH₃), 122.55 (C4/C5), 145.50 (C2), 161.03 (HCO₃); ¹H NMR (500 MHz, [D₄] MeOH) δ = 2.51 (s, 3H; C2-CH₃), 3.72 (s, 6H, N-CH₃), 7.36 (s, 2H, C4/C5-H); ¹³C NMR (125 MHz, [D₄] MeOH) δ = 9.37 (C2-CH₃), 35.44 (N-CH₃), 123.35 (C4/C5), 146.48 (C2), 161.32 (CH₃CO₃). Single crystal X-ray diffraction analysis of [1,2,3-triMeIM][HCO₃].H₂O: colorless needles; C₇H₁₄N₂O₄; MW 190.20; T = 173 K; Monoclinic; $P2_1/n$; a = 7.479(2) Å; b = 13.289(4) Å; c = 9.636(3) Å; β = 90.011(5)°; V = 954.0(5) Å³; Z = 4; D_{calc} = 1.324 g cm⁻³; R₁, wR₂ [I > 2 σ (I)] = 0.0719, 0.1097; R₁, wR₂ (all data) = 0.1822, 0.1407.”

Synthesis of N,N-Dimethylpyrrolidinium Hydrogen Carbonate ([N,N-diMePyr][HCO₃]).
 4.0 g (50 mmol) of N-methylpyrrolidine was initially dissolved in 5 mL of EtOH and transferred into a 20 mL thick-walled pressure tube. Next, 9 g (100 mmol) of DMC was added to the solution at room temperature. The tube was sealed, stirred vigorously, placed in the oven, and heated to 90 °C. The reaction mixture was kept at those conditions for 14 days, and then cooled to room temperature (Figure 3c) giving a dark red liquor. Excess unreacted substrates were removed using a rotary evaporator at 90 °C, and later high vacuum at 70 °C. No product crystallized from the mother liquor.

Due to problems with isolating the product from the red liquor, the intermediate was converted *in situ* into *N,N*-dimethylpyrrolidinium hydrogen carbonate. To the oily-red concentrated reaction mixture 10 mL of wet acetone was added resulting in the complete dissolution of reaction mixture. After 1 h a crystalline product slowly started to appear. After 24 h at room temperature, the vessel was placed in the refrigerator and kept at this temperature for an additional 72 h. A white, solid, very hygroscopic product was separated from the red liquor by centrifugation, and washed twice with cold acetone. The remaining extract was concentrated, more solid product precipitated, and later was separated by centrifugation. After combining the two precipitation batches, the product was dried under high vacuum for 12 h at room temperature, resulting in a white, hygroscopic solid (5.80 g; 72% total yield and 98% purity), with a melting point at the decomposition temperature.

***N,N*-Dimethylpyrrolidinium Hydrogen Carbonate ([*N,N*-diMePyr][HCO₃]):** White solid, very hygroscopic, 72% yield, m.p. at $T_{5\%dec}$, $T_{5\%dec}$ 158 °C; ¹H NMR (500 MHz, D₂O) δ = 2.23 (t, 4H; CH₂), 3.14 (s, 6H, N-CH₃), 3.51 (t, 4H, N-CH₂); ¹³C NMR (125 MHz, D₂O) δ = 21.65 (CH₂), 51.67 (N-CH₃), 65.82 (N-CH₂), 160.17 (HCO₃); ¹H NMR (500 MHz, [D₆] DMSO) δ = 2.08 (t, 4H; CH₂), 3.05 (s, 6H, N-CH₃), 3.42 (t, 4H, N-CH₂); ¹³C NMR (125 MHz, [D₆] DMSO) δ = 21.76 (CH₂), 51.50 (N-CH₃), 65.33 (N-CH₂), 158.93 (HCO₃). Single crystal X-ray diffraction analysis: colorless plates; C₇H₁₅NO₃; MW 161.20; Monoclinic; *P*2₁/*n*; *a* = 6.6199(6) Å; *b* = 13.9451(12) Å; *c* = 9.2587(8) Å; β = 101.760(2)°; *V* = 836.8(1) Å³; *Z* = 4; *D*_{calc} = 1.280 g cm⁻³; *R*₁, *wR*₂ [*I* > 2 σ (*I*)] = 0.0356, 0.0890; *R*₁, *wR*₂ (all data) = 0.0445, 0.0937.

Preparation of ILs from hydrogen carbonate IL precursors. In order to show the possible synthetic applications of [HCO₃]⁻-based salts as IL precursors, the newly formed [1,2,3-triMeIM][HCO₃] and [*N,N*-diMePyr][HCO₃] salts were reacted with a group of organic and inorganic acids (HCl, HNO₃, picric acid), and ammonium perchlorate ([NH₄][ClO₄]; considered here as a very weak acid (p*K*_a=9.2)).⁸⁰ In all cases but one, [NH₄][ClO₄], the p*K*_a values of the acids were lower than that of H₂CO₃ (p*K*_{a1}=6.35),⁸¹ thus complete conversion was expected with the formation of H₂CO₃ as byproduct. H₂CO₃, due to its low stability, was expected to readily decompose to H₂O and gaseous CO₂, thus shifting the reaction equilibrium towards product formation, and after solvent evaporation, to result in byproduct free salts.

In the case of the reaction of [HCO₃]⁻-based IL precursors with [NH₄][ClO₄], a different reaction pathway was expected. Instead of relying on a lower p*K*_a of the acidic reagent in comparison to H₂CO₃, the kinetic equilibrium between [NH₄]⁺ + [HCO₃]⁻ and NH₃ + H₂CO₃ was expected to produce volatile products which could be removed from the system shifting the reaction toward products (Figure 11, where [X]⁻ = [ClO₄]⁻). All eight product salts were confirmed using ¹H and ¹³C NMR. In all cases, no remaining signal for [HCO₃]⁻ was recorded in the ¹³C NMR confirming the anticipated quantitative conversion of [HCO₃]⁻ IL precursors into new salt products.

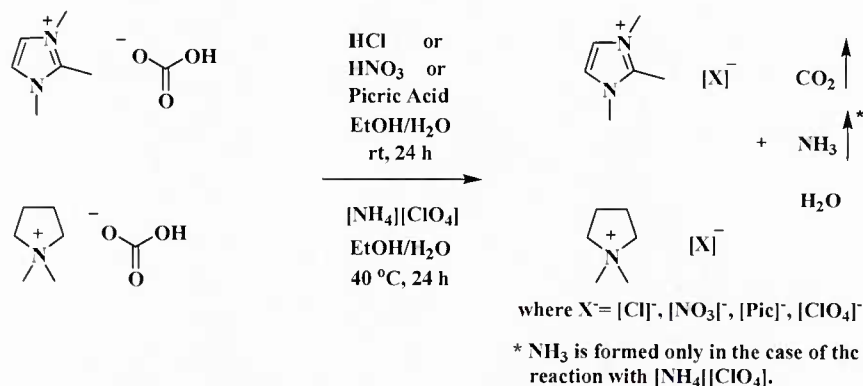


Figure A2.2. Reactions of [1,2,3-triMeIM][HCO₃] and [N,N-diMePyr][HCO₃] with hydrochloric, nitric, and picric acids, as well as ammonium perchlorate.

General Procedure for the Preparation of 1,2,3-Trimethylimidazolium and N,N-Dimethylpyrrolidinium Chloride [Cl], Nitrate [NO₃], Picrate [Pic], and Perchlorate [ClO₄] Salts. All reactions were performed using the same procedure: 0.01 mol of the appropriate acid (HPF₆, HCl, H₂SO₄, picric acid) or salt ([NH₄][ClO₄]) was dissolved in 10 mL of H₂O (ethanol in the case of picric acid) and added dropwise, at room temperature (40 °C in case of [NH₄][ClO₄]), to a stirred solution of 0.01 mol of [1,2,3-triMeIM][HCO₃] or [N,N-diMePyr][HCO₃] in 50% aqueous ethanol (v/v, 20 mL). The mixture was stirred for an additional 24 h in a closed flask (to avoid inorganic acid evaporation) and the solvent and gaseous byproducts were evaporated on a rotary evaporator under vacuum. All samples were then dried under high vacuum at room temperature. All salts obtained were checked for the presence of starting material using ¹H and ¹³C NMR, and none of the spectra revealed any residual peaks for the [HCO₃]⁻ anion.

1,2,3-Trimethylimidazolium Chloride ([1,2,3-triMeIM][Cl]): White solid, very hygroscopic, 99% yield, m.p. 71 °C, $T_{5\%dec} = 205$ °C; ¹H NMR (500 MHz, [D₄] MeOH) $\delta = 2.62$ (s, 3H, C2-CH₃), 3.83 (s, 6H, N-CH₃), 7.46 (s, 2H, C4/C5-H); ¹³C NMR (125 MHz [D₄] MeOH) $\delta = 10.38$ (C2-CH₃), 35.57 (N-CH₃), 123.26 (C4/C5), 146.45 (C2).

1,2,3-Trimethylimidazolium Nitrate ([1,2,3-triMeIM][NO₃): White crystalline solid, 98% yield, m.p. 63 °C, $T_{5\%dec} = 259$ °C; ¹H NMR (500 MHz, [D₄] MeOH) $\delta = 2.60$ (s, 3H, C2-CH₃), 3.84 (s, 6H, N-CH₃), 7.43 (s, 2H, C4/C5-H); ¹³C NMR (125 MHz [D₄] MeOH) $\delta = 10.01$ (C2-CH₃), 35.34 (N-CH₃), 123.26 (C4/C5), 146.40 (C2).

1,2,3-Trimethylimidazolium Picrate ([1,2,3-triMeIM][Pic]): Yellow crystalline solid, 98% yield, m.p. 104 °C, $T_{5\%dec} = 224$ °C; ¹H NMR (500 MHz, [D₄] MeOH) $\delta = 2.56$ (s, 3H, C2-CH₃), 3.76 (s, 6H, N-CH₃), 7.58 (s, 2H, C4/C5-H), 8.59 (s, 2H, picrate); ¹³C NMR (125 MHz [D₄] MeOH) $\delta = 9.48$ (C2-CH₃), 34.54 (N-CH₃), 121.82 (C4/C5), 124.03 (picrate), 125.07 (picrate), 141.73 (picrate), 144.59 (C2), 160.68 (picrate).

1,2,3-Trimethylimidazolium Perchlorate ([1,2,3-triMeIM][ClO₄): White crystalline solid, 98% yield, m.p. at $T_{5\%dec}$ (hot stage apparatus) ~ 220 °C, $T_{5\%dec} = 220$ °C; ¹H NMR (500 MHz, [D₄] MeOH) $\delta = 2.57$ (s, 3H, C2-CH₃), 3.77 (s, 6H, N-CH₃), 7.50 (s, 2H, C4/C5-H); ¹³C NMR (125 MHz [D₄] MeOH) $\delta = 10.00$ (C2-CH₃), 35.81 (N-CH₃), 123.36 (C4/C5), 146.35 (C2).

N,N-Dimethylpyrrolidinium Chloride ([N,N-diMePyr][Cl]): White solid, very hygroscopic, 99% yield, m.p. at $T_{5\%dec}$ (hot stage apparatus) ~ 260 °C, $T_{5\%dec} = 231$ °C; ¹H NMR

(500 MHz, [D₄] MeOH) δ = 2.26 (t, 4H, -CH₂-), 3.20 (s, 6H, N-CH₃), 3.58 (t, 4H, N-CH₂); ¹³C NMR (125 MHz [D₄] MeOH) δ = 22.99 (-CH₂-) 52.55 (t, N-CH₃), 66.95 (t, N-CH₂).

***N,N*-Dimethylpyrrolidinium Nitrate ([*N,N*-diMePyr][NO₃]):** White solid, 98% yield, m.p. at T_{5%dec} (hot stage apparatus) ~220 °C, T_{5%dec} = 276 °C; ¹H NMR (500 MHz, [D₄] MeOH) δ = 2.26 (t, 4H, -CH₂-), 3.18 (s, 6H, N-CH₃), 3.55 (t, 4H, N-CH₂); ¹³C NMR (125 MHz [D₄] MeOH) δ = 22.97 (-CH₂-) 52.45 (t, N-CH₃), 66.93 (t, N-CH₂).

***N,N*-Dimethylpyrrolidinium Picrate ([*N,N*-diMePyr][Pic]):** Yellow crystalline solid, 98% yield, m.p. at T_{5%dec} (hot stage apparatus) ~280 °C, T_{5%dec} = 269 °C; ¹H NMR (500 MHz, [D₄] MeOH) δ = 2.28 (t, 4H, -CH₂-), 3.19 (s, 6H, N-CH₃), 3.56 (t, 4H, N-CH₂), 8.87 (s, 2H, picrate); ¹³C NMR (125 MHz [D₄] MeOH) δ = 22.79 (-CH₂-) 52.69 (N-CH₃), 66.96 (N-CH₂), 127.54 (picrate), 128.52 (picrate), 142.76 (picrate), 163.52 (picrate).

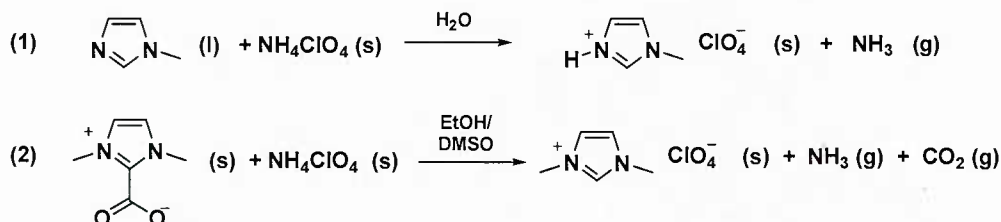
***N,N*-Dimethylpyrrolidinium Perchlorate ([*N,N*-diMePyr][ClO₄]):** White solid, 97% yield, m.p. at T_{5%dec} (hot stage apparatus) ~280 °C, T_{5%dec} = 254 °C; ¹H NMR (500 MHz, [D₄] MeOH) δ = 2.26 (t, 4H, -CH₂-), 3.17 (s, 6H, N-CH₃), 3.55 (t, 4H, N-CH₂); ¹³C NMR (125 MHz [D₄] MeOH) δ = 22.97 (-CH₂-) 52.50 (N-CH₃), 66.97 (N-CH₂).

Appendix A3

Ionic Liquid-Based Routes to Conversion or Reuse of Recycled Ammonium Perchlorate

Using three different routes (Figure A3.1) and AP as the perchlorate source, we have prepared 1-methylimidazolium perchlorate, ([Hmim][ClO₄], **1**), 1,3-dimethylimidazolium perchlorate, ([C₁mim][ClO₄], **2**), 1-butyl-3-methylimidazolium perchlorate, ([C₄mim][ClO₄], **3**), and trihexyl(tetradecyl)phosphonium perchlorate, ([P₆₆₆₁₄][ClO₄], **4**). All four of these salts were formed in high yield, requiring little purification; **3** and **4** are ILs by definition, while **1** and **2** melt at temperatures above 100 °C.

Acid-base reaction:



Anion metathesis:

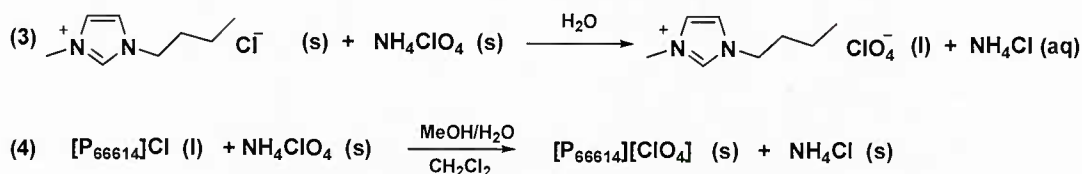


Figure A3.1. Synthetic routes to perchlorate ILs.

The first, and simplest method involves the reaction of a neutral amine (1-methylimidazole) with AP in aqueous solution, resulting in the formation of **1** and ammonia gas which due to its volatility and thus easy removal, allows a shift in the reaction equilibrium to completion. Ultimately, the ammonia generated by this process could be recovered and reused, making this reaction very atom efficient. The reaction was conducted in water followed by evaporation to yield a colorless crystalline hygroscopic solid. Protonation of the imidazole ring was shown to be quantitative both by the presence of the NH peak, and the shift in position of all the 1-methylimidazole peaks in the ¹H NMR spectrum. The IR spectrum showed one peak in the [ClO₄][−] stretching region, a strong and broad peak at 1044 cm^{−1}, with a shoulder at 1005 cm^{−1}, consistent with the symmetry of the [ClO₄][−] anion being slightly altered,⁸³ probably by hydrogen-bonding. An additional peak was observed at 3081 cm^{−1} indicative of the protonation of the imidazole ring.⁸²

The second method involves utilization of a previously reported protocol for the formation of a permanent cation, *i.e.* the preparation of imidazolium based salts via the decarboxylation reaction of 1,3-dimethylimidazolium-2-carboxylate.⁴⁶ When reacted with AP, this compound is transformed to [C₁mim][ClO₄], **2**, and easily removable gaseous by-products ammonia and CO₂. The Krapcho decarboxylation of 1,3-dimethylimidazolium-2-carboxylate was carried out in a mixture of EtOH and DMSO. Evaporation of the solvents gave **2** as a colorless, crystalline, extremely hygroscopic solid, in quantitative yield. The decarboxylation of the zwitterion was

confirmed by both the ^1H and ^{13}C NMR spectra; the ^1H NMR showing a resonance for the C2 proton, and the ^{13}C NMR showing neither R-COO^- nor $[\text{HCO}_3]^-/[\text{CO}_3]^{2-}$ species. Production of pure **2** was confirmed by single crystal X-ray diffraction (Figure A3.2).

The compounds **3** and **4** were prepared by metathesis of NH_4ClO_4 with $[\text{C}_4\text{mim}]\text{Cl}$ in water or with $[\text{P}_{66614}]\text{Cl}$ in methanol, respectively. The IL products phase separated from the corresponding solution to give **3** as a pale yellow viscous liquid and **4** as a clear liquid that transformed into a white solid at around $20\text{ }^\circ\text{C}$. AgCl precipitation tests were negative indicating the absence of Cl^- in each product to the limit of detection. The lack of an absorption band for water in the IR spectra after drying and the measured water contents of 0.17% w/w (**3**) and 0.12% w/w (**4**) indicated the materials to be quite hydrophobic. The IR spectra showed a strong and broad peak in the $[\text{ClO}_4]^-$ stretching region (1068 cm^{-1} , **3**; 1081 cm^{-1} , **4**) for each compound consistent with the symmetry of the $[\text{ClO}_4]^-$ anion being unbroken.⁸³

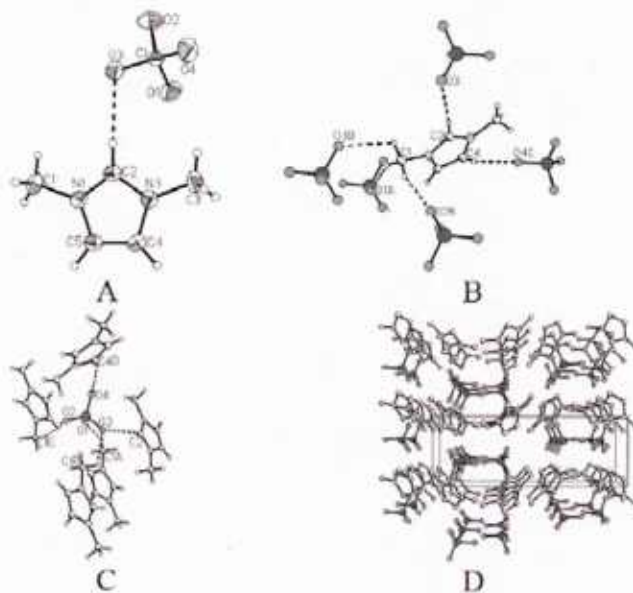


Figure A3.2. The crystal structure of $[\text{C}_1\text{mim}][\text{ClO}_4]$ (**2**) showing (A) the asymmetric unit with the dominating interaction of the most acidic proton in the cation (C2-H) with the perchlorate anion indicated; the interactions (distances less than the sum of the van der Waals' radii minus 0.1 \AA) to the (B) cation and (C) anion; and (D) the packing down the crystallographic c axis showing the distinct cationic and anionic layers (hydrogen atoms were omitted).

Synthesis of $[\text{Hmim}][\text{ClO}_4]$ (1**).** 0.50 g (4.3 mmol) of NH_4ClO_4 was dissolved in 3 mL DI water. 0.44 mL (0.35 g, 4.3 mmol) N-methylimidazole was dissolved in 1 mL DI water, the solutions were mixed and stirred overnight. The water was evaporated under a N_2 gas stream to give an off-white solid. A further portion of DI water was added and the evaporation repeated. The solid material was dried under high vacuum at room temperature to give 0.76 g of the desired product as a white hygroscopic solid in quantitative yield. Melting point (DSC): $148\text{ }^\circ\text{C}$, onset for 5 % decomposition $T_{5\%dec} = 241\text{ }^\circ\text{C}$, second decomposition $T_{dec} = 495\text{ }^\circ\text{C}$; ^1H NMR (500 MHz, $[\text{D}_6]\text{DMSO}$, $25\text{ }^\circ\text{C}$, TMS): $\delta=8.51$ (1H, s, NCHN), 7.48 (1H, s, NCHCHN), 7.38 (1H, s, NCHCHN), 7.07 ppm (1H, br s, NH), 3.78 (3H, s, NCH_3); ^{13}C NMR (125 MHz, $[\text{D}_6]\text{DMSO}$, $25\text{ }^\circ\text{C}$, TMS): $\delta=136.48$ (NCHN), 122.72 (NCHCHN), 122.18 (NCHCHN), 34.45 ppm (CH_3);

selected IR (neat sample) cm^{-1} : 3154, 3116, 3081, 3022, 2976, 2880, 1587, 1550, 1439, 1308, 1280, 1044 ($[\text{ClO}_4]^-$), 1005 ($[\text{ClO}_4]^-$), 931, 914, 856, 747. MS: m/z (%): 83.06 (100) $[\text{Hmim}^+]$, 265.06 (90) $[\text{Hmim}_2\text{ClO}_4^+]$, 82.9 (35) $[\text{ClO}_3^-]$, 98.9 (100) $[\text{ClO}_4^-]$.

Synthesis of $[\text{C}_1\text{mim}][\text{ClO}_4]$ (2). 1,3-dimethylimidazolium-2-carboxylate was prepared according to the literature method.⁸⁴ 0.50 g (4.3 mmol) of NH_4ClO_4 was dissolved in 2.5 mL DMSO/EtOH (3:1 v/v) and added to a warmed solution of 0.60 g (4.3 mmol) 1,3-dimethylimidazolium-2-carboxylate dissolved in 2 mL EtOH. The mixture was heated to 70 °C and then stirred for 3 days. The solvent was removed under high vacuum to leave the desired product as a white and extremely hygroscopic solid in quantitative yield. X-ray quality crystals were grown by the diffusion of ether vapor into a solution of **2** in dry EtOH. The melting point was not determined. Due to the discovered instability of the investigated compound (the TGA experiment resulted in an energetic decomposition), the DSC experiment was not conducted above 150 °C, to which temperature no thermal transition was recorded. Onset temperature for 5% decomposition $T_{5\%dec} = 244$ °C (followed by explosive decomposition); ^1H NMR (500 MHz, $[\text{D}_6]\text{DMSO}$, 25 °C, TMS): $\delta=8.99$ (1H, s, NCHN), 7.65 (2H, s, NCHCHN), 3.84 ppm (6H, s, NCH₃); ^{13}C NMR (125 MHz, $[\text{D}_6]\text{DMSO}$, 25 °C, TMS): $\delta=136.93$ (NCHN), 123.34 (NCHCHN), 35.58 ppm (CH₃).

Synthesis of $[\text{C}_4\text{mim}][\text{ClO}_4]$ (3). 0.50 g (4.3 mmol) of NH_4ClO_4 was dissolved in 3 mL DI water. 0.74 g (4.3 mmol) $[\text{C}_4\text{mim}]\text{Cl}$ (BASF, Ludwigshafen, Germany) was dissolved in 1 mL DI water and added with initial mixing. The mixture was left to stand for 2 h. The water was evaporated under a N_2 gas stream to give a mixture of solid and liquid residue. The liquid was separated from the solid by extraction with CH_2Cl_2 , and the solvent removed *in vacuo*. The resulting viscous liquid was taken up in CH_2Cl_2 and extracted with DI water until the washing water did not form a precipitate when tested with a solution of AgNO_3 . The CH_2Cl_2 was removed *in vacuo* and the resulting pale yellow viscous liquid dried under high vacuum at room temperature to give 0.91 g (89 % yield) of the desired product. No melting point was detected in the compound's DSC trace, but a glass transition was observed at $T_g = -77$ °C; onset for 5 % decomposition $T_{5\%dec} = 282$ °C; ^1H NMR (500 MHz, $[\text{D}_6]\text{DMSO}$, 25 °C, TMS): $\delta=9.10$ (1H, s, NCHN), 7.77 (1H, s, NCHCHN), 7.70 (1H, s, NCHCHN), 4.16 (2H, t, $^3J(\text{H,H})=7.0$ Hz, NCH₂), 3.85 (3H, s, NCH₃), 1.77 (2H, m, NCH₂CH₂), 1.27 (2H, m, CH₂CH₃), 0.91 ppm (3H, t, $^3J(\text{H,H})=7.5$ Hz, CH₂CH₃); ^{13}C NMR (125 MHz, $[\text{D}_6]\text{DMSO}$, 25 °C, TMS): $\delta=136.45$ (NCHN), 123.57 (NCHCHN), 122.22 (NCHCHN), 48.47 (NCH₂), 35.71 (NCH₃), 31.29 (CH₂CH₂CH₂), 18.72 (CH₂CH₃), 13.21 ppm (CH₃); selected IR (neat sample) cm^{-1} : 3156, 3116, 2962, 2933, 2874, 1572, 1464, 1168, 1068 ($[\text{ClO}_4]^-$), 842, 751. MS: m/z (%): 83.07 (25) $[\text{Hmim}^+]$, 139.1 (100) $[\text{C}_4\text{mim}^+]$, 239.2 (30) [mol. peak + H^+], 82.9 (5) $[\text{ClO}_3^-]$, 97.0 (15) $[\text{dimim}^-]$, 98.9 (100) $[\text{ClO}_4^-]$. The compound appears to be slightly hygroscopic, as the elemental analysis suggests that a substoichiometric hydrate formed after several days with contact to the atmosphere. elemental analysis calcd (%) for $\text{C}_8\text{H}_{15}\text{N}_2\text{ClO}_4 \cdot 0.25 \text{H}_2\text{O}$ (243.2): C 39.52, H 6.42, N 11.52; found: C 39.41, H 6.23, N 11.32.

Synthesis of $[\text{P}_{66614}][\text{ClO}_4]$ (4). A mixture of 4.07 g (7.8 mmol) of $[\text{P}_{66614}]\text{Cl}$ (Cytec, Niagara Falls, Canada) and 0.922 g (7.8 mmol) of NH_4ClO_4 in 10 mL MeOH containing a few drops of water was stirred at room temperature. A phase separation was observed after 15 min (precipitation of NH_4Cl), but the stirring was continued overnight to ensure the completion of the reaction. The product was extracted using CH_2Cl_2 . The organic phase was washed until chloride free, and the solvent was removed *in vacuo*. The product was dried under high vacuum at 35 °C overnight to give a colorless liquid in 91% yield that slowly crystallized. Melting point (DSC):

24.7 °C, single decomposition $T_{5\%dec} = 254.5$ °C; ^1H NMR (500 MHz, $[\text{D}_6]\text{DMSO}$, 25 °C): $\delta=2.17$ (8H, m, PCH_2), 1.34 (48H, m, CH_2), 0.88 ppm (12H, m, CH_3); ^{13}C NMR (125 MHz, $[\text{D}_6]\text{DMSO}$, 25 °C): $\delta=31.27$ (CH_2), 30.36 (CH_2), 30.02 (CH_2), 29.81 (CH_2), 29.61 (CH_2), 29.01 (CH_2), 28.93 (CH_2), 28.68 (CH_2), 28.61 (CH_2), 28.05 (CH_2), 22.06 (CH_2), 21.77 (CH_2), 20.48 (d, CH_2), 17.46 (d, CH_2), 13.89 (CH_3), 13.80 ppm (CH_3); ^{31}P NMR (202 MHz, $[\text{D}_6]\text{DMSO}$, 25 °C): $\delta=34.96$ ppm; ^{35}Cl NMR (49 MHz, D_2O , 25 °C, NaCl): $\delta=1010.80$ ppm; selected IR (neat sample) cm^{-1} : 2955, 2923, 2854, 1465, 1412, 1378, 1215, 1081 ($[\text{ClO}_4]^-$), 812, 720. MS: m/z (%): 483.5 (100) $[\text{P}_{66614}^+]$, 82.9 (5) $[\text{ClO}_3^-]$, 98.9 (100) $[\text{ClO}_4^-]$, 202.9 (95) $[\text{P}_{66}\text{H}]$; elemental analysis calcd (%) for $\text{PC}_{32}\text{H}_{68}\text{ClO}_4$ (583.3): C 65.89, H 11.75; found: C 66.32, H 11.88.

Appendix A4

Azolium azolates from reactions of neutral azoles with 1,3-diemthylimidazolium-2-carboxylate, 1,2,3-trimethylimidazolium hydrogen carbonate, and *N,N*-dimethylpyrrolidinium hydrogen carbonate

Utilizing the concepts developed previously, 18 new azolate-based salts were synthesized via halide free, fast, and clean decarboxylation of the IL cation precursors [1,3-diMeIM-2-COO], [1,2,3-triMeIM][HCO₃], and [N,N-diMePyr][HCO₃] with neutral azoles acting as weak acids in these systems. All salts presented were synthesized in one step, simply by preparing standard solutions of all reagents in an EtOH/H₂O solvent system, and then mixing reactants in a 1:1 molar ratio (Figure 2). Most of the reaction mixtures (with 4,5-diNO₂-IM, 4-NO₂-1,2,3-tri, and 5-NH₂-tetr), evolved gas from the vial at the point of adding the reagents, confirming that the decarboxylation reaction was taking place in these systems. In reactions involving [1,3-diMeIM-2-COO] a spike of DMSO was added to the system to enhance the decarboxylation process. All reactions were kept in open vials for an additional 48 h with constant stirring at 40 °C. After that time, the solvent was evaporated using rotary evaporator at 90 °C, allowing for the recovery of the product.

Successful conversion of the IL precursors to the desired products was monitored using ¹³C NMR via simple analysis of the spectral region where presence of the [HCO₃]⁻ or carboxylate group of the zwitterion from the substrate would be expected in case of incomplete conversion. The absence of the relevant signal also served to indicate the completion of the reaction. None of the analyzed salts showed the presence of the carboxylate signal at ~160 ppm, indicating no residual substrate. In evaluating the ¹³C NMR results, it was concluded that all 18 new salts were formed approaching quantitative yield.

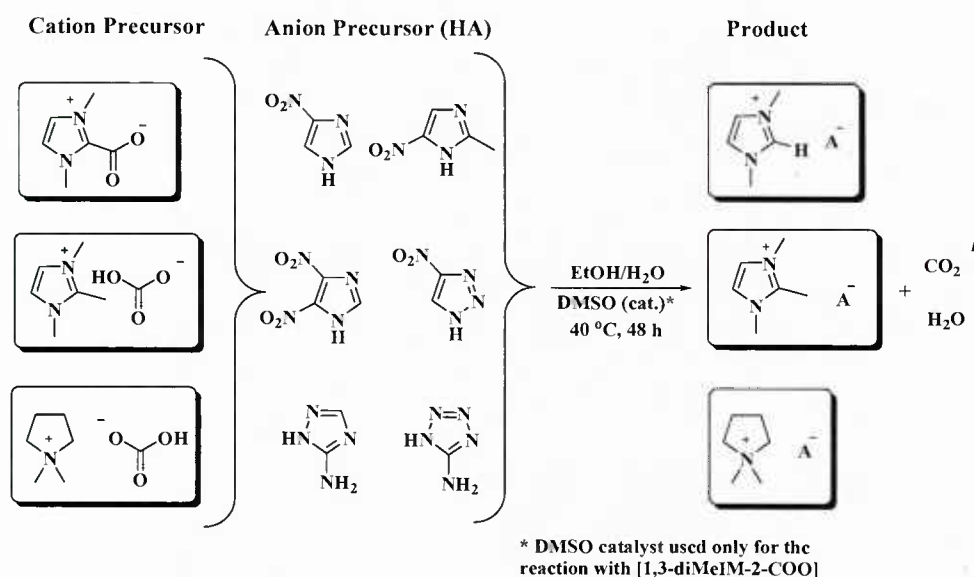


Figure A4.1. Reaction of [1,3-diMeIM-2-COO], [1,2,3-triMeIM][HCO₃], and [N,N-diMePyr][HCO₃] with neutral azole acids.

General Protocol for the Preparation of Azolate Base Salts. The IL precursors were prepared according to the literature protocol. The precursors were prepared in 2-3 gram scale and used as obtained. 5 mmol of the appropriate IL precursor ([1,3-diMeIM-2-COO], [1,2,3-triMeIM][HCO₃] \cdot H₂O, and [N,N-diMePyr][HCO₃]) was placed into a 10 mL volumetric flask and dissolved in 50 % aqueous ethanol (v/v). Similarly, 2.5 mmol of the appropriate neutral azole (4-NO₂-IM, 2-Me-5-NO₂-IM, 4,5-diNO₂-IM, 4-NO₂-1,2,3-tri, 3-NH₂-1,2,4-tri, and 5-NH₂-tetr) was placed into a 5 mL volumetric flask and dissolved in 50 % aqueous ethanol (v/v). Next, 1 mL of each prepared solution of IL precursor (0.5 mmol) was placed in the reaction vial and 1 mL of the solution of neutral azole (0.5 mmol) was added dropwise. Upon mixing of the reagents, in reactions involving 4,5-diNO₂-IM, 4-NO₂-1,2,3-tri, and 5-NH₂-tetr, evolution of the gas from the solution was observed. In the reactions involving [1,3-diMeIM-2-COO], 0.1 mL of DMSO was added to each reaction to facilitate the decarboxylation process.

The reaction mixture was kept under moderate heating (40 °C) for 48 h. After 48 h, the solvent was removed on the rotary evaporator under vacuum at 90 °C. The successful reactions were identified by disappearance of carboxylate (in the case of the zwitterion) or carbonate (in the case of the [HCO₃]⁻) signature in the ¹³C NMR spectra. In none of the analyzed salts, after completion of the reaction, was the characteristic carbonate or carboxylate peak observed. Only in the case of salts with [3-NH₂-1,2,4-tri]⁺ and [5-NH₂-tetr]⁺, another peak at ~160 ppm appeared on the ¹³C NMR spectra resulting from the carbon atom in the anion directly bound to the amine group.

1,3-Dimethylimidazolium 4-Nitroimidazolate ([1,3-diMeIM][4-NO₂-IM]): Yellow, crystalline solid, hygroscopic, mp 78 °C, T_{5%dec} 182 °C; ¹H NMR (360 MHz, [D₆] DMSO) δ = 3.79 (s, 6H, N-CH₃), 7.11 (s, 1H, C5'-H), 7.60 (s, 2H, C4/C5-H), 9.02 (s, 1H, C2-H); ¹³C NMR (90 MHz, [D₆] DMSO) δ = 35.69 (N-CH₃), 123.47 (C4/C5), 131.07 (C5'), 137.15 (C2'), 145.66 (C4'), 148.11 (C2).

1,3-Dimethylimidazolium 2-Methyl-5-nitroimidazolate ([1,3-diMeIM][2-Me-5-NO₂-IM]): Yellow, crystalline solid, hygroscopic, mp 112 °C, T_{5%dec} 178 °C; ¹H NMR (360 MHz, [D₆] DMSO) δ = 2.10 (s, 3H, C2'-CH₃), 3.79 (s, 6H, N-CH₃), 7.64 (s, 1H, C4'-H), 7.64 (s, 2H, C4/C5-H), 9.09 (s, 1H, C2-H); ¹³C NMR (90 MHz [D₆] DMSO) δ = 17.31 (C2'-CH₃), 35.59 (N-CH₃), 123.40 (C4/C5), 132.69 (C4'), 137.13 (C2'), 147.36 (C2), 154.12 (C5').

1,3-Dimethylimidazolium 4,5-Dinitroimidazolate ([1,3-diMeIM][4,5-diNO₂-IM]): Yellow, crystalline solid, mp 96 °C, T_{5%dec} 215 °C; ¹H NMR (360 MHz, [D₆] DMSO) δ = 3.84 (s, 6H, N-CH₃), 6.94 (C2'-H), 7.67 (s, 2H, C4/C5-H), 9.02 (s, 1H, C2-H); ¹³C NMR (90 MHz [D₆] DMSO) δ = 35.55 (N-CH₃), 123.33 (C4/C5), 136.92 (C2), 139.25 (C2'), 140.16 (C4'/5').

1,3-Dimethylimidazolium 4-Nitro-1,2,3-triazolate ([1,3-diMeIM][4-NO₂-tri]): Yellow, crystalline solid, mp 74 °C, T_{5%dec} 187 °C; ¹H NMR (360 MHz, [D₆] DMSO) δ = 3.86 (s, 6H, N-CH₃), 7.69 (d, 2H, C4/C5-H), 8.04 (s, 1H, C4'-H), 9.08 (s, 1H, C2-H); ¹³C NMR (90 MHz [D₆] DMSO) δ = 35.57 (N-CH₃), 123.34 (C4/C5), 129.39 (C5'), 136.99 (C2), 154.1 (C4').

1,3-Dimethylimidazolium 3-Amino-1,2,4-triazolate ([1,3-diMeIM][3-HN₂-1,2,4-tri]): Yellow, viscous liquid, no mp observed, T_{5%dec} 190 °C; ¹H NMR (360 MHz, [D₆] DMSO) δ = 3.75 (s, 6H, N-CH₃), 5.25 (b, C3'-NH₂), 7.29 (s, 2H, C4/5), 7.64 (s, 1H, C5'-H), 9.21 (s, 1H, C2-H); ¹³C NMR (90 MHz [D₆] DMSO) δ = 35.59 (N-CH₃), 123.40 (C4/C5), 137.40 (C2), 147.80 (C5'), 159.74 (C3').

1,3-Dimethylimidazolium 5-Aminotetrazolate ([1,3-diMeIM][5-NH₂-tetr]): White solid, hygroscopic, mp 84 °C, T_{5%dec} 206 °C; ¹H NMR (360 MHz, [D₆] DMSO) δ = 3.77 (s, 6H,

N-CH₃), 4.08 (b, C5'-NH₂), 7.58 (s, 2H, C4/C5-H), 8.87 (s, 1H, C2-H); ¹³C NMR (90 MHz [D₆] DMSO) δ = 36.11 (N-CH₃), 123.83 (C4/C5), 137.38 (C2), 164.53 (C5').

1,2,3-Trimethylimidazolium 4-Nitroimidazolate ([1,2,3-triMeIM][4-NO₂-IM]): Yellow viscous liquid, no mp observed, T_{5%dec} 171 °C; ¹H NMR (500 MHz, [D₄] MeOH) δ = 2.60 (s, 3H, C2-CH₃), 3.82 (s, 6H, N-CH₃), 7.31 (s, 1H, C4'-H), 7.44 (s, 2H, C4/C5-H), 7.81 (s, 1H, C2'); ¹³C NMR (125 MHz [D₄] MeOH) δ = 9.43 (C2-CH₃), 35.52 (N-CH₃), 123.44 (C4/C5), 126.30 (C5'), 129.64 (C2), 145.07 (C2'), 148.46 (C4').

1,2,3-Trimethylimidazolium 2-Methyl-5-nitroimidazolate ([1,2,3-triMeIM][2-Me-5-NO₂-IM]): Yellow, crystalline solid, mp 126 °C, T_{5%dec} 182 °C; ¹H NMR (500 MHz, [D₄] MeOH) δ = 2.41 (s, 3H, C2'-CH₃), 2.60 (s, 3H, C2-CH₃), 3.80 (s, 6H, N-CH₃), 7.37 (s, 2H, C4/C5-H), 8.00 (s, 1H, C4'); ¹³C NMR (125 MHz [D₄] MeOH) δ = 9.51 (C2-CH₃), 14.17 (C2'-CH₃), 35.56 (N-CH₃), 121.47 (C4'), 123.08 (C4/C5), 147.52 (C2), 148.46 (C2'), 151.22 (C5').

1,2,3-Trimethylimidazolium 4,5-Dinitroimidazolate ([1,2,3-triMeIM][4,5-diNO₂-IM]): Yellow solid, mp 86 °C, T_{5%dec} 198 °C; ¹H NMR (500 MHz, [D₄] MeOH) δ = 2.59 (s, 3H, C2-CH₃), 3.80 (s, 6H, N-CH₃), 7.15 (s, 1H, C2'-H), 7.43 (s, 2H, C4/C5-H); ¹³C NMR (125 MHz [D₄] MeOH) δ = 9.31 (C2-CH₃), 35.41 (N-CH₃), 123.33 (C4/C5), 139.10 (C2'), 148.95 (C2).

1,2,3-Trimethylimidazolium 4-Nitro-1,2,3-triazolate ([1,2,3-triMeIM][4-NO₂-tri]): Yellow, crystalline solid, mp 107 °C, T_{5%dec} 195 °C; ¹H NMR (500 MHz, [D₄] MeOH) δ = 2.59 (s, 3H, C2-CH₃), 3.80 (s, 6H, N-CH₃), 7.42 (s, 2H, C4/C5-H), 8.33 (s, 1H, C5'-H); ¹³C NMR (125 MHz [D₄] MeOH) δ = 9.35 (C2-CH₃), 35.42 (N-CH₃), 123.37 (C4/C5), 128.47 (C5'), 146.43 (C2), 155.42 (C4').

1,2,3-Trimethylimidazolium 3-Amino-1,2,4-triazolate ([1,2,3-triMeIM][3-HN₂-1,2,4-tri]): Yellow solid, very hygroscopic, no mp observed, T_{5%dec} 179 °C; ¹H NMR (500 MHz, [D₄] MeOH) δ = 2.58 (s, 3H, C2-CH₃), 3.79 (s, 6H, N-CH₃), 7.42 (s, 2H, C4/C5-H), 7.53 (s, 1H, C5'-H); ¹³C NMR (125 MHz [D₄] MeOH) δ = 9.29 (C2-CH₃), 34.30 (N-CH₃), 123.20 (C4/C5), 148.59 (C2), 146.28 (C5'), 160.11 (C3').

1,2,3-Trimethylimidazolium 5-Aminotetrazolate ([1,2,3-triMeIM][5-NH₂-tetr]): White solid, hygroscopic, mp 160 °C, T_{5%dec} 202 °C; ¹H NMR (500 MHz, [D₄] MeOH) δ = 2.55 (s, 3H, C2-CH₃), 3.77 (s, 6H, N-CH₃), 7.39 (s, 2H, C4/C5-H); ¹³C NMR (125 MHz [D₄] MeOH) δ = 9.33 (C2-CH₃), 35.41 (N-CH₃), 123.39 (C4/C5), 146.25 (C2), 163.40 (C5').

N,N-Dimethylpyrrolidinium 4-Nitroimidazolate ([N,N-diMePyr][4-NO₂-IM]): Yellow, viscous liquid, no mp observed, T_{5%dec} 175 °C; ¹H NMR (500 MHz, [D₄] MeOH) δ = 2.23 (t, 4H, -CH₂-), 3.15 (s, 6H, N-CH₃), 3.51 (t, 4H, N-CH₂), 7.32 (s, 1H, C4'-H), 7.82 (s, 1H, C2'-H); ¹³C NMR (125 MHz [D₄] MeOH) δ = 23.09 (-CH₂-), 52.58 (N-CH₃), 69.07 (N-CH₂), 129.16 (C5'), 144.80 (C2'), 149.06 (C4').

N,N-Dimethylpyrrolidinium 2-Methyl-5-nitroimidazolate ([N,N-diMePyr][2-Me-5-NO₂-IM]): Yellow, crystalline solid, mp 128 °C, T_{5%dec} 179 °C; ¹H NMR (500 MHz, [D₄] MeOH) δ = 2.22 (t, 4H, -CH₂-), 2.26 (s, 3H, C2'-CH₃), 3.14 (s, 6H, N-CH₃), 3.51 (t, 4H, N-CH₂), 7.75 (s, 1H, C5'-H); ¹³C NMR (125 MHz [D₄] MeOH) δ = 16.49 (C2'-CH₃), 23.07 (-CH₂-), 52.58 (N-CH₃), 67.05 (N-CH₂), 131.12 (C4'), 148.29 (C2'), 154.82 (C5').

N,N-Dimethylpyrrolidinium 4,5-Dinitroimidazolate ([N,N-diMePyr][4,5-diNO₂-IM]): Yellow, crystalline solid, mp at T_{5%dec} (hot stage apparatus) ~220 °C, T_{5%dec} 221 °C; ¹H NMR (500 MHz, [D₄] MeOH) δ = 2.25 (t, 4H, -CH₂-), 3.17 (s, 6H, N-CH₃), 3.53 (t, 4H, N-CH₂), 7.06 (s, 1H, C2'); ¹³C NMR (125 MHz [D₄] MeOH) δ = 23.00 (-CH₂-), 52.51 (N-CH₃), 67.00 (N-CH₂), 139.85 (C2').

***N,N*-Dimethylpyrrolidinium 4-Nitro-1,2,3-triazolate ([*N,N*-diMePyr][4-NO₂-tri]):**
Yellow, viscous liquid, mp 57 °C, T_{5%dec} 173 °C; ¹H NMR (500 MHz, [D₄] MeOH) δ = 2.24 (t, 4H, -CH₂-), 3.16 (s, 6H, N-CH₃), 3.52 (t, 4H, N-CH₂), 8.23 (s, 1H, C5'-H); ¹³C NMR (125 MHz [D₄] MeOH) δ = 22.99 (-CH₂-), 52.49 (N-CH₃), 66.98 (N-CH₂), 129.12 (C5'), 155.12 (C4').

***N,N*-Dimethylpyrrolidinium 3-Amino-1,2,4-triazolate ([*N,N*-diMePyr][3-HN₂-1,2,4-tri]):**
Yellow, viscous liquid, no mp observed, T_{5%dec} 143 °C; ¹H NMR (500 MHz, [D₄] MeOH) δ = 2.23 (t, 4H, -CH₂-), 3.12 (s, 6H, N-CH₃), 3.49 (t, 4H, N-CH₂), 7.52 (s, 1H, C5'-H); ¹³C NMR (125 MHz [D₄] MeOH) δ = 22.98 (-CH₂-), 52.47 (N-CH₃), 66.93 (N-CH₂), 148.87 (C5'), 159.94 (C3').

***N,N*-Dimethylpyrrolidinium 5-Aminotetrazolate ([*N,N*-diMePyr][5-NH₂-tetr]):** White solid, hygroscopic, mp 138 °C, T_{5%dec} 178 °C; ¹H NMR (500 MHz, [D₄] MeOH) δ = 2.23 (t, 4H, -CH₂-), 3.14 (s, 6H, N-CH₃), 3.51 (t, 4H, N-CH₂); ¹³C NMR (125 MHz [D₄] MeOH) δ = 22.99 (-CH₂-), 52.47 (N-CH₃), 66.96 (N-CH₂), 163.50 (C5').

Appendix A5

Synthesis of *N*-cyanoalkyl-substituted imidazolium halide and nitrate salts with variable *N*-alkyl and *N*-cyanoalkyl chain lengths, and the characterization of their structural and thermal properties as potential energetic ionic liquids

The synthesis of both *N*-cyanoalkyl-functionalized imidazolium halides and their nitrate analogues are depicted in Figure A5.1.

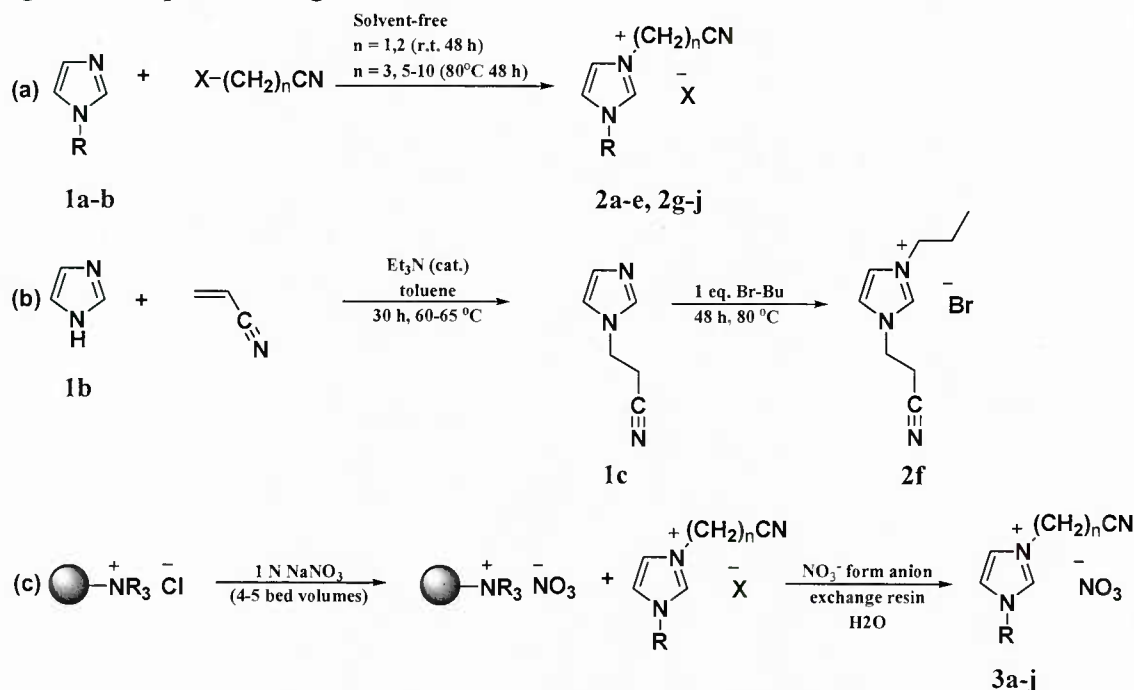


Figure A5.1. Preparation of (a-b) *N*-cyanoalkyl-functionalized imidazolium halides **2a-j** (c) subsequent exchange of halides **2a-j** to obtain nitrate analogues **3a-j**.

The preparation of *N*-cyanoalkyl-functionalized imidazolium halides (precursors) (**2a-j**). A 20 mL Ace GlassTM high pressure vial with Teflon screw cap is charged with 1-methyl- or 1-butylimidazole (15 mmol, **1a** or **1b**, respectively), the appropriate haloalkylnitrile (15 mmol), and stored in a furnace set to 70 °C for 48 h (Figure A5.1a) to obtain halide precursors **2a-e** and **2g-j**. A slightly modified procedure was used in obtaining **2f**, where 1-(2-cyanoethyl)imidazole, **1c**, was first obtained by literature methods followed by alkylation with 1-bromobutane to form the desired 1-butyl-3-(2-cyanoethyl)imidazolium bromide (**2f**). The products were washed several times with ethyl acetate or acetone to extract unreacted starting materials, and residual solvent was removed overnight on high vacuum.

1-cyanomethyl-3-methylimidazolium chloride (2a): $T_{5\%dec} = 214.01$ °C, $T_{onset} = 237.35$ °C, $T_{dec} = 295.35$ °C, $T_g = 23.90$ °C. 1H -NMR ($[D_6]DMSO$): $\delta = 9.55$ (s, 1H), 7.99 (s, 1H), 7.86 (s, 1H), 5.82 (s, 2H), 3.91 (s, 3H) ppm. ^{13}C -NMR ($[D_6]DMSO$): $\delta = 137.7, 124.1, 122.4, 114.7, 36.60, 36.04$ ppm.

1-butyl-3-cyanomethylimidazolium chloride (2b): $T_{5\%dec} = 200.91$ °C, $T_{onset} = 238.32$ °C, $T_{dec} = 258.12$ °C. 1H -NMR ($[D_6]DMSO$): $\delta = 9.70$ (s, 1H), 8.04 (d, 1H), 7.99 (d, 1H), 5.83 (s,

2H), 4.27 (t, 2H), 1.75 (pent, 2H), 1.23 (hex, 2H), 0.88 (t, 3H). ^{13}C -NMR ($[\text{D}_6]\text{DMSO}$): δ = 137.2, 123.0, 122.6, 114.7, 48.79, 36.66, 31.10, 18.61, 13.14 ppm.

1-(1-cyanoethyl)-3-methylimidazolium bromide (2c): $T_{5\% \text{dec}} = 220.09\text{ }^\circ\text{C}$, $T_{\text{onset}} = 270.37\text{ }^\circ\text{C}$, $T_{\text{dec}} = 284.19\text{ }^\circ\text{C}$, $T_{\text{cryst}} = 86.94\text{ }^\circ\text{C}$, $T_{\text{m}} = 138.05\text{ }^\circ\text{C}$. ^1H -NMR ($[\text{D}_6]\text{DMSO}$): δ = 9.53 (s, 1H), 8.12 (s, 1H), 7.79 (s, 1H), 6.17 (q, 1H), 3.90 (s, 3H), 1.90 (d, 3H) ppm. ^{13}C -NMR ($[\text{D}_6]\text{DMSO}$): δ = 137.5, 125.1, 121.4, 117.5, 45.74, 36.70, 19.54 ppm.

1-butyl-3-(1-cyanoethyl)imidazolium bromide (2d): $T_{5\% \text{dec}} = 224.66\text{ }^\circ\text{C}$, $T_{\text{onset}} = 282.03\text{ }^\circ\text{C}$, $T_{\text{dec}} = 293.58\text{ }^\circ\text{C}$, $T_{\text{g}} = -7.64\text{ }^\circ\text{C}$. ^1H -NMR ($[\text{D}_6]\text{DMSO}$): δ = 9.71 (s, 1H), 8.19 (s, 1H), 8.04 (s, 1H), 6.27 (q, 1H), 4.24 (t, 2H), 1.90 (d, 3H), 1.79 (pent, 2H), 1.27 (sext, 2H), 0.88 (t, 3H) ppm. ^{13}C -NMR ($[\text{D}_6]\text{DMSO}$): δ = 136.4, 123.3, 121.0, 117.0, 48.91, 46.22, 31.04, 18.69, 13.22 ppm.

1-(2-cyanoethyl)-3-methylimidazolium bromide (2e): $T_{5\% \text{dec}} = 222.30\text{ }^\circ\text{C}$, $T_{\text{onset}} = 266.19\text{ }^\circ\text{C}$, $T_{\text{dec}} = 281.61\text{ }^\circ\text{C}$, $T_{\text{g}} = -9.65\text{ }^\circ\text{C}$, $T_{\text{m}} = 149.30\text{ }^\circ\text{C}$. ^1H -NMR ($[\text{D}_6]\text{DMSO}$): δ = 9.31 (s, 1H), 7.88 (s, 1H), 7.80 (s, 1H), 4.53 (t, 2H), 3.90 (s, 3H), 3.25 (t, 2H) ppm. ^{13}C -NMR ($[\text{D}_6]\text{DMSO}$): δ = 137.5, 124.4, 122.8, 118.2, 44.91, 36.46, 19.21 ppm.

1-butyl-3-(2-cyanoethyl)imidazolium bromide (2f): $T_{\text{onset}} = 278.74\text{ }^\circ\text{C}$, $T_{\text{dec}} = 287.35\text{ }^\circ\text{C}$, $T_{\text{g}} = -29.90\text{ }^\circ\text{C}$, $T_{\text{m}} = 91.57\text{ }^\circ\text{C}$. ^1H -NMR ($[\text{D}_6]\text{DMSO}$): δ = 9.43 (s, 1H), 7.92 (d, 1H), 7.91 (d, 1H), 4.53 (t, 2H), 4.23 (t, 2H), 3.28 (t, 2H), 1.78 (pent, 2H), 1.24 (hext, 2H), 0.89 (t, 3H) ppm. ^{13}C -NMR ($[\text{D}_6]\text{DMSO}$): δ = 136.4, 122.6, 122.3, 117.5, 48.57, 44.31, 31.10, 18.54, 18.53, 13.08 ppm.

1-(3-cyanopropyl)-3-methylimidazolium chloride (2g): $T_{5\% \text{dec}} = 247.38\text{ }^\circ\text{C}$, $T_{\text{onset}} = 295.74\text{ }^\circ\text{C}$, $T_{\text{dec}} = 314.71\text{ }^\circ\text{C}$, $T_{\text{g}} = -30.55\text{ }^\circ\text{C}$, $T_{\text{cryst}} = 29.38\text{ }^\circ\text{C}$, $T_{\text{m}} = 96.31\text{ }^\circ\text{C}$. ^1H -NMR ($[\text{D}_6]\text{DMSO}$): δ = 9.42 (s, 1H), 7.87 (t, 1H), 7.78 (t, 1H), 4.28 (t, 2H), 3.86 (s, 3H), 2.61 (t, 2H), 2.14 (pent, 2H) ppm. ^{13}C -NMR ($[\text{D}_6]\text{DMSO}$): δ = 136.9, 123.5, 122.2, 119.5, 47.43, 35.62, 25.16, 13.37 ppm.

1-butyl-3-(3-cyanopropyl)imidazolium chloride (2h): $T_{5\% \text{dec}} = 259.84\text{ }^\circ\text{C}$, $T_{\text{onset}} = 306.04\text{ }^\circ\text{C}$, $T_{\text{dec}} = 317.76\text{ }^\circ\text{C}$, $T_{\text{g}} = -31.21\text{ }^\circ\text{C}$. ^1H -NMR ($[\text{D}_6]\text{DMSO}$): δ = 9.44 (s, 1H), 7.87 (s, 1H), 7.85 (s, 1H), 4.28 (t, 2H), 4.17 (t, 2H), 2.61 (t, 2H), 2.15 (pent, 2H), 1.78 (pent, 2H), 1.28 (sext, 2H), 0.90 (t, 3H) ppm. ^{13}C -NMR ($[\text{D}_6]\text{DMSO}$): δ = 136.3, 122.4, 122.3, 119.5, 48.48, 47.60, 31.13, 25.02, 18.66, 13.42, 13.16 ppm.

1-(4-cyanobutyl)-3-methylimidazolium chloride (2i): $T_{5\% \text{dec}} = 239.53\text{ }^\circ\text{C}$, $T_{\text{onset}} = 285.09\text{ }^\circ\text{C}$, $T_{\text{g}} = -22.99\text{ }^\circ\text{C}$. ^1H -NMR ($[\text{D}_6]\text{DMSO}$): δ = 9.39 (s, 1H), 7.84 (s, 1H), 7.77 (s, 1H), 4.25 (t, 2H), 3.86 (s, 3H), 2.58 (t, 2H), 1.89 (tt, 2H), 1.53 (sext, 2H) ppm. ^{13}C -NMR ($[\text{D}_6]\text{DMSO}$): δ = 136.7, 123.5, 122.1, 120.2, 47.67, 35.62, 28.38, 21.39, 15.56 ppm.

1-butyl-3-(4-cyanobutyl)imidazolium chloride (2j): $T_{5\% \text{dec}} = 310.63\text{ }^\circ\text{C}$, $T_{\text{onset}} = 256.58\text{ }^\circ\text{C}$, $T_{\text{g}} = -38.49\text{ }^\circ\text{C}$. ^1H -NMR ($[\text{D}_6]\text{DMSO}$): δ = 9.62 (s, 1H), 7.91 (d, 1H), 7.90 (d, 1H), 4.27 (t, 2H), 4.20 (t, 2H), 2.59 (t, 2H), 1.89 (pent, 2H), 1.78 (pent, 2H), 1.53 (pent, 2H), 1.24 (sext, 2H), 0.89 (t, 3H) ppm. ^{13}C -NMR ($[\text{D}_6]\text{DMSO}$): δ = 136.2, 122.4, 122.3, 120.2, 48.39, 47.70, 31.12, 28.30, 21.42, 18.63, 15.54, 13.11 ppm.

The preparation of N-cyanoalkyl-functionalized imidazolium nitrates (3a-j). From the halide salts obtained (2a-j), each was eluted as an aqueous solution through a column of BioRad® AG 1-X8 strongly basic anion exchange resin that had been previously converted to (NO₃⁻)-form (Figure A5.1c). Completion of the exchange was confirmed by spot testing the eluted fractions with 1 M AgNO₃ to confirm the absence of precursor halide in the aqueous solution of the final products, 3a-j.

1-cyanomethyl-3-methylimidazolium nitrate (3a): $T_{5\%dec} = 189.05\text{ }^{\circ}\text{C}$, $T_{onset} = 212.32\text{ }^{\circ}\text{C}$, $T_{dec} = 225.42\text{ }^{\circ}\text{C}$ (tto 46% wt.), 415.55 $^{\circ}\text{C}$ (to 22% wt.), $T_g = -45.39\text{ }^{\circ}\text{C}$. ¹H-NMR ([D₆]DMSO): $\delta = 9.26$ (s, 1H), 7.89 (t, 1H), 7.79 (t, 1H), 5.59 (s, 2H), 3.89 (s, 3H) ppm. ¹³C-NMR ([D₆]DMSO): $\delta = 137.7, 124.3, 122.4, 114.6, 36.66, 36.02$ ppm.

1-butyl-3-cyanomethylimidazolium nitrate (3b): $T_{5\%dec} = 176.97\text{ }^{\circ}\text{C}$, $T_{onset} = 184.74\text{ }^{\circ}\text{C}$, $T_{dec} = 196.69\text{ }^{\circ}\text{C}$, $T_g = -43.28\text{ }^{\circ}\text{C}$. ¹H-NMR ([D₆]DMSO): $\delta = 9.39$ (s, 1H), 7.93 (t, 1H), 7.91 (t, 1H), 5.61 (s, 2H), 4.22 (t, 2H), 1.77 (pent, 2H), 1.26 (hext, 2H), 0.89 (t, 3H) ppm. ¹³C-NMR ([D₆]DMSO): $\delta = 137.3, 123.1, 122.7, 114.6, 48.92, 36.77, 31.11, 18.66, 13.17$ ppm.

1-(1-cyanoethyl)-3-methylimidazolium nitrate (3c): $T_{5\%dec} = 192.82\text{ }^{\circ}\text{C}$, $T_{onset} = 237.63\text{ }^{\circ}\text{C}$, $T_{dec} = 270.21\text{ }^{\circ}\text{C}$ (to 18% wt.), $T_g = -42.95\text{ }^{\circ}\text{C}$, $T_{cryst} = 12.42$, $T_m = 53.31\text{ }^{\circ}\text{C}$. ¹H-NMR ([D₆]DMSO): $\delta = 9.44$ (s, 1H), 8.09 (s, 1H), 7.85 (s, 1H), 6.05 (q, 1H), 3.89 (s, 3H), 1.89 (d, 3H) ppm. ¹³C-NMR ([D₆]DMSO): $\delta = 137.0, 124.5, 120.8, 116.9, 45.13, 36.00, 18.83$ ppm.

1-butyl-3-(1-cyanoethyl)imidazolium nitrate (3d): $T_{5\%dec} = 189.99\text{ }^{\circ}\text{C}$, $T_{onset} = 234.77\text{ }^{\circ}\text{C}$, $T_{dec} = 260.12\text{ }^{\circ}\text{C}$, $T_g = -50.87\text{ }^{\circ}\text{C}$. ¹H-NMR ([D₆]DMSO): $\delta = 9.49$ (s, 1H), 8.12 (t, 1H), 7.95 (t, 1H), 6.01 (q, 1H), 4.21 (t, 2H), 1.90 (d, 3H), 1.79 (pent, 2H), 1.28 (sext, 2H), 0.90 (t, 3H) ppm. ¹³C-NMR ([D₆]DMSO): $\delta = 136.4, 123.3, 121.0, 116.9, 48.97, 42.24, 31.00, 18.77, 18.66, 13.13$ ppm.

1-(2-cyanoethyl)-3-methylimidazolium nitrate (3e): $T_{5\%dec} = 183.96\text{ }^{\circ}\text{C}$, $T_{onset} = 213.36\text{ }^{\circ}\text{C}$, $T_{dec} = 236.99\text{ }^{\circ}\text{C}$, $T_g = -58.44\text{ }^{\circ}\text{C}$, $T_m = 52.16\text{ }^{\circ}\text{C}$. ¹H-NMR ([D₆]DMSO): $\delta = 9.28$ (s, 1H), 7.82 (t, 1H), 7.76 (t, 1H), 4.51 (t, 2H), 3.89 (s, 3H), 3.21 (t, 2H) ppm. ¹³C-NMR ([D₆]DMSO): $\delta = 137.0, 123.9, 122.2, 117.6, 44.30, 35.78, 18.47$ ppm.

1-butyl-3-(2-cyanoethyl)imidazolium nitrate (3f): $T_{5\%dec} = 191.67\text{ }^{\circ}\text{C}$, $T_{onset} = 221.44\text{ }^{\circ}\text{C}$, $T_g = -30.49\text{ }^{\circ}\text{C}$, $T_m = 91.57\text{ }^{\circ}\text{C}$. ¹H-NMR ([D₆]DMSO): $\delta = 9.34$ (s, 1H), 7.88 (t, 1H), 7.86 (t, 1H), 4.51 (t, 2H), 4.22 (t, 2H), 3.23 (t, 2H), 1.77 (pent, 2H), 1.26 (sext, 2H), 0.88 (t, 3H) ppm. ¹³C-NMR ([D₆]DMSO): $\delta = 136.5, 122.8, 122.4, 117.7, 48.68, 44.42, 31.22, 18.64, 18.53, 13.18$ ppm.

1-(3-cyanopropyl)-3-methylimidazolium nitrate (3g): $T_{5\%dec} = 280.82\text{ }^{\circ}\text{C}$, $T_{onset} = 310.20\text{ }^{\circ}\text{C}$, $T_{dec} = 319.73\text{ }^{\circ}\text{C}$, $T_g = -51.99\text{ }^{\circ}\text{C}$. ¹H-NMR ([D₆]DMSO): $\delta = 9.18$ (s, 1H), 7.80 (t, 1H), 7.73 (t, 1H), 4.24 (t, 2H), 3.84 (s, 3H), 2.58 (t, 2H), 2.13 (pent, 2H) ppm. ¹³C-NMR ([D₆]DMSO): $\delta = 136.8, 123.63, 122.2, 119.5, 47.53, 35.62, 25.12, 13.33$ ppm.

1-butyl-3-(3-cyanopropyl)imidazolium nitrate (3h): $T_{5\%dec} = 273.63\text{ }^{\circ}\text{C}$, $T_{onset} = 313.11\text{ }^{\circ}\text{C}$, $T_{dec} = 322.43\text{ }^{\circ}\text{C}$, $T_g = -59.01\text{ }^{\circ}\text{C}$. ¹H-NMR ([D₆]DMSO): $\delta = 9.28$ (s, 1H), 7.83 (s, 1H), 7.82 (s, 1H), 4.26 (t, 2H), 4.17 (t, 2H), 2.59 (t, 2H), 2.15 (pent, 2H), 1.78 (pent, 2H), 1.26 (sext, 2H), 0.90 (t, 3H) ppm. ¹³C-NMR ([D₆]DMSO): $\delta = 136.3, 122.5, 122.3, 119.5, 48.54, 47.68, 31.14, 25.03, 18.66, 13.34, 13.13$ ppm.

1-(4-cyanobutyl)-3-methylimidazolium nitrate (3i): $T_{5\%dec} = 279.85\text{ }^{\circ}\text{C}$, $T_{onset} = 316.51\text{ }^{\circ}\text{C}$, $T_{dec} = 328.43\text{ }^{\circ}\text{C}$, $T_g = -55.81\text{ }^{\circ}\text{C}$. ¹H-NMR ([D₆]DMSO): $\delta = 9.17$ (s, 1H), 7.78 (t, 1H), 7.72 (t, 1H), 4.21 (t, 2H), 3.85 (s, 3H), 2.54 (t, 2H), 1.87 (dt, 2H), 1.54 (dt, 2H) ppm. ¹³C-NMR ([D₆]DMSO): $\delta = 136.6, 123.6, 122.1, 120.2, 47.81, 35.61, 28.42, 21.45, 15.54$ ppm.

1-butyl-3-(4-cyanobutyl)imidazolium nitrate (3j): $T_{5\%dec} = 276.22\text{ }^{\circ}\text{C}$, $T_{onset} = 316.03\text{ }^{\circ}\text{C}$, $T_{dec} = 328.80\text{ }^{\circ}\text{C}$, $T_g = -58.86\text{ }^{\circ}\text{C}$. $^1\text{H-NMR}$ ($[\text{D}_6]\text{DMSO}$): $\delta = 9.25$ (s, 1H), 7.82 (d, 1H), 7.81 (d, 1H), 4.21 (t, 2H), 4.17 (t, 2H), 2.56 (t, 2H), 1.88 (dt, 2H), 1.79 (dt, 2H), 1.54 (dt, 2H), 1.26 (dt, 2H), 0.90 (t, 3H) ppm. $^{13}\text{C-NMR}$ ($[\text{D}_6]\text{DMSO}$): $\delta = 136.0$, 122.4, 122.3, 120.2, 48.51, 47.90, 31.12, 28.34, 21.48, 18.66, 15.54, 13.11 ppm.

Appendix A6

Synthesis of *N*-cyanoalkyl- and *N,N*-dicyanoalkyl-substituted imidazolium halide and dicyanamide salts with variable *N*-cyanoalkyl chain lengths, and the characterization of their structural and thermal properties as potential energetic ionic liquids

The synthesis of all *N*-cyanoalkyl and *N,N*-dicyanoalkyl-functionalized imidazolium halide salts and their dicyanamide analogues are depicted below in Figure A6.1.

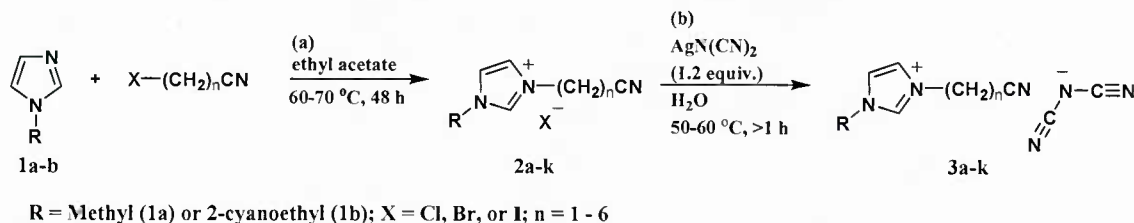


Figure A6.1. Synthesis of (a) *N*-cyanoalkyl and *N,N*-dicyanoalkyl-functionalized imidazolium (a) halides **2a-k** by alkylation of **1a-b** and (b) dicyanamide salts **3a-k** via exchange with prepared AgN(CN)_2 .

The preparation of *N*-cyanoalkyl-functionalized imidazolium halide precursors (2a-e). Typical synthesis of *N*-cyanoalkyl-*N*-alkylimidazolium halide salts (precursors, **2c-f**): A 20 mL Ace GlassTM high pressure vial with Teflon screw cap is charged with 1-methylimidazole (15 mmol, **1a**), the appropriate haloalkylnitrile (15 mmol), and mixed with a stir bar in an oil bath at about 50-60 °C for 48 h (Figure A6.1a). The products **2c-f** were washed several times with ethyl acetate to extract unreacted starting materials, and residual ethyl acetate was removed overnight on high vacuum.

Alternative syntheses for precursors 2a-b: Precursors **2a** and **2b** were synthesized by alternate means, due to the tendency towards thermal decomposition when heated in the case of **2a** and the predominance of β -elimination over *N*-substitution for **2b** under the conditions described above for **2c-f** when using 3-bromopropionitrile as the alkylating agent. To synthesize **2a**, 1-methylimidazole (50 mmol, **1a**) and chloroacetonitrile (50 mmol) were combined in a 100 mL round-bottom flask and stirred together for 48 hours. The product **2a** was removed as a solid precipitate from solution that was subsequently washed with acetonitrile and dried under high vacuum to obtain the final product. For the synthesis of **2b**, a 20 mL Ace GlassTM high pressure vial with a Teflon screw cap with 1-(2-cyanoethyl)imidazole (20 mmol, **1b**) and methyl iodide (40 mmol) in ethyl acetate (20 mL) was mixed with a stir bar at room temperature for 48 hours. The formed yellow-orange solid was washed with diethyl ether prior to drying on high vacuum overnight to isolate the final product.

The preparation of *N,N*-dicyanoalkyl-functionalized imidazolium halide precursors (2f-k). To a 20 mL Ace GlassTM high pressure vial with Teflon screw cap, the appropriate haloalkylnitrile (20 mmol) is combined with previously prepared 1-(2-cyanoethyl)imidazole (20 mmol, **1b**) in ethyl acetate and stirred for 48 hours on an oil bath at 70-80 °C (Figure A6.1a). The products separate as an amber liquid lower phase, where the upper solvent phase is decanted and the product is washed several times with ethyl acetate to remove residual starting material prior to drying on high vacuum for 48 hours.

Alternative synthesis for 2g: To a 50 mL round bottom flask, chloroacetonitrile (22 mmol) is combined with prepared 1-(2-cyanoethyl)imidazole (20 mmol, **1b**) and stirred for 24 hours at room temperature. The resulting mixture is washed several times with acetone to remove residual starting material and then dried on high vacuum for 48 hours to yield an amber liquid product.

The preparation of *N*-cyanoalkyl- and *N,N*-dicyanoalkyl-functionalized imidazolium dicyanamide salts (3a-k). To a tared 100 mL round bottom flask, halide precursor salt **2a-k** (2.8 to 18.7 mmol, depending on precursor availability) is dissolved in 40 mL deionized water (Figure A6.1b). A Teflon stirbar is added, and then previously prepared silver dicyanamide (1.2 equivalents) is added and the suspension is stirred in darkness for more than 1 hour at 40-50 °C. The resulting yellowish/white solids are filtered and washed several times with water. The aqueous filtrate is reduced in volume by evaporation in an air stream prior to final drying on high vacuum for 48 hours at 60 °C to obtain the final dicyanamide salts **3a-k**.

1-cyanomethyl-3-methylimidazolium dicyanamide (3a): White solid. Yield 2.605 g (87.1 % of theory). Thermal analysis: $T_{5\% \text{ onset}} = 186.57$ °C, $T_{5\% \text{ dec}} = 222.11$ °C, $T_{\text{onset}} = 233.99$ °C, $T_{\text{dec}} = 210.49$ °C, $T_g = -58.94$ °C, $T_m = 53.94$ °C. IR (absorption frequency): 3681 (m), 3493 (w), 3149 (m), 3088 (m), 2953 (s), 2867 (w), 2230 (s), 2195 (m), 2125 (s), 1712 (w), 1612 (w), 1577 (w), 1558 (m), 1419 (w), 1410 (w), 1305 (s), 1218 (w), 1170 (s), 1111 (w), 1055 (m), 1033 (m), 933 (w), 906 (w), 857 (m), 745 (s) cm^{-1} . $^1\text{H-NMR}$ ($[\text{D}_6]$ DMSO): $\delta = 9.24$ (s, 1H), 7.88 (t, 1H), 7.78 (t, 1H), 5.58 (s, 2H), 3.89 (s, 3H) ppm. $^{13}\text{C-NMR}$ ($[\text{D}_6]$ DMSO): $\delta = 137.6$, 124.2, 122.5, 119.0, 114.6, 36.7, 36.0 ppm. Impact sensitivity: > 200 kg·cm.

1-(2-cyanoethyl)-3-methylimidazolium dicyanamide (3b): Amber liquid. Yield 2.057 g (74.5 % of theory). Thermal analysis: $T_{5\% \text{ onset}} = 158.45$ °C, $T_{5\% \text{ dec}} = 171.08$ °C, $T_{\text{onset}} = 172.75$ °C, $T_{\text{dec}} = 200.37$ °C (42% wt.), $T_g = -66.71$ °C, $T_m = 11.87$ °C (2nd heating cycle). IR (absorption frequency): 3681 (m), 3494 (w), 3150 (w), 3108 (m), 2967 (m), 2865 (w), 2229 (s), 2192 (m), 2119 (s), 1577 (m), 1562 (m), 1455 (w), 1420 (w), 1306 (s), 1165 (s), 1108 (w), 1053 (m), 1033 (m), 904 (w), 844 (m), 750 (m) cm^{-1} . $^1\text{H-NMR}$ ($[\text{D}_6]$ DMSO): $\delta = 9.11$ (s, 1H), 7.80 (t, 1H), 7.48 (t, 1H), 4.50 (t, 2H), 3.89 (s, 3H), 3.19 (s, 2H) ppm. $^{13}\text{C-NMR}$ ($[\text{D}_6]$ DMSO): $\delta = 136.9$, 123.9, 122.2, 119.0, 117.6, 44.3, 35.8, 18.5 ppm. Impact sensitivity: 172 kg·cm.

1-(3-cyanopropyl)-3-methylimidazolium dicyanamide (3c): Amber liquid. Yield 1.363 g (92.7 % of theory). Thermal analysis: $T_{5\% \text{ onset}} = 243.20$ °C, $T_{5\% \text{ dec}} = 260.45$ °C, $T_{\text{onset}} = 272.20$ °C, $T_{\text{dec}} = 308.93$ °C (to 36.3 wt%), $T_g = -79.70$ °C, $T_m = 49.71$ °C. IR (absorption frequency): 3681 (m), 3428 (m), 3152 (w), 3108 (w), 3010 (w), 2966 (m), 2866 (w), 2233 (s), 2196 (m), 2125 (s), 1632 (w), 1575 (m), 1565 (m), 1454 (w), 1425 (w), 1309 (s), 1166 (s), 1054 (m), 1033 (m), 1015 (w), 905 (w), 843 (w), 751 (m) cm^{-1} . $^1\text{H-NMR}$ ($[\text{D}_6]$ DMSO): $\delta = 9.11$ (s, 1H), 7.76 (s, 1H), 7.70 (s, 1H), 4.23 (t, 2H), 3.84 (s, 3H), 2.57 (t, 2H), 2.13 (m, 2H) ppm. $^{13}\text{C-NMR}$ ($[\text{D}_6]$ DMSO): $\delta = 136.7$, 123.6, 122.2, 119.5, 119.0, 47.6, 35.7, 25.1, 13.4 ppm. Impact sensitivity: 170 kg·cm.

1-(4-cyanobutyl)-3-methylimidazolium dicyanamide (3d): Amber liquid. Yield 0.533 g (82.6 % of theory). Thermal analysis: $T_{5\% \text{ onset}} = 238.24$ °C, $T_{5\% \text{ dec}} = 257.93$ °C, $T_{\text{onset}} = 259.49$ °C, $T_{\text{dec}} = 284.58$ °C (to 71.7 wt%), $T_g = -77.35$ °C. IR (absorption frequency): 3681 (m), 3489 (w), 3149 (w), 3104 (w), 3011 (w), 2950 (m), 2867 (w), 2227 (s), 2192 (m), 2125 (s), 1623 (w), 1574 (m), 1456 (w), 1425 (w), 1305 (s), 1163 (s), 1055 (m), 1033 (w), 1017 (w), 903 (w), 842 (w), 749 (m) cm^{-1} . $^1\text{H-NMR}$ ($[\text{D}_6]$ DMSO): $\delta = 9.10$ (s, 1H), 7.76 (t, 1H), 7.71 (t, 1H), 4.20 (t, 2H), 3.85 (s, 3H), 2.55 (q, 2H), 1.87 (m, 2H), 1.55 (m, 2H) ppm. $^{13}\text{C-NMR}$ ($[\text{D}_6]$ DMSO): $\delta = 136.5$, 123.6, 122.1, 120.2, 119.0, 47.8, 35.7, 28.4, 21.4, 15.6 ppm. Impact sensitivity: 170 kg·cm.

1-(5-cyanopentyl)-3-methylimidazolium dicyanamide (3e): Amber liquid. Yield 1.833 g (84.3 % of theory). Thermal analysis: $T_{5\% \text{ onset}} = 260.31\text{ }^{\circ}\text{C}$, $T_{5\% \text{ dec}} = 278.62\text{ }^{\circ}\text{C}$, $T_{\text{onset}} = 287.34\text{ }^{\circ}\text{C}$, $T_{\text{dec}} = 314.76\text{ }^{\circ}\text{C}$ (to 46.9 wt%), $T_g = -78.47\text{ }^{\circ}\text{C}$, $58.38\text{ }^{\circ}\text{C}$. IR (absorption frequency): 3681 (w), 3491 (w), 3149 (w), 3104 (w), 3011 (w), 2941 (m), 2866 (w), 2227 (s), 2192 (m), 2125 (s), 1624 (w), 1574 (m), 1460 (w), 1425 (w), 1304 (s), 1168 (s), 1055 (m), 1033 (w), 1017 (w), 903 (w), 841 (w), 751 (m) cm^{-1} . $^1\text{H-NMR}$ ($[\text{D}_6]\text{DMSO}$): $\delta = 9.11$ (s, 1H), 7.77 (t, 1H), 7.71 (t, 1H), 4.18 (t, 2H), 3.86 (s, 3H), 2.51 (t, 2H), 1.82 (m, 2H), 1.60 (m, 2H), 1.34 (m, 2H) ppm. $^{13}\text{C-NMR}$ ($[\text{D}_6]\text{DMSO}$): $\delta = 136.4$, 123.5, 122.1, 120.4, 119.0, 48.3, 35.6, 28.4, 24.4, 23.9, 15.8 ppm. Impact sensitivity: 170 $\text{kg}\cdot\text{cm}$.

1-(6-cyanoheptyl)-3-methylimidazolium dicyanamide (3f): White solid product. Yield 1.126 g (86.8 % of theory). Thermal analysis: $T_{5\% \text{ onset}} = 263.11\text{ }^{\circ}\text{C}$, $T_{5\% \text{ dec}} = 280.08\text{ }^{\circ}\text{C}$, $T_{\text{onset}} = 288.20\text{ }^{\circ}\text{C}$, $T_{\text{dec}} = 318.39\text{ }^{\circ}\text{C}$ (to 39.4 wt%), $T_g = -78.47\text{ }^{\circ}\text{C}$, $58.38\text{ }^{\circ}\text{C}$. IR (absorption frequency) = 3667 (w), 3490 (w), 3149 (w), 3104 (w), 2938 (m), 2865 (w), 2230 (s), 2194 (m), 2125 (s), 1625 (w), 1573 (m), 1460 (w), 1425 (w), 1308 (s), 1167 (s), 1055 (m), 1033 (w), 903 (w), 842 (w), 753 (m) cm^{-1} . $^1\text{H-NMR}$ ($[\text{D}_6]\text{DMSO}$): $\delta = 9.10$ (s, 1H), 7.76 (ts, 1H), 7.69 (s, 1H), 4.16 (t, 2H), 3.85 (s, 3H), 2.48 (t, 2H), 1.80 (m, 2H), 1.56 (m, 2H), 1.40 (m, 2H), 1.34 (m, 2H) ppm. $^{13}\text{C-NMR}$ ($[\text{D}_6]\text{DMSO}$): $\delta = 136.4$, 123.5, 122.1, 120.5, 190.0, 48.6, 35.6, 29.0, 27.3, 24.6, 24.4, 15.9 ppm. Impact sensitivity: 174 $\text{kg}\cdot\text{cm}$.

1-cyanomethyl-3-(2-cyanoethyl)imidazolium dicyanamide (3g): White solid product. Yield 1.505 g (88.3 % of theory). Thermal analysis: $T_{5\% \text{ onset}} = 144.80\text{ }^{\circ}\text{C}$, $T_{5\% \text{ dec}} = 163.51\text{ }^{\circ}\text{C}$, $T_{\text{onset}} = 161.89\text{ }^{\circ}\text{C}$, $T_{\text{dec}} = 209.44\text{ }^{\circ}\text{C}$ (to 55.7% wt.), $T_g = -27.59\text{ }^{\circ}\text{C}$, $59.95\text{ }^{\circ}\text{C}$. IR (absorption frequency): 3427 (w), 3145 (w), 3114 (w), 3015 (w), 2981 (w), 2233 (s), 2195 (m), 2125 (s), 1692 (w), 1623 (w), 1562 (m), 1457 (w), 1418 (w), 1310 (s), 1233 (w), 1164 (s), 1107 (w), 1080 (w), 1027 (w), 909 (w), 846 (w), 747 (m) cm^{-1} . $^1\text{H-NMR}$ ($[\text{D}_6]\text{DMSO}$): $\delta = 9.38$ (s, 1H), 7.96 (t, 1H), 7.91 (t, 1H), 5.63 (s, 2H), 4.56 (t, 2H), 3.21 (s, 2H) ppm. $^{13}\text{C-NMR}$ ($[\text{D}_6]\text{DMSO}$): $\delta = 138.3$, 123.7, 123.6, 119.6, 118.1, 115.1, 45.3, 37.6, 19.0 ppm. Impact sensitivity: 176 $\text{kg}\cdot\text{cm}$.

1-(2-cyanoethyl)-3-(3-cyanopropyl)imidazolium dicyanamide (3h): Amber liquid product. Yield 4.19 g (91.8 % of theory). Thermal analysis: $T_{5\% \text{ onset}} = 161.78\text{ }^{\circ}\text{C}$, $T_{5\% \text{ dec}} = 178.86\text{ }^{\circ}\text{C}$, $T_{\text{onset}} = 182.30\text{ }^{\circ}\text{C}$, $T_{\text{dec}} = 242.61\text{ }^{\circ}\text{C}$ (to 27.9 % wt.), $T_g = -61.20\text{ }^{\circ}\text{C}$, $71.22\text{ }^{\circ}\text{C}$. IR (absorption frequency): 3491 (w), 3144 (w), 3108 (w), 3015 (w), 2967 (w), 2229 (s), 2193 (m), 2125 (s), 1624 (w), 1564 (m), 1504 (w), 1452 (w), 1420 (w), 1306 (s), 1233 (w), 1161 (s), 1108 (w), 1079 (w), 1047 (w), 1023 (w), 906 (w), 844 (w), 750 (m) cm^{-1} . $^1\text{H-NMR}$ ($[\text{D}_6]\text{DMSO}$): $\delta = 9.26$ (s, 1H), 7.85 (t, 1H), 7.84 (t, 1H), 4.50 (t, 2H), 4.29 (t, 2H), 3.19 (t, 2H), 2.58 (t, 2H), 2.15 (m, 2H) ppm. $^{13}\text{C-NMR}$ ($[\text{D}_6]\text{DMSO}$): $\delta = 136.7$, 122.7, 122.5, 119.4, 119.0, 117.6, 47.8, 44.4, 25.1, 18.5, 13.4 ppm. Impact sensitivity: 176 $\text{kg}\cdot\text{cm}$.

1-(2-cyanoethyl)-3-(4-cyanobutyl)imidazolium dicyanamide (3i): Amber liquid product. Yield 1.33 g (90.8 % of theory). Thermal analysis: $T_{5\% \text{ onset}} = 167.48\text{ }^{\circ}\text{C}$, $T_{5\% \text{ dec}} = 180.99\text{ }^{\circ}\text{C}$, $T_{\text{onset}} = 179.60\text{ }^{\circ}\text{C}$, $T_{\text{dec}} = 249.11\text{ }^{\circ}\text{C}$ (to 29.7 % wt.), $T_g = -60.84\text{ }^{\circ}\text{C}$, $50.35\text{ }^{\circ}\text{C}$. IR (absorption frequency): 3697 (w), 3665 (w), 3488 (w), 3144 (w), 2981 (m), 2939 (m), 2923 (m), 2866 (m), 2844 (m), 2233 (s), 2195 (m), 2125 (s), 1631 (w), 1563 (m), 1509 (w), 1455 (w), 1420 (w), 1310 (s), 1239 (w), 1159 (s), 1107 (w), 1055 (s), 1033 (s), 1016 (s), 908 (w), 827 (w), 748 (m) cm^{-1} . $^1\text{H-NMR}$ ($[\text{D}_6]\text{DMSO}$): $\delta = 9.25$ (s, 1H), 7.84 (s, 2H), 4.50 (t, 2H), 4.26 (t, 2H), 3.20 (t, 2H), 2.55 (t, 2H), 1.89 (m, 2H), 1.55 (m, 2H) ppm. $^{13}\text{C-NMR}$ ($[\text{D}_6]\text{DMSO}$): $\delta = 136.5$, 122.7, 122.5, 120.2, 119.0, 117.6, 48.1, 44.4, 28.4, 21.4, 18.5, 15.6 ppm. Impact sensitivity: 174 $\text{kg}\cdot\text{cm}$.

1-(2-cyanoethyl)-3-(5-cyanopentyl)imidazolium dicyanamide (3j): Amber liquid product. Yield 1.837 g (85.4 % of theory). Thermal analysis: $T_{5\% \text{ onset}} = 162.60\text{ }^{\circ}\text{C}$, $T_{5\% \text{ dec}} =$

176.77 °C, T_{onset} = 191.74 °C, T_{dec} = 253.26 °C (to 29.5 % wt.), T_g = -65.65 °C, 53.33 °C. IR (absorption frequency): 3707 (w), 3681 (w), 3488 (w), 3144 (w), 2981 (m), 2967 (m), 2939 (m), 2866 (m), 2844 (m), 2229 (s), 2193 (m), 2125 (s), 1563 (m), 1509 (w), 1455 (w), 1420 (w), 1345 (m), 1308 (s), 1160 (s), 1055 (s), 1033 (s), 1016 (s), 906 (w), 826 (w), 749 (m) cm^{-1} . ^1H -NMR ($[\text{D}_6]$ DMSO): δ = 9.26 (s, 1H), 7.85(s, 2H), 4.50 (t, 2H), 4.24 (t, 2H), 3.21 (t, 2H), 2.49 (t, 2H), 1.84 (m, 2H), 1.60 (m, 2H), 1.36 (m, 2H) ppm. ^{13}C -NMR ($[\text{D}_6]$ DMSO): δ = 136.4, 122.7, 122.4, 120.4, 119.0, 117.6, 48.5, 28.4, 24.4, 23.9, 18.6, 15.9 ppm. Impact sensitivity: 164 kg·cm.

1-(2-cyanoethyl)-3-(6-cyanoethyl)imidazolium dicyanamide (3k): Amber liquid product. Yield 1.837 g (85.4 % of theory). Thermal analysis: $T_{5\% \text{ onset}}$ = 154.13 °C, $T_{5\% \text{ dec}}$ = 171.34 °C, T_{onset} = 192.12 °C, T_{dec} = 239.95 °C (to 23.1 % wt.), T_g = -66.72 °C, 57.71 °C. IR (absorption frequency): 3697 (w), 3681 (w), 3489 (w), 3144 (w), 2966 (m), 2939 (m), 2866 (m), 2844 (m), 2231 (s), 2194 (m), 2125 (s), 1624 (w), 1563 (m), 1508 (w), 1455 (w), 1421 (w), 1308 (s), 1162 (s), 1055 (s), 1033 (s), 1017 (s), 906 (w), 825 (w), 752 (m) cm^{-1} . ^1H -NMR ($[\text{D}_6]$ DMSO): δ = 9.25 (s, 1H), 7.85(q, 2H), 4.49 (t, 2H), 4.21 (t, 2H), 3.21 (t, 2H), 2.49 (t, 2H), 1.80 (m, 2H), 1.54 (m, 2H), 1.36 (m, 2H), 1.22 (m, 2H) ppm. ^{13}C -NMR ($[\text{D}_6]$ DMSO): δ = 136.4, 122.7, 122.4, 120.5, 119.0, 117.6, 48.8, 44.4, 28.9, 27.2, 24.5, 24.3, 18.6, 15.9 ppm. Impact sensitivity = 170 kg·cm.

Appendix A7

Introduction and initial demonstration of synthetic design platform for bridged multi-heterocycles with variable charge, structure, and symmetry options: Formation of 5-tetrazole-based products using a three step procedure of azole 'click' functionalization, 'click' synthesis of bi-heterocyclic precursors, and further product modification utilizing IL-based synthetic strategies

The synthesis involved for the initial demonstration of the design platform concept is depicted in Figure A7.1 and A7.2.

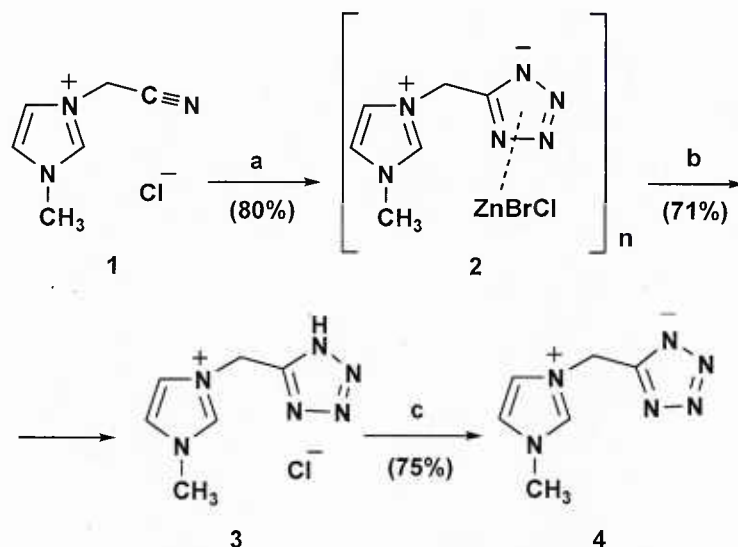


Figure A7.1. Synthesis of imidazole-tetrazole bicyclic targets: (a) NaN_3 (1.1 eq.), ZnBr_2 , water (24 h, RT); (b) BioRad AG 1-X8 (Cl^- form) in 9 N HCl; (c) BioRad AG 1-X8 (OH^- form) from ionic precursor 1.

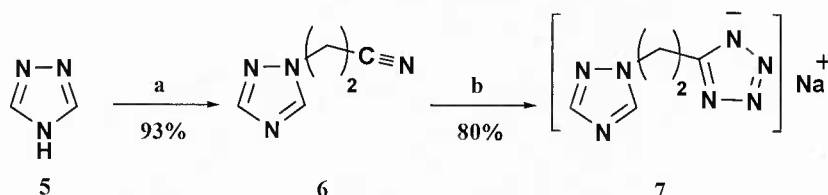


Figure A7.2. Synthesis of sodium 5-(2-(1,2,4-triazol-1-yl)ethyl)tetrazolate, 7, from neutral 1-(2-cyanoethyl)-1,2,4-triazole, 6: (a) acrylonitrile (1 eq.), Et_3N (cat.), toluene, reflux, 30 h; (b) NaN_3 (1.1 eq.), AcOH, 60-70 °C, 24 h.

The preparation of 1-cyanomethyl-3-imidazolium chloride (1). As shown above in Figure A7.1, compound 1 was prepared by a solvent-free adaptation of a previously reported method. Yields and reaction times are unoptimized. The following serves as general procedure. In a 50 mL round bottom flask with magnetic stirbar, chloroacetonitrile (2.867 g, 37.9 mmol) was slowly added to 1-methylimidazole (2.87 g, 35 mmol). The mixture was stirred at room temperature overnight, and the resulting white solid precipitate washed with ethyl acetate (4 x 10

mL) and dried by rotary evaporation then high vacuum at room temperature for 24 h. White solid, water soluble, 90% yield. mp (DSC) $T_m = 178.7\text{ }^\circ\text{C}$, onset for 5% decomposition $T_{5\%\text{onset}} = 221.1\text{ }^\circ\text{C}$; ^1H NMR (500 MHz, DMSO- d_6) δ ppm 9.56 (s, 1H), 8.00 (t, $J = 1.73\text{ Hz}$, 1H), 7.87 (t, $J = 1.64\text{ Hz}$, 1H), 5.82 (s, 2H), 3.92 (s, 3H); ^{13}C (125 MHz, DMSO- d_6) δ ppm 138.292, 124.800, 123.026, 115.342, 37.207, 36.641. FT-IR (ν_{max}): 3392 (w), 3032 (s), 2977 (s), 2906 (s), 1575 (s), 1565 (s), 1439 (m), 1337 (m), 1254 (s), 1168 (s), 915 (m).

The preparation of zinc-coordinated 1-(5-tetrazolidyl)methyl-3-methyl-imidazolium zwitterion (2). As shown in Figure Ax.1 above, compound **2** was prepared from the halide salt 1-cyanomethyl-3-methylimidazolium chloride (**1**). Subsequent monitoring of the reaction by way of ^1H -NMR spectroscopy resulted in $\sim 85\%$ conversion of **1** to product **2** under room temperature conditions with all other factors the same. 1-cyanomethyl-3-methylimidazolium chloride (**1**) (2.81 g, 17.2 mmol) was combined with NaN_3 (1.30 g, 20 mmol) in a 100 mL round-bottom flask with 50 mL water and stirred to dissolve with a magnetic stir bar. Zinc bromide was added (4.49 g, 20 mmol), and the mixture stirred to reflux overnight. The resultant white solid was rinsed with water and filtered. The final product was dried at $60\text{ }^\circ\text{C}$ for 24 h in an oven. White powder, 80% yield. glass transition temperature (DSC) $T_m =$ at decomposition temperature; onset for 5% decomposition, $T_{5\%\text{onset}} = 306.9\text{ }^\circ\text{C}$; ^1H NMR (360 MHz, DMSO- d_6) δ ppm 9.18 (s, 1H), 7.75 (t, $J = 1.72\text{ Hz}$, 1H), 7.68 (t, $J = 1.74\text{ Hz}$, 1H), 5.57 (s, 2H); 3.87 (3H, s); ^{13}C NMR (125 MHz, DMSO- d_6) δ ppm 154.171, 138.060, 124.442, 123.563, 42.915, 36.557. FT-IR (ν_{max}): 3498 (w), 3103 (s), 3078 (s), 2076 (s), 16128 (w), 1572 (s), 1446 (s), 1433 (s), 1421 (s), 1340 (m), 1171 (s), 1072 (m), 839 (s), 816 (s), 776 (s), 692 (s).

The preparation of 1-(5-1H-tetrazolyl)methyl-3-methylimidazolium chloride (Zn-free salt) (3). Compound **3** (Figure A7.1, above) was obtained from the Zn-coordination polymer (**2**) via a preparatory adaptation of an anion exchange resin technique reported to remove trace Zn selectively from water and industrial waste samples⁸⁵. Yields and reaction times are unoptimized.

Conditioning of anion exchange resin: To 15.167 g of BioRad AG 1-X8 strongly basic anion exchange resin (100-200 mesh), 40 mL D.I. water was added and the resin stirred in a 125 mL flask to a slurry for 20 min. The slurry was then introduced into a glass column ($\sim 0.5\text{ cm ID}$, 40 cm length; prewashed with 9 N HCl and rinsed several times with D.I. water) with a sand and glass wool plug. 9 N HCl was then eluted through the column (2 x 30 mL) and discarded upon neutralization.

Sample preparation for anion exchange: The Zn-coordination polymer **2** was added to a 50 mL Erlenmeyer flask (0.508 g, 1.473 mmol) and 15 mL of 9 N HCl was added and stirred to dissolve the solid material. The solution was sonicated briefly to break up residual solids suspended in the acidic solution, and an additional 10 mL 9 N HCl was added to completely dissolve the material.

Zn separation from 2 by anion exchange resin: 10 mL collection vials were numbered and arranged to collect eluted fractions from the column, and **2** dissolved in minimal 9 N HCl was introduced by 3 mL increments to the top of the resin bed and eluted at a rate of $\sim 1\text{ drop/sec}$ (controlled by positive pressure introduced to top of column). When sample introduction was complete, 9 N HCl was eluted for complete removal of the salt **3**. After this step, the column was eluted with 0.005 M HCl followed by eluting the column with enough water until elution had tested negative for chloride by silver nitrate spot test ($\sim 1:1\text{ v/v}$ ratio of eluted fraction to 0.1 M AgNO_3). In all, 24 vials were collected from the exchange resin, where each vial contained approximated 5-10 mL of eluted material.

Qualitative analysis of Zn removal by pH measurement and $K_2[Hg(CNS)_4]$ spot test: Determination of Zn in eluted fractions was estimated by two methods. First, the approximate pH of the elution in each collected vial was obtained by pH indicator paper (Vials 1-19, pH < 1; Vial 20, pH ~ 3-5; Vials 21-24, pH ~ 5). As the $[ZnCl_4]^{2-}$ anion is present at high chloride concentrations, the zinc should remain supported on the resin and it may be assumed that the earlier elution volumes were relatively Zn-free. Next, a solution of $K_2[Hg(CNS)_4]$ (prepared the previous day by established methods,⁸⁶ 2.7% $HgCl_2$ and 3.9% in D.I. water) was used to test each of the eluted fractions for Zn by spot test (1:1 ratio of 0.5 mL each, sample to test solution; concentration limit = 1/10,000). A white precipitate indicating the presence of Zn formed quickly (less than 1 min) for elution vials #14-22, where 14-16 only had a slight precipitate. To ensure the quality of the samples, only vials 2-5 and 7-11 were included for sample collection. Vials #1 and #6 seemed to visually contain column impurity (yellow coloring) and were stored separately. Vials 12 and 13, although not obviously precipitating, were kept separate as well to increase the window between the eluted sample and Zn-containing eluted solution.

Isolation of 1-(5-1H-tetrazolyl)methyl-3-methylimidazolium chloride (3): Each of the eluted fractions of **3** was heated (~60 °C, 24 h) to remove water and excess HCl, and the residual solids were triturated with dry ethanol. From evaporating the reserved ethanol solution, the product was obtained as a white solid. White solid, 71% yield. mp (DSC) T_m = 155.5 °C (melts during early onset of decomposition); onset for 5% decomposition, $T_{5\%onset}$ = 213.1 °C, 1H -NMR (500 MHz, DMSO- d_6) δ ppm 9.35 (s, 1H), 7.86 (t, J = 1.65 Hz, 1H), 7.77 (t, J = 1.61 Hz, 1H), 5.89 (s, 2H), 3.89 (s, 3H); ^{13}C -NMR (125 MHz, DMSO- d_6) δ ppm 153.375, 137.561, 123.841, 122.956, 42.292, 36.914. FT-IR (ν_{max}): 3107 (m), 3001 (s), 2468 (w), 2395 (s), 1801 (m), 1668 (w), 1584 (m), 1552 (s), 1424 (w), 1178 (m), 1084 (s), 1027 (s), 1015 (s); 790 (s), 785 (s), 740 (s).

The preparation of 1-(5-tetrazolidyl)methyl-3-methylimidazolium as a free zwitterion (4). As shown in Figure A7.1 above, compound **4** was obtained from the 1-(5-1H-tetrazolyl)methyl-3-methylimidazolium chloride salt (**3**) via neutralization reaction using hydroxide-exchanged anion exchange resin as solid-supported base. Yields and reaction times are not optimized.

Conditioning of anion exchange resin (OH): Approximately 5 g of BioRad AG 1-X8 strongly basic anion exchange resin in chloride form was eluted with ~20 bed volumes (~1 L) of 1 N NaOH and each eluted volume was tested for Cl^- anion by using the silver nitrate test⁸⁷. The column was then washed with 2 bed volumes of D.I. water, filtered, and rinsed dry with ethanol before storing under high vacuum for 48 h.

Neutralization of 3 by OH form of anion exchange resin: The required volume of dry resin needed to convert **3** to the zwitterion **4** (EQ. 1) was added to a 125 mL Erlenmeyer flask, washed three times with 25 mL of D.I. water and decanted to remove fines from ruptured resin beads, and then **3** (0.240 g, 1.20 mmol) was added to the flask as a solution in 25 mL of water.

$$\begin{aligned} \text{Dry Resin required (g)} &= (\text{mmol } Cl^- \text{ salt}) \times \left(\frac{1 \text{ g dry resin}}{(2.6 \text{ meq exchange capacity})} \right) & [\text{EQ. 1}] \\ &= (1.2 \text{ mmol}) \times \left(\frac{1 \text{ g}}{2.6 \text{ meq}} \right) = 0.46 \text{ g dry resin needed} \\ &= 2.30 \text{ g dry resin (5} \times \text{ excess)} \end{aligned}$$

The mixture was gently stirred by rotating the flask for 20 min prior to spot checking the solution for Cl^- anion by silver nitrate test (0.1 M $AgNO_3$), the resin was filtered and washed

with 3 x 10 mL D.I. water, and the resulting aqueous filtrates combined and evaporated to dryness at room temperature in an open beaker.

Isolation of 1-(5-tetrazolidyl)methyl-3-methylimidazolium (4): Neutralized fractions were combined and allowed to evaporate at room temperature to remove water. Additional Recrystallization of isolated **4** from slow evaporation from hot methanol resulted in the final product. A crystal from this batch was submitted for single crystal X-ray diffraction analysis. White solid, 75% yield. mp (DSC) $T_m = 124.8\text{ }^{\circ}\text{C}$; onset for 5% decomposition, $T_{5\%\text{onset}} = 241.0\text{ }^{\circ}\text{C}$, $^1\text{H-NMR}$ (500 MHz, DMSO- d_6) δ ppm 9.15 (s, 1H), 7.72 (t, $J = 1.50\text{ Hz}$, 1H), 7.65 (t, $J = 1.51\text{ Hz}$, 1H), 5.52 (s, 2H), 3.84 (s, 3H); $^{13}\text{C-NMR}$ (125 MHz, DMSO- d_6) δ ppm 155.584, 136.458, 123.226, 122.650, 44.619, 35.614. FT-IR (ν_{max}): 3146 (m), 3094 (s), 3074 (s), 1575 (m), 1560 (m), 1402 (w), 1331 (s), 1193 (w), 1150 (s), 1122 (m), 1080 (w), 862 (s), 815 (s), 780 (s), 751 (s), 698 (s).

The preparation of neutral azole precursor 1-(2-cyanoethyl)-1,2,4-triazole (6). As shown in Figure A7.2 above, compound **6** was prepared from the 1,2,4-triazole, **5**. Yields and reaction times are unoptimized. The following serves as a general procedure. A sample of 1,2,4-triazole (1.724 g, 25 mmol) was dissolved in toluene (10 mL) and placed into a 50 mL round bottom flask to which a Teflon stirbar was added. Acrylonitrile (1.3562 g, 25 mmol) was added to the flask drop-wise as a solution in toluene (2 mL) followed by addition of triethylamine (0.5 mL) directly to the reaction mixture. The reaction mixture was fitted with a condenser and heated to reflux. The reaction mixture was then refluxed for an additional 30 h.

At the end of the reaction time, **6** separated from the toluene as a second amber liquid phase and was isolated by decanting the toluene from the mixture and washing the residue with additional toluene. Residual solvent was then removed by rotary evaporation. White solid, 93.3% yield. mp (DSC) $T_m = 31.4\text{ }^{\circ}\text{C}$; onset for 5% decomposition, $T_{5\%\text{onset}} = 120.4\text{ }^{\circ}\text{C}$, $^1\text{H NMR}$ (360 MHz, DMSO- d_6) δ ppm 8.62 (s, 1H), 8.07 (s, 1H), 4.51 (d, $J = 6.38\text{ Hz}$, 2H), 3.13 (t, $J = 6.38\text{ Hz}$, 2H); $^{13}\text{C NMR}$ (90 MHz, DMSO- d_6) δ ppm 152.411, 144.958, 118.691, 44.737, 18.864. FT-IR (ν_{max}): 3406 (br m), 3120 (m), 2253 (m), 1508 (s), 1450 (m), 1418 (m), 1274 (s) 1206 (m), 1135 (s), 1040 (m), 1022 (m), 1003 (s), 919 (m), 872 (m), 679 (s).

Caution: Acrylonitrile is a very hazardous irritant and permeator for skin and eyes, so protective clothing and a properly ventilated workspace should be utilized when handling this material. Prolonged exposure should be avoided, as there are possible carcinogenic/tetratogenic/mutagenic effects as well as toxicity related to target organs including blood, liver, central nervous system and kidneys. Additionally, explosive mixtures can be formed when vapors are allowed to mix with air, so accumulation of evaporated material is to be avoided. Please refer to Material Safety Data Sheet (MSDS) for further precautionary details (CAS # 107-13-1).

The preparation of sodium coordination polymer 5-(2-(1,2,4-triazol-1-yl)ethyl)tetrazolate (7). Compound **7** (Figure A7.2, above) was prepared from 1-(2-cyanoethyl)-1,2,4-triazole (**6**). Yields and reaction times are not optimized. The following serves as a general procedure. In an Ace Glass high-pressure glass vial with a Teflon screw-cap, 1-(2-cyanoethyl)-1,2,4-triazole (1.195 g, 9.8 mmol) was combined with sodium azide (0.6437 g, 9.8 mmol) in glacial acetic acid (0.6 mL, 10 mmol). A Teflon magnetic stir bar was added, the vial sealed, and the mixture stirred on an oil bath at 60-70 $^{\circ}\text{C}$ for 24 h. At the end of the reaction period, the vial was set on a rotary evaporator at 70-80 $^{\circ}\text{C}$ for 4 h to remove residual acetic acid followed by dissolving the white solids with dry ethanol. Single crystals were obtained from slow evaporation of ethanol from the crude reaction mixture, and the final product, **6**, was

obtained from removal of residual solvent by high vacuum. White solid, 48.5% yield. mp (DSC) T_m = decomposition temperature; onset for 5% decomposition, $T_{5\%onset} = 313.7\text{ }^{\circ}\text{C}$, ^1H NMR (360 MHz, DMSO- d_6) δ ppm 8.42 (s, 1H), 7.92 (s, 1H), 4.47 (t, $J = 7.62\text{ Hz}$, 2H), 3.15 (t, $J = 7.59\text{ Hz}$, 2H); ^{13}C NMR (90 MHz, DMSO- d_6) δ ppm 157.889, 151.547, 144.329, 48.809, 26.953. FT-IR (ν_{max}): 3322 (s), 3219 (s), 3144 (s), 1687 (m), 1571 (s), 1516 (s), 1468 (m), 1435 (m), 1380 (s), 1277 (s), 1205 (s), 1139 (s), 1104 (w), 1043 (w), 1014 (s), 970 (w), 923 (w), 858 (m), 673 (m).

Appendix A8

Click synthesis and thermal characterization of zinc-containing, alkyl-bridged imidazolium-tetrazolates with highly variable *N*-alkyl and alkyl bridge lengths as expansion of bridged multiheterocyclic design platform

The synthesis of 7 Zn-containing imidazolium-tetrazolate zwitterions **3a-g** via Click chemical methods was achieved, where variable alkyl bridge lengths are established early from the synthesis of the *N*-cyanoalkyl-functionalized imidazolium halide precursors **2a-g** (Figure A8.1).

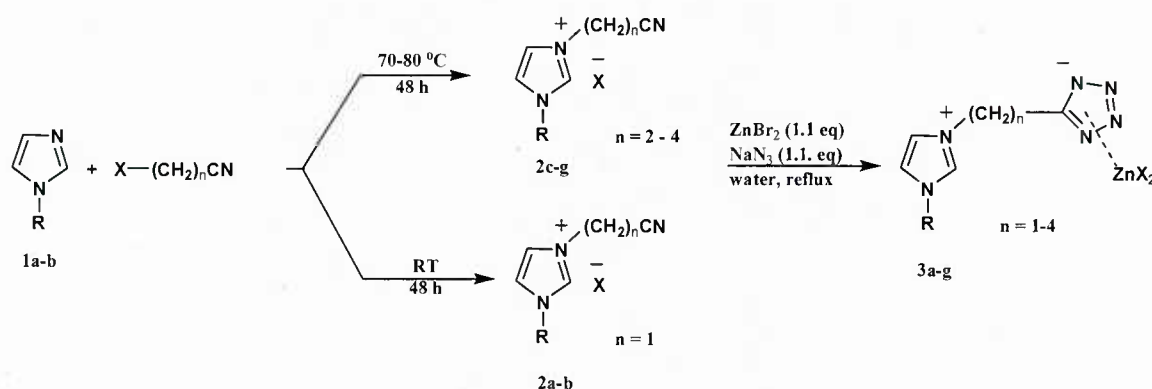


Figure A8.1. Synthesis of *N*-cyanoalkyl-functionalized imidazolium halide salts **2a-g** from 1-alkylimidazoles **1a-b** and their use as precursors for the formation of Zn-containing imidazolium-tetrazolate based zwitterions **3a-g**.

The preparation of *N*-cyanoalkyl-functionalized imidazolium halide (precursors) (2a-g**).**

Preparation of *N*-cyanoalkyl-*N*-alkylimidazolium halide salts (2a-g**):** Compounds **2a-b** and **2c-g** were prepared by solvent-free modification of reported methods from the respective haloalkyl nitriles under room-temperature or heated conditions, respectively. Yields and reaction times were not optimized, and the following general procedure is representative of our work.

Compounds **2a-b:** Chloroacetonitrile (1.1 equiv.) was added to 1-alkylimidazole (1 equiv.) in a small, round-bottom flask, fitted with a magnetic stir bar and sealed. The reaction is stirred vigorously for 48 hours, when the reaction mixture is washed with ethyl acetate. Products are dried overnight under high vacuum at room temperature.

Compounds **2c-g:** Starting 1-alkylimidazole (1 equiv.) was combined with the corresponding haloalkyl nitrile (1.1 equiv.) in a 20 mL high pressure vial, sealed with a Teflon screw cap, and mixed vigorously prior to storing in a furnace at 70 °C for 48 hours. An exception was for **2c**, where the reaction was run for 20 days. After cooling, the reaction mixture is washed several times with acetone, and the product is dried by high vacuum at 50 °C overnight.

1-cyanomethyl-3-methylimidazolium chloride (2a**).** White solid, water soluble, 90 % yield, m. p. (DSC) $T_m = 23.90$ °C, onset for 5% decomposition $T_{5\%dec} = 214.01$ °C; 1H NMR (500 MHz, DMSO- d_6) δ ppm 9.56 (s, 1H), 8.00 (t, $J = 1.73$ Hz, 1H), 7.87 (t, $J = 1.64$ Hz, 1H), 5.82 (s, 2H), 3.92 (s, 3H); ^{13}C (125 MHz, DMSO- d_6) δ ppm 138.292, 124.800, 123.026, 115.342, 37.207, 36.641. FT-IR: 3392 (w), 3032 (s), 2977 (s), 2906 (s), 2229 (m), 1575 (s), 1565 (s), 1439 (m), 1337 (m), 1254 (s), 1168 (s), 915 (m).

1-butyl-3-cyanomethylimidazolium chloride (2b). Amber viscous liquid, water soluble, 78 % yield, glass transition temperature (DSC) $T_g =$; onset for 5% decomposition $T_{5\%dec} = 200.91$ °C; ^1H NMR (500 MHz, DMSO- d_6) δ ppm 9.69 (s, 1H), 8.04 (t, $J = 1.76$ Hz, 1H), 7.99 (t, $J = 1.73$ Hz, 1H), 5.82 (s, 1H), 4.26 (t, $J = 7.21$ Hz, 2H), 1.90-1.67 (m, 2H), 1.27 (dd, $J = 15.04$, 7.47 Hz, 2H), 0.90 (t, $J = 7.38$ Hz, 3H); ^{13}C (125 MHz, DMSO- d_6) δ ppm 137.848, 123.583, 123.225, 115.285, 49.432, 37.290, 31.688, 19.224, 13.744; FT-IR: 3372 (w), 3058 (m), 2957 (s), 2931 (s), 2225 (m), 1557 (s), 1461 (m), 1335 (w), 1161 (s), 1029 (m), 925 (w).

1-(2-cyanoethyl)-3-methylimidazolium bromide (2c). Yellow solid, water soluble, 89 % yield, melting point and glass transition temperature (DSC) $T_m = 149.30$ °C, $T_g = -9.65$ °C; onset for 5% decomposition $T_{5\%dec} = 222.30$ °C; ^1H NMR (500 MHz, DMSO- d_6) δ ppm 9.32 (s, 1H), 7.89 (s, 1H), 7.80 (s, 1H), 4.54 (t, $J = 6.52$ Hz, 2H), 3.91 (s, 2H), 3.26 (t, $J = 6.52$ Hz, 2H); ^{13}C (125 MHz, DMSO- d_6) δ ppm 137.547, 124.405, 122.831, 118.157, 44.915, 36.462, 19.196. FT-IR: 3078 (s), 3038 (s), 2251 (s), 1572 (s), 1555 (s), 1446 (m), 1426 (m), 1400 (m), 1279 (m), 1163 (s), 862 (s), 789 (s), 741 (m).

1-(3-cyanopropyl)-3-methylimidazolium (2d). White solid, water soluble, 92 % yield, melting point and glass transition temperature (DSC) $T_m = 96.31$ °C, $T_g = -30.55$ °C; onset for 5% decomposition $T_{5\%dec} = 247.38$ °C; ^1H NMR (500 MHz, DMSO- d_6) δ ppm 9.42 (s, 1H), 7.87 (t, $J = 1.65$ Hz, 1H), 7.78 (t, $J = 1.56$ Hz, 1H), 4.28 (t, $J = 6.97$ Hz, 2H), 3.86 (s, 3H), 2.61 (t, $J = 7.23$ Hz, 2H), 2.14 (p, $J = 7.12$ Hz, 2H); ^{13}C (125 MHz, DMSO- d_6) δ ppm 137.527, 124.174, 122.774, 120.151, 48.051, 36.248, 25.789, 13.981. FT-IR: 3433 (s), 3367 (s), 3058 (s), 2246 (m), 1618 (m), 1573 (s), 1562 (s), 1451 (m), 1423 (m), 1158 (s), 1089 (m), 867 (s), 773 (s), 665 (m).

1-butyl-3-(3-cyanopropyl)imidazolium chloride (2e). Amber viscous liquid, water soluble, 45 % yield, glass transition temperature (DSC) $T_g = -31.21$ °C; onset for 5% decomposition $T_{5\%dec} = 259.84$ °C; ^1H NMR (500 MHz, DMSO- d_6) δ ppm 9.44 (s, 1H), 7.88 (t, 1H), 7.86 (t, 1H), 4.28 (t, $J = 6.96$ Hz, 2H), 4.18 (t, $J = 7.20$ Hz, 2H), 2.62 (t, $J = 7.12$ Hz, 2H), 2.16 (p, $J = 7.08$ Hz, 2H), 1.83-1.75 (m, 2H), 1.28 (dd, $J = 15.02$, 7.46 Hz, 2H), 0.91 (t, $J = 7.38$ Hz, 3H); ^{13}C (125 MHz, DMSO- d_6) δ ppm 136.921, 123.068, 122.961, 120.107, 49.108, 48.230, 31.755, 25.642, 19.276, 14.044, 13.780. FT-IR: 3372 (w), 2956 (s), 2931 (s), 2870 (m), 2249 (m), 1560 (s), 1458 (m), 1161 (s), 864 (m), 751 (m).

1-(4-cyanobutyl)-3-methylimidazolium chloride (2f). Amber viscous liquid, water soluble, 95 % yield, glass transition temperature (DSC) $T_g = -22.99$ °C; onset for 5% decomposition $T_{5\%dec} = 239.53$ °C; ^1H NMR (500 MHz, DMSO- d_6) δ ppm 9.35 (s, 1H), 7.80 (t, $J = 1.61$ Hz, 1H), 7.73 (t, 1H), 4.21 (t, $J = 6.98$ Hz, 2H), 3.82 (s, 3H), 2.54 (t, $J = 7.16$ Hz, 2H), 1.93-1.67 (q, 2H), 1.50 (q, 2H), ^{13}C (125 MHz, DMSO- d_6) δ ppm 137.289, 124.143, 122.706, 120.859, 48.294, 36.247, 29.003, 22.016, 16.186. FT-IR: 3372 (m), 3058 (s), 2946 (s), 2931 (s), 2247 (m), 1633 (m), 1570 (s), 1456 (m), 1423 (m), 1161 (s), 869 (m), 758 (m).

1-butyl-3-(4-cyanobutyl)imidazolium chloride (2g). Amber viscous liquid, water soluble, 97 % yield, glass transition temperature (DSC) $T_g = -38.49$ °C; onset for 5% decomposition $T_{5\%dec} = 256.58$ °C; ^1H NMR (500 MHz, DMSO- d_6) δ ppm 9.61 (s, 1H), 7.90 (t, $J = 1.62$ Hz, 1H), 7.89 (t, $J = 1.67$ Hz, 1H), 4.26 (t, $J = 6.98$ Hz, 2H), 4.19 (t, $J = 7.18$ Hz, 2H), 2.58 (t, $J = 7.16$ Hz, 2H), 1.93-1.84 (m, 2H), 1.80-1.73 (m, 2H), 1.61-1.40 (m, 2H), 1.23 (dd, $J = 15.01$, 7.46 Hz, 2H), 0.88 (t, $J = 7.38$ Hz, 3H); ^{13}C (125 MHz, DMSO- d_6) δ ppm 136.901, 123.089, 122.995, 120.944, 49.125, 48.430, 31.847, 29.030, 22.150, 19.366, 16.276, 13.843. FT-IR: 3372 (w), 3043 (m), 2956 (s), 2931 (s), 2247 (m), 1638 (w), 1560 (s), 1456 (s), 1161 (s), 877 (m), 753 (m).

The preparation of alkyl-bridged, Zn-containing imidazolium-tetrazolate zwitterions (3a-g). All Zn-containing Click products, **3a-b,d-g**, were obtained by using a similar procedure. To an aqueous solution (40 mL water) of the *N*-cyanoalkyl-functionalized imidazolium halide salt (**2a-b,d-g**, 20 mmol) in a 100 mL round bottom flask, 1.1 equivalents of sodium azide were added and stirred to dissolve. Immediately afterwards, 1.1 equivalents of zinc bromide was combined with the reaction mixture, and set to reflux with stirring overnight. Next, the aqueous solution was decanted from the resulting amorphous, white solid. The solids were washed several times with water, filtered, and the resulting white powder was dried under high vacuum at 50 °C for at least 24 hours. An exception is the synthesis of **3c** from **2c** (1 mmol), where the product was obtained from exploratory conditions utilizing a mixture of isopropyl alcohol and water (1 mL/2 mL) as solvent mixture with 1 mmol of ZnBr₂ and 2 equivalents of NaN₃.

catena-poly[(bromochlorozinc)-μ-[1-(5-tetrazoyl)methyl-3-methylimidazolium]-N':N'] (3a).⁸⁸ White powder, 80 % yield, glass transition temperature (DSC) T_g = none observed; onset for 5% decomposition, $T_{5\%dec} = 307.17$ °C; ¹H NMR (360 MHz, DMSO-*d*₆) δ ppm 9.18 (s, 1H), 7.75 (t, *J* = 1.72 Hz, 1H), 7.68 (t, *J* = 1.74 Hz, 1H), 5.57 (s, 2H); 3.87 (3H, s); ¹³C NMR (125 MHz, DMSO-*d*₆) δ ppm 154.171, 138.060, 124.442, 123.563, 42.915, 36.557. FT-IR: 3498 (w), 3103 (s), 3078 (s), 2076 (s), 1618 (w), 1572 (s), 1446 (s), 1433 (s), 1421 (s), 1340 (m), 1171 (s), 1072 (m), 839 (s), 816 (s), 776 (s), 692 (s).

A crystal submitted for XRD analysis was obtained from dissolving **3a** in a minimal volume of concentrated HNO₃, evaporating the resulting mixture to near dryness, washing the residual with dry acetone, and slowly evaporating in open air to form colorless plates.

Zn-containing 1-butyl-3-(5-tetrazoyl)methylimidazolium (3b). White powder, 89.1 % yield, glass transition temperature (DSC) T_g = none observed; onset for 5% decomposition, $T_{5\%dec} = 305.13$ °C; ¹H NMR (500 MHz, DMSO-*d*₆) δ ppm 9.26 (s, 1H), 7.78 (d, *J* = 29.47 Hz, 2H), 5.80 (s, 2H), 4.20 (t, *J* = 7.07 Hz, 2H), 1.83-1.72 (m, 2H), 1.26 (qd, *J* = 14.38, 7.08 Hz, 2H), 0.90 (t, *J* = 7.29 Hz, 3H); ¹³C NMR (125 MHz, DMSO-*d*₆) δ ppm 156.276, 136.964, 123.330, 122.953, 49.194, 44.002, 31.787, 19.264, 13.745. FT-IR: 3098 (s), 2946 (m), 2865 (w), 2075 (m), 1565 (s), 1441 (s), 1335 (m), 1161 (s), 1138 (m), 1075 (m), 822 (s), 746 (s), 710 (s), 672 (s).

Zn-containing 1(2-(5-tetrazoyl)ethyl)-3-methylimidazolium (3c). White powder, < 60 % yield (not optimized), glass transition temperature (DSC) T_g = none observed; onset for 5% decomposition, $T_{5\%dec} = 266.56$ °C; ¹H NMR (360 MHz, DMSO-*d*₆) δ ppm 9.08 (s, 1H), 7.65 (td, *J* = 4.48, 1.80 Hz, 2H), 4.58 (t, *J* = 6.91 Hz, 2H), 3.84 (s, 3H), 3.45 (t, *J* = 6.92 Hz, 2H); ¹³C NMR (125 MHz, DMSO-*d*₆) δ ppm 157.957, 137.412, 124.114, 122.950, 48.102, 36.425, 26.205. FT-IR: 3569 (m), 3103 (m), 3098 (m), 2146 (m), 2066 (s), 1575 (m), 1560 (m), 1487 (m), 1421 (s), 1335 (m), 1161 (s), 1082 (m), 854 (s), 761 (s), 705 (m).

Zn-containing 1-(3-(5-tetrazoyl)propyl)-3-methylimidazolium (3d). White powder, 52 % yield, glass transition temperature (DSC) T_g = 91.57 °C; onset for 5% decomposition, $T_{5\%dec} = 322.81$ °C; ¹H NMR (500 MHz, DMSO-*d*₆) δ ppm 9.10 (s, 1H), 7.70 (d, *J* = 25.61 Hz, 2H), 4.21 (t, *J* = 6.40 Hz, 2H), 3.85 (s, 3H), 3.00-2.86 (m, 2H), 2.18 (t, 2H); ¹³C NMR (125 MHz, DMSO-*d*₆) δ ppm 160.327, 137.087, 124.085, 122.739, 48.827, 36.316, 29.012, 21.325. FT-IR: 3518 (w), 3104 (m), 3083 (m), 2066 (s), 1570 (s), 1560 (s), 1489 (s), 1439 (s), 1428 (s), 1156 (s), 1064 (m), 837 (s), 748 (s), 698 (m).

Zn-containing 1-butyl-3-(3-(5-tetrazoyl)propyl)imidazolium (3e). White powder, 76 % yield, glass transition temperature (DSC) T_g = 91.29 °C; onset for 5% decomposition, $T_{5\%dec} = 321.12$ °C; ¹H NMR (500 MHz, DMSO-*d*₆) δ ppm 9.14

(s, 1H), 9.14 (s, 1H), 7.73 (s, 1H), 4.16 (t, $J = 6.89$ Hz, 2H), 4.11 (t, $J = 7.23$ Hz, 2H), 2.86 (t, $J = 7.35$ Hz, 2H), 2.20-2.11 (m, 2H), 1.78-1.69 (m, 2H), 1.22 (dd, $J = 14.99, 7.45$ Hz, 2H), 0.85 (t, $J = 7.37$ Hz, 3H); ^{13}C NMR (125 MHz, DMSO- d_6) δ ppm 160.335, 136.502, 122.943, 122.914, 49.182, 48.929, 31.673, 28.979, 21.405, 19.343, 13.807. FT-IR: 3493 (w), 3108 (w), 2942 (w), 2061 (s), 1565 (s), 1426 (s), 1337 (m), 1161 (s), 1074 (m), 1021 (s), 834 (m), 743 (s).

Zn-containing 1-(4-(5-tetrazoyl)butyl)-3-methylimidazolium (3f). Yellowish solid, 79 % yield, glass transition temperature (DSC), none observed; onset for 5% decomposition, $T_{5\% \text{dec}} = 304.31$ °C; ^1H NMR (500 MHz, DMSO- d_6) δ ppm 9.07 (s, 1H), 7.68 (d, $J = 24.35$ Hz, 2H), 4.14 (t, $J = 6.96$ Hz, 2H), 3.83 (s, 1H), 2.87 (t, $J = 6.82$ Hz, 3H), 1.79-1.75 (m, 2H), 1.58 (q, 2H); ^{13}C NMR (125 MHz, DMSO- d_6) δ ppm 161.375, 137.000, 124.183, 122.774, 49.114, 36.443, 29.628, 25.685, 23.769. FT-IR: 3514 (w), 3104 (w), 2946 (w), 2061 (s), 1570 (s), 1486 (m), 1426 (s), 1337 (m), 1161 (s), 1074 (m), 1019 (w), 829 (m), 743 (s).

Zn-containing 1-butyl-3-(4-(5-tetrazolyl)butyl)imidazolium (3g). Dark yellow waxy solid, 67 % yield, glass transition temperature (DSC) $T_g = 71.93$ °C; onset for 5% decomposition, $T_{5\% \text{dec}} = 306.44$ °C; 9.19 (s, 1H), 7.77 (d, $J = 10.07$ Hz, 2H), 4.32-3.89 (m, 4H), 2.92 (t, $J = 7.34$ Hz, 2H), 1.79 (dd, $J = 14.80, 7.23$ Hz, 4H), 1.64-1.55 (m, 2H), 1.26 (dd, $J = 14.94, 7.44$ Hz, 2H), 0.90 (t, $J = 7.34$ Hz, 3H); ^{13}C NMR (125 MHz, DMSO- d_6) δ ppm 161.037, 136.346, 122.930, 122.890, 49.155, 49.115, 31.685, 29.466, 25.547, 23.826, 19.313, 13.753. FT-IR: 3503 (w), 3099 (w), 2956 (w), 2066 (s), 1560 (s), 1489 (m), 1429 (s), 1158 (s), 1075 (m), 1019 (w), 829 (m), 743 (s).

Appendix A9

Utilization of ionic liquid-based synthetic strategies for the targeting of properties via the multiheterocyclic design platform

To complete the demonstration of the design platform for bridged multi-heterocycle synthesis initially addressed with formation of bicyclic zwitterion, cation, and anion products, it is necessary to show that IL-based synthetic strategies can be employed to direct the physiochemical properties of multi-heterocyclic targets within a desired range for specific properties (melting point, for example). Here, the synthesis of a novel tri-heterocyclic system **10** as a zwitterion capable of being chemically transformed to either cationic (**11**) or anionic (**12**) components of new IL-based products is illustrated in Figure A9.1.

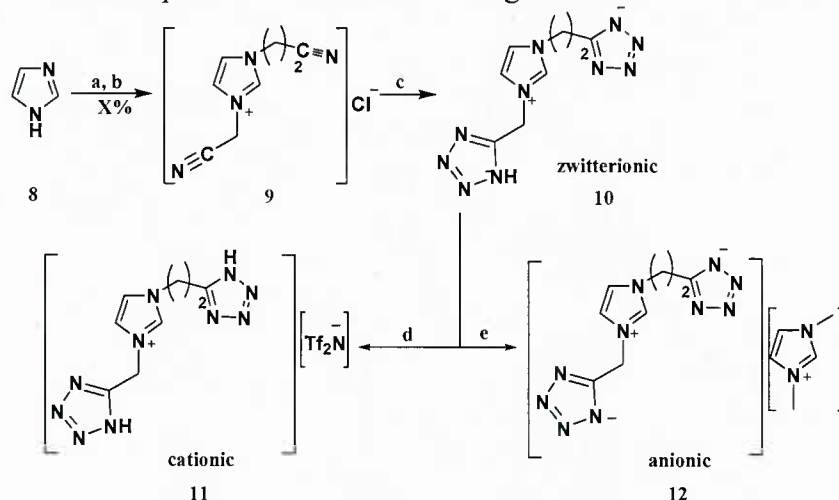


Figure A9.1. Top: Synthesis of zwitterionic **10** from **8**: (a) acrylonitrile (1 eq.), Et₃N (cat.), toluene, reflux, 30 h; (b) chloroacetonitrile, 70 °C, (c) NaN₃ (2.2 eq.), AcOH, 70 °C, 24 h.

Bottom: Synthesis of **11**, and **12** from zwitterionic **10**: (d) hydrogen bis(trifluoromethanesulfonyl)amide (HNTf₂), MeOH/Water 1/1, RT; (e) 1,3-dimethylimidazolium-2-carboxylate, MeOH/water 1/1, DMSO (cat.), RT, 6 h.

The preparation of 1-cyanomethyl-3-(2-cyanoethyl)imidazolium bromide (9). To a 50 mL round bottom flask, chloroacetonitrile (22 mmol, 1.627 g) is combined with 1-(2-cyanoethyl)imidazole (20 mmol, 2.423 g) and stirred for 24 hours at room temperature. The resulting mixture is washed several times with acetone to remove residual starting material and then dried on high vacuum for 48 hours to yield an amber liquid product, 87.0 % yield.

The preparation of 1-(2-(5-tetrazolidyl)ethyl)-3-(5-1H-tetrazolyl)methylimidazolium zwitterion (10). Azolium zwitterion, **10**, was achieved by reacting **9** (3.037 g, 20 mmol) with sodium azide (2.880 g, 44 mmol) in 10 mL of glacial acetic acid in a heated oil bath (60-70 °C) for 48 h. The mixture resulted in a suspended white solid in amber liquid, and the solid product was washed several times with dry ethanol. Final drying at high vacuum resulted in the final product. White solid, 78% yield. mp (DSC) $T_m = 49.4$ °C; onset of 5% decomposition, $T_{5\%onset} = 237.5$ °C, ¹H NMR (500 MHz, DMSO- *d*₆) δ ppm 9.27 (s, 1H), 7.75 (dd, $J = 10.47$ Hz, 2H), 5.55 (s, 2H), 4.64 (t, $J = 6.95$ Hz, 2H), 3.50 (t, $J = 6.97$ Hz, 2H); ¹³C (500 MHz, DMSO- *d*₆) δ ppm: 155.953, 154.151, 137.013, 123.361, 122.885, 46.868, 45.196, 24.732. FTIR (ν_{max}): 3143 (m), 3113 (m), 3043 (m), 2344 (br m), 1945 (br m), 1567 (s), 1459 (m), 1434 (m), 1234 (m), 1211

(m), 1170 (s), 1099 (s), 1045 (m), 950 (m), 872 (m), 860 (m), 802 (s), 761 (s), 744 (s), 690 (s), 665 (s).

The preparation of 1-(2-(5-1*H*-tetrazolyl)ethyl)-3-(5-1*H*-tetrazolyl)methylimidazolium bis(trifluoromethanesulfonyl)amide (11). The synthesis of **11** was carried out in the hood by reacting 123 mg (0.5 mmol) of zwitterion **10** and 140 mg (0.5 mmol) of hydrogen bis(trifluoromethanesulfonyl)amide (HNTf₂) in 10 mL of 1:1 methanol:water at RT for about 72 h in a 20 mL borosilicate glass vial. The mixture was kept at ambient conditions in order to allow the volatile solvent to evaporate and then water was removed by air stream. The product **11** was kept under high vacuum to afford a clear, viscous oil. Colorless oil, 80% yield. glass transition temperature (DSC) $T_g/T_m = 10.5\text{ }^{\circ}\text{C}$, $50.8\text{ }^{\circ}\text{C}$; onset for 5% decomposition, $T_{5\%\text{onset}} = 245.6\text{ }^{\circ}\text{C}$, ¹H NMR (500 MHz, DMSO- *d*₆) δ ppm 9.35 (s, 1H), 7.87 (dt, $J = 24.61\text{ Hz}$, 2H), 5.91 (s, 2H), 4.71 (t, $J = 6.81\text{ Hz}$, 2H), 3.54 (t, $J = 6.82\text{ Hz}$, 2H); ¹³C NMR (500 MHz, DMSO- *d*₆) δ ppm: 138.05, 123.83, 123.40, 121.40, 121.23, 118.67, 467.84, 43.07, 24.37. FTIR (ν_{max}): 3531 (w), 3245 (w), 3153 (m), 3090 (m), 1562 (s), 1442 (m), 1345 (s), 1183 (s), 1134 (s), 1054 (s), 791 (m), 741 (s).

The preparation of 1,3-dimethylimidazolium 1-(2-(5-tetrazolidyl)ethyl)-3-(5-tetrazolidyl)methyl-imidazolium (12). The synthesis of **12** was carried out in the hood by reacting 123 mg (0.5 mmol) of zwitterion **10** and 70 mg (0.5 mmol) of 1,3-dimethylimidazolium-2-carboxylate in 10 mL of a 1:1 solution of methanol:water (and 2 drops of DMSO) at RT for about 72 h in a 20 mL borosilicate glass vial. The mixture was kept at ambient conditions in order to allow the volatile solvent to evaporate and then water was removed by air stream. The compound was kept under high vacuum to afford a clear, viscous oil. Colorless oil, 78% yield. The NMR spectrum revealed the presence of 33% 1,3-dimethylimidazolium-2-carboxylate, which was removed by slow dissolution in hot acetone (6 x 2 mL). Yield of **12** after purification, 52%. glass transition temperature (DSC) $T_g/T_m = -24.4\text{ }^{\circ}\text{C}$, $44.9\text{ }^{\circ}\text{C}$; onset of 5% decomposition, $T_{5\%\text{onset}} = 224.4\text{ }^{\circ}\text{C}$, ¹H NMR (500 MHz, DMSO- *d*₆) δ ppm 9.21 (d, $J = 78.05\text{ Hz}$, 2H), 7.69 (dt, $J = 15.80, 15.54, 1.47\text{ Hz}$, 4H), 5.51 (s, 2H), 4.52 (t, $J = 7.23\text{ Hz}$, 2H), 3.84 (s, 1H), 3.21 (t, $J = 7.24\text{ Hz}$, 2H); ¹³C NMR (500 MHz, DMSO- *d*₆) δ ppm: 157.28, 156.11, 137.54, 136.70, 123.93, 122.93, 122.90, 48.66, 45.18, 36.15, 26.93. FTIR (ν_{max}): 3372 (w), 3149 (w), 3096 (m), 2956 (w), 2858 (w), 2602 (w), 2338 (w), 1727 (w), 1701 (w), 1656 (m), 1567 (s), 1516 (w), 1439 (m), 1397 (m), 1326 (m), 1229 (m), 1170 (s), 1111 (w), 1083 (w), 1051 (w), 1019 (w), 990 (w), 836 (w), 742 (s), 693 (w), 662 (w).

Appendix A10

Hypergolic Ionic Liquids for Monopropellant Applications

The published acid-base reaction (Drake, et al.,⁸⁹) was used to prepare 2-hydroxyethylhydrazinium nitrate $[\text{HO}(\text{CH}_2)_2\text{NHNH}_3][\text{NO}_3]$ (HEHN) and 2-hydroxyethylhydrazinium dinitrate $[\text{HO}(\text{CH}_2)_2\text{NH}_2\text{NH}_3][\text{NO}_3]$ (HEH2N). A preweighed 50 mL round bottom flask equipped with a condenser, a teflon stirbar, and a cooling bath was charged with 2-hydroxyethyl hydrazine (15 mmol, 1.140 g). Aqueous nitric acid (15.8 M, 15 mmol, 0.95 mL for HEHN or 1.9 mL for HEH2N) was added dropwise by means of an addition funnel. Excess heat evolved upon addition was removed via an ice bath. The clear homogenous solutions were stirred at ambient temperature overnight (*ca.* 12 h). At the end of this time, the stirbar was removed and the solvent removed by air stream for 12 h, resulting in colorless, viscous oils. The flasks and the viscous products were transferred to a vacuum line and kept under vacuum for another 10 h. The resulting materials were additionally dried in a 50 °C furnace, resulting in a yellowish viscous oil (HEHN; Yield: 97.6 %) and a viscous, clear oil liquid (HEH2N, Yield: 98.1 %), that crystallized within a week.

2-hydroxyethylhydrazinium nitrate $[\text{HO}(\text{CH}_2)_2\text{NHNH}_3][\text{NO}_3]$: ^1H NMR (360 MHz, DMSO- d_6) δ ppm 6.82 (s, 4H), 3.60 (t, $J = 5.29$ Hz, 2H), 2.98 (t, $J = 5.33$ Hz, 2H); ^{13}C (360 MHz, DMSO- d_6) δ ppm 56.641, 52.641; 3320 (w), 3052 (w), 2891 (w), 1610 (w), 1297 (s), 1154 (m), 1067 (m), 1040 (m), 926 (m), 823 (m); water contents of HEHN (7.8 %); density 1.423 g/mL

2-hydroxyethylhydrazinium dinitrate $[\text{HO}(\text{CH}_2)_2\text{NH}_2\text{NH}_3][\text{NO}_3]$: ^1H NMR (360 MHz, DMSO- d_6) δ ppm 7.06 (s, 5H), 3.61 (t, $J = 5.37$ Hz, 3H), 2.98 (t, $J = 5.40$ Hz, 3H); ^{13}C (360 MHz, DMSO- d_6) δ ppm 56.641, 52.641; 3141 (w), 2884 (w), 2641 (w), 1613 (w), 1556 (w), 1395 (m), 1280 (s), 1065 (m), 1023 (m), 970 (m), 821 (m); water contents HEH2N (3.9 %)

Appendix A11

Eutectic mixtures of Ionic Liquids

Synthesis of Azolium Azolate Salts. To 0.5 mmol of 4,5-dinitroimidazole or 5-nitro-1,2,3-triazole, dissolved in 50% aqueous ethanol (v/v), 0.5 mmol of 1,3-dimethylimidazolium-2-carboxylate, dissolved in 2 mL 50% aqueous ethanol (v/v) and 0.5 mL of DMSO was added dropwise. The reaction mixture was heated to 40 °C for 48 h, after which the solvent was removed *in vacuo* at 90 °C. Both samples were dried under high vacuum for 48 h at 50 °C to ensure all moisture was removed.

[1,3-diMeIm][4,5-diNO₂-Im]: Yellow, crystalline solid, mp 96 °C, $T_{5\%dec}$ (onset to 5% decomposition) 215 °C; ¹H NMR (360 MHz, [D₆] DMSO) δ = 3.84 (s, 6H, N-CH₃), 6.94 (C2'-H), 7.67 (s, 2H, C4/C5-H), 9.02 (s, 1H, C2-H); ¹³C NMR (90 MHz, [D₆] DMSO) δ = 35.55 (N-CH₃), 123.33 (C4/C5), 136.92 (C2), 139.25 (C2'), 140.16 (C4'/5'). [1,3-diMeIm][4-NO₂-1,2,3-Tri]: Yellow, crystalline solid, mp 74 °C, $T_{5\%dec}$ 187 °C; ¹H NMR (360 MHz, [D₆] DMSO) δ = 3.86 (s, 6H, N-CH₃), 7.69 (d, 2H, C4/C5-H), 8.04 (s, 1H, C4'-H), 9.08 (s, 1H, C2-H); ¹³C NMR (90 MHz [D₆] DMSO) δ = 35.57 (N-CH₃), 123.34 (C4/C5), 129.39 (C5'), 136.99 (C2), 154.1 (C4').

Synthesis of the Eutectic Mixture: 100.0 mg (0.714 mmol) of [1,3-dimethylimidazolium-2-carboxylate] was placed in a 10 mL round bottom flask and 2 mL of 9:1 EtOH:DMSO was added. To this solution, 40.6 mg (0.257 mmol) of 4,5-dinitroimidazole and 52.1 mg (0.457 mmol) of 5-nitro-1,2,3-triazole was added. The reaction was stirred for 24 h at 50 °C, after which time the solvents were evaporated first on the rotary evaporator at 60 °C, and then placed under high vacuum for an additional 12 h at 60 °C. The product, a eutectic mixture with the formula [1,3-diMeIm][4,5-diNO₂-Im]_{0.36}[4-NO₂-Tri]_{0.64} was obtained as a yellow solid in quantitative yield. The sample was analyzed by NMR and the spectra corresponds to the spectra of [1,3-diMeIm][4,5-diNO₂-Im] and [1,3-diMeIm][4-diNO₂-Tri] with the integration of peaks in the correct ratios for the ratio of starting materials. No carboxylate peak from the starting material was observed in the ¹³C NMR.

Appendix B

Analytical data for EILs (DSC, TGA, ARC, IR, etc.)

Appendix B1

Ionic Liquids Based on Azolate Anions

Melting point analyses.

Table B1.1. Melting point and glass transitions (°C) for **3-9(a-i)**[§]

		[Ph ₄ P] ⁺ (3)	[EtPh ₃ P] ⁺ (4)	[N-PhPyrr] ⁺ (5)	[1-Bu-3-Me-im] ⁺ (6)	[Bu ₄ N] ⁺ (7)	[Et ₄ N] ⁺ (8)	[Me ₄ N] ⁺ (9)
		mp (°C)	mp (°C)	mp (°C)	mp (°C)	mp (°C)	mp (°C)	mp (°C)
[5-NO ₂ -benztri] ⁻	(a)	145 ^[a,b]	131 ^[a]	75 ^[a]	-41 ^[c]	60 ^[a,b]	64 ^[a]	192 (at <i>T</i> _{dec})
[5-NO ₂ -benzim] ⁻	(b)	55 ^[a]	88 ^[a]	---	-34 ^[c]	81 ^[a]	101 ^[a,b]	119 ^[a,b]
[4-NO ₂ -1,2,3-tri] ⁻	(c)	155	97 ^[a]	135 ^[a,b]	-73 ^[c,d]	87 ^[d]	82 ^[d]	157 ^[d]
[4-NO ₂ -im] ⁻	(d)	171	100 ^[b]	---	-63 ^[c,d]	106 ^[d]	124 ^[d]	185 ^[d] (at <i>T</i> _{dec})
[3,5-diNO ₂ -1,2,4-tri] ⁻	(e)	171	127 ^[a]	167	33 ^[d]	139 ^[d]	114 ^[d]	214 ^[d] (at <i>T</i> _{dec})
[2,4-diNO ₂ -im] ⁻	(f)	195	70 ^[a]	143	-53 ^[c,d]	81 ^[d]	86 ^[d]	181 ^[d]
[4,5-diNO ₂ -im] ⁻	(g)	145 ^[a,b]	97 ^[a]	140	-64 ^[c,d]	85 ^[d]	84 ^[d]	215 ^[d] (at <i>T</i> _{dec})
[4,5-diCN-im] ⁻	(b)	149 ^[b]	-29 ^[c]	---	-74 ^[c,d]	79 ^[d]	118 ^[d]	197 ^[d] (at <i>T</i> _{dec})
[tetr] ⁻	(i)	290 (at <i>T</i> _{dec})	51 ^[a,b]	---	-82 ^[c,d]	-66 ^[c,d]	114 ^[d]	216 ^[d] (at <i>T</i> _{dec})

[§] Melting (mp) or glass transition (*T*_g) points (°C) were measured from the transition onset temperature and determined by DSC from the second heating cycle at 5 °C min⁻¹, after initially melting and then cooling samples to -100 °C unless otherwise indicated. Salts meeting the definition of ionic liquids (mp < 100 °C) are in **bold**. [a] Glass transition temperatures (°C) of supercooled liquids (i) with consecutive crystallization and melting on heating; **3a**, 30; **3b**, 22; **3g**, 15; **4a**, 9; **4c**, -8; **4e**, -5; **5c**, -19; **7a**, -32; **7b**, -21; **8a**, -38; **8b**, -30; **9b**, 22 (°C); (ii) with no crystallization and melting under experimental conditions: **4b**, 15; **4f**, -4; **4g**, -11; **4i**, 2; **5a**, 7 (°C). [b] Irreversible transition, from first heating; **3a**, 133; **3g**, 151; **3h**, 159; **4d**, 71, **4h**, 159; **4i**, 94; **5c**, 114; **7a**, 92; **8b**, 37; **9b**, 66 (°C). [c] Glass transitions on heating. [d] Reference 25.

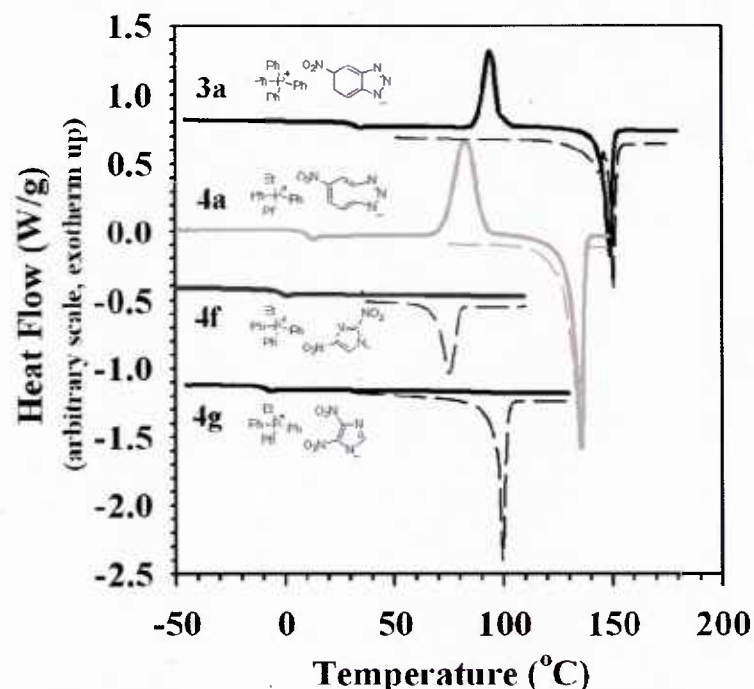


Figure B1.1. Examples of supercooled liquid behavior. The first heating cycle is shown as a dashed line and the second heating cycle is shown as a solid line. Samples **3a** and **4a** after initial melting did not crystallize on cooling, but formed supercooled phases, which upon the second heating cycle underwent a consecutive glass transition, crystallization, and melting. Samples **4f** and **4g** after initial melting did not crystallize, but formed supercooled phases, which upon heating exhibited glass transitions with no further thermal phase transitions.

Thermal Stability Analyses.

Table B1.2. Thermal stabilities (°C) for **3-9(a-i)**[§]

		[Ph ₄ P] ⁺ (3)	[EtPh ₃ P] ⁺ (4)	[N-PhPyr] ⁺ (5)	[1-Bu-3-Me-im] ⁺ (6)	[Bu ₄ N] ⁺ (7)	[Et ₄ N] ⁺ (8)	[Me ₄ N] ⁺ (9)
		<i>T</i> _{5%dec} (<i>T</i> _{dec}) (°C)	<i>T</i> _{5%dec} (<i>T</i> _{dec}) (°C)	<i>T</i> _{5%dec} (<i>T</i> _{dec}) (°C)	<i>T</i> _{5%dec} (<i>T</i> _{dec}) (°C)	<i>T</i> _{5%dec} (<i>T</i> _{dec}) (°C)	<i>T</i> _{5%dec} (<i>T</i> _{dec}) (°C)	<i>T</i> _{5%dec} (<i>T</i> _{dec}) (°C)
[5-NO ₂ -benztri] ⁻	(a)	273 (305) ^[a]	247 (279) ^[a]	158 (162) ^[a]	186 (209) ^[a]	174 (202)	178 (205)	177 (197)
[5-NO ₂ -benzim] ⁻	(b)	223 (256)	220 (270) ^[a]	---	177 (189) ^[a]	169 (194)	169 (193)	141 (161) ^[a]
[4-NO ₂ -1,2,3-tri] ⁻	(c)	273 (308) ^[a]	241 (284) ^[a]	192 (201) ^[a]	219 ^[b]	192 ^[b]	194 ^[b]	180 ^[b]
[4-NO ₂ -im] ⁻	(d)	232 (283) ^[a]	220 (253) ^[a]	---	200 ^[b]	193 ^[b]	188 ^[b]	165 ^[b]
[3,5-diNO ₂ -1,2,4-tri] ⁻	(e)	368 (402) ^[a]	284 (321) ^[a]	277 (296) ^[a]	239 ^[b]	219 ^[b]	205 ^[b]	235 ^[b]
[2,4-diNO ₂ -im] ⁻	(f)	339 (379) ^[a]	281 (317) ^[a]	258 (281) ^[a]	254 ^[b]	221 ^[b]	216 ^[b]	222 ^[b]
[4,5-diNO ₂ -im] ⁻	(g)	279 (322)	248 (289)	204 (224) ^[a]	241 ^[b]	222 ^[b]	215 ^[b]	225 ^[b]
[4,5-diCN-im] ⁻	(h)	361 (399) ^[a]	291 (330) ^[a]	---	230 ^[b]	215 ^[b]	212 ^[b]	202 ^[b]
[tetr] ⁻	(i)	291 (311) ^[a]	248 (285) ^[a]	---	208 ^[b]	180 ^[b]	184 ^[b]	198 ^[b]

[§] Decomposition temperatures shown were determined by TGA, heating at 5 °C min⁻¹ under dried air atmosphere and are reported as (i) onset to 5 wt% mass loss (*T*_{5%dec}) and (ii) onset to total mass loss (*T*_{dec}) (in parentheses). [a] *T*_{onset} data for a second decomposition step at temperature (°C) with percent decomposition (%), respectively: **3a**, 495 (35%); **3c**, 487 (12%); **3d**, 490 (18%); **3e**, 509, (20%); **3f**, 509 (13%); **3h**, 528 (14%); **3i**, 501 (10%); **4a**, 466 (35%); **4b**, 497 (17%); **4c**, 471 (12%); **4d**, 480 (16%); **4e**, 535 (8%); **4f**, 482 (11%); **4h**, 486 (9%); **4i**, 500 (10%); **5a**, 441 (65%); **5c**, 454 (61%); **5e**, 486 (59%); **5f**, 499 (62%); **5g**, 440 (60%); **6a**, 499 (36%); **6b**, 511 (45%); **9b**, 328 (31%). [b] Reference 25

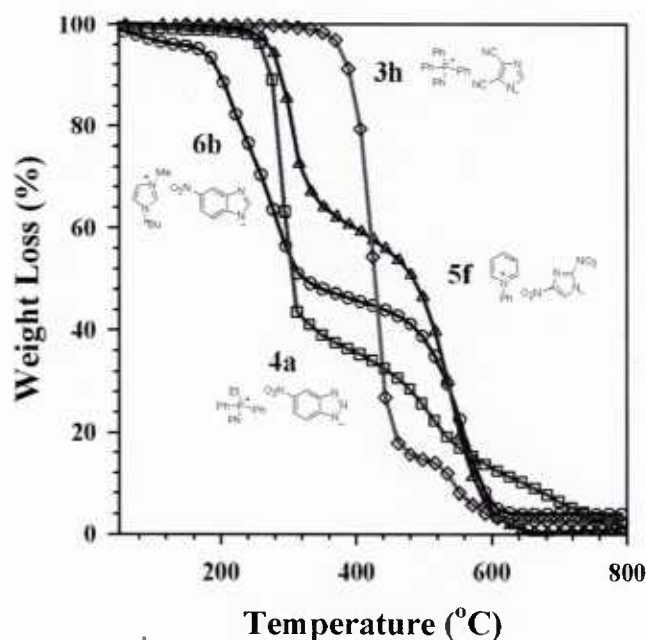


Figure B1.2. Examples of the observed thermal decomposition with distinguishable two step degradation: [Ph₄P][4,5-diCN-im] **3h** (-◇-), [Ph₃EtP][5-NO₂-benztri] **4a** (-□-), [N-PhPyr][2,4-diNO₂-im] **5f** (-Δ-), and [1-Bu-3-Me-im][5-NO₂-benzim] **6b** (-○-).

Appendix B2

New Hydrogen Carbonate Precursors for Efficient and Byproduct-Free Syntheses of Ionic Liquids Based

Melting point and thermal analysis. All synthesized compounds, along with their $[\text{HCO}_3]^-$ IL precursors, were thermally characterized. Melting points and decomposition temperatures were analyzed (Table 1) using differential scanning calorimetry (DSC) and thermogravimetric analysis (TGA). The results indicated the thermal stabilities of $[\text{MeCO}_3]^-$ and $[\text{HCO}_3]^-$ salts to be very low, with the lowest thermal stability recorded for $[1,2,3\text{-triMeIM}][\text{MeCO}_3]$ (onset temperature for 5% decomposition, $T_{5\%dec}$ = 104 °C). The $[\text{HCO}_3]^-$ salt of this cation exhibited a similar $T_{5\%dec}$ of 112 °C. In comparison, the thermal stability of $[N,N\text{-diMePyr}][\text{HCO}_3]$ was substantially higher ($T_{5\%dec}$ = 158 °C) than observed for the imidazolium salts.

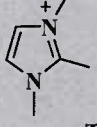
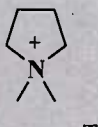
All of the analyzed salts formed by the reaction of the IL precursors with acids, exhibited thermal stabilities >200 °C. This increase in stability was expected since the new products are composed of stable anions that do not undergo any simple thermal decomposition, as normally found for $[\text{HCO}_3]^-$ and $[\text{MeCO}_3]^-$. The thermal stabilities of the $[1,2,3\text{-triMeIM}]^+$ -based salts ranged from 205 °C for $[1,2,3\text{-triMeIM}][\text{Cl}]$, to 258 °C for $[1,2,3\text{-triMeIM}][\text{NO}_3]$. In the case of the $[N,N\text{-diMePyr}]^+$ -based salts, the thermal stabilities ranged between 231 °C for $[N,N\text{-diMePyr}][\text{Cl}]$ to 276 °C $[N,N\text{-diMePyr}][\text{NO}_3]$.

The melting points of the obtained salts were also analyzed, however, due to the extreme hygroscopic nature of both $[\text{HCO}_3]^-$ -based salts, the determination of the melting point using DSC did not provide reliable results and visual melting point determination was attempted. In each of the $[\text{HCO}_3]^-$ -based samples, placing them directly on a glass slide resulted in fast moisture absorption and deliquescence of the compounds due to the water absorbed from the atmosphere. When the glass slide was placed on the hot stage apparatus and heated to ~100 °C, the absorbed water appeared to evaporate leaving a white powder on the slide. Continuous heating of the sample was carried out to the decomposition temperature, at which point the compounds simultaneously melted, evolved gasses, and turned brown in color.

DSC analyses of the $[1,2,3\text{-triMeIM}]^+$ salts, except for the $[\text{HCO}_3]^-$ and $[\text{ClO}_4]^-$ analogs, exhibited a sharp melting transition (on heating) and a sharp crystallization transition (on cooling). The melting points of the $[1,2,3\text{-triMeIM}]^+$ salts were surprisingly low, considering the high symmetry of the cation, and were between 64 °C for $[1,2,3\text{-triMeIM}][\text{NO}_3]$ and 104 °C for $[1,2,3\text{-triMeIM}][\text{Pic}]$. The melting transition for $[1,2,3\text{-triMeIM}][\text{ClO}_4]$ was not detected on the DSC instrument due to the safety limitations set for the DSC experimental protocol. Visual melting point analysis revealed that the sample remained solid until ~220 °C, at which point it melted and decomposed simultaneously. This finding was supported by a literature report where the melting point for $[1,2,3\text{-triMeIM}][\text{ClO}_4]$ was reported to be >250 °C.⁹²

DSC analysis of the melting points for the $[N,N\text{-diMePyr}]^+$ -based salts, did not result in determination of any melting point transitions within the allowed DSC temperature ranges (up to $T_{\text{DSCmax}} = T_{5\%dec} - 50$ °C to avoid decomposition of the analyzed compound in the DSC cell and its contamination). Thus, visual melting point analyses were performed, and revealed that the analyzed salts remain solid until, or very close to, their decomposition temperatures. In all cases the melting points were recorded to be >220 °C, and the melting transition translated directly to the beginning of the decomposition process. Literature reports, although limited, confirm these findings.^{90,91,93}

Table B2.1. Melting point transitions and decomposition temperatures of the [1,2,3-triMeIM]⁺ and [N,N-diMePyr]⁺-based salts.^a

Anion\Cation	 m.p. (°C) T _{5%dec} (°C)		 m.p. (°C) T _{5%dec} (°C)	
[MeCO ₃] ⁻	79	104	N/A	N/A
[HCO ₃] ⁻	-- ^c	112 ^d	-- ^c	158
[Cl] ⁻	71	205	~260 ^a (lit >350) ⁹⁰	231
[NO ₃] ⁻	63	259	~220 ^b	276
[Pic] ⁻	104	224	~280 ^b (lit >310) ⁹¹	269
[ClO ₄] ⁻	~220 ^b (lit >250) ⁹²	220	~280 ^b (lit >330) ⁹³	254

^aSalts melting below 100 °C, are shown in **bold**. ^bUsing a standard DSC protocol, the m.p. was not observed; visual m.p. analysis confirmed that the salt remains solid until its decomposition temperature, at which point it melts and decomposes simultaneously, changing to dark brown in color. ^cDue to the extreme hygroscopic nature of the sample, the determination of the m.p. was not possible. ^dHydrated salt decomposition.

Appendix B3

Ionic Liquid-Based Routes to Conversion or Reuse of Recycled Ammonium Perchlorate

Thermal Investigations. All four salts were examined by DSC and TGA using a standard protocol. From the DSC of **1**, a melting point of 148 °C (lit. 154–158 °C)^{94,95} was observed, with an additional transition observed at 2 °C. This melting point is a bit lower than the one found in the literature, and we assume that this may be caused by the compound's high hygroscopicity and thus fast absorption of water from the atmosphere. However, no detailed information on the methods used to determine the melting point range was provided in the literature. From its appearance, the transition at 2 °C was identified as a solid-state polymorph transition, and its reversibility indicated it to be polytropic.

Compound **2** proved to be comparably unstable and the TGA experiment resulted in an energetic decomposition at 262 °C. DSC runs were therefore not conducted past 150 °C, up to which temperature no thermal transitions were observed. In **3**, only a glass transition at $T_g = -77$ °C was observed. The DSC of **4** showed a melting point at 24.7 °C and from this standpoint it can be classified an IL.

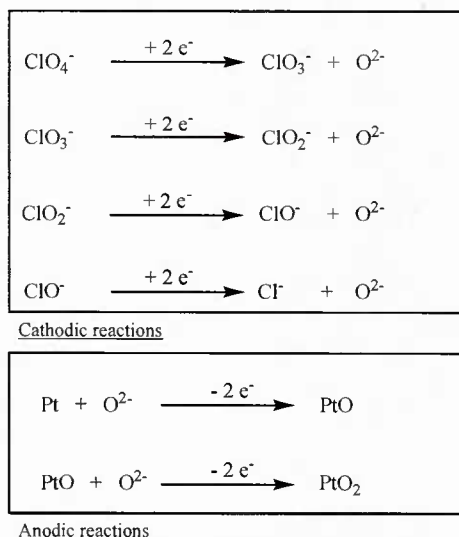
In TGA investigations, all salts showed stability at lower temperatures with almost no mass loss observed below 200 °C. Compound **1** exhibited a two-step decomposition with $T_{5\%dec} = 241$ °C, and an onset temperature for the second decomposition step of 495 °C. Salt **2** showed a more violent decomposition with $T_{5\%dec} = 244$ °C, after which a steady rate of decomposition was observed until 262 °C when it underwent extremely rapid, energetic decomposition. Compound **3** exhibited $T_{5\%dec} = 282$ °C. Above this temperature the IL showed a steady rate of decomposition up to 310 °C, when it underwent very rapid, total decomposition. Compound **4** decomposes in one step with $T_{5\%dec} = 254.5$ °C.

In contrast to these materials, AP itself generally shows a more controllable thermal decomposition,⁹⁶ which begins around 130 °C, but below its phase transition temperature of ~240 °C, does not undergo complete decomposition. While it is regarded as more generally thermally stable than NH₄NO₃, the stability of AP does depend on a variety of factors, including method of crystallization, preliminary treatment of crystals, how long they have been stored, and the purity of the salt.

Electrochemical investigation. To test the ability of a perchlorate-based IL to serve as reagent and electrolyte, we chose [P₆₆₆₁₄][ClO₄] (**4**) since the phosphonium cation is electrochemically more stable than imidazolium cations,⁹⁷ and this provides a wider electrochemical window. The cyclic voltammetry (CV) experiments carried out with neat **4** indicated that the perchlorate anions can be reduced on both gold (at -1.3 V and -2 V vs. Ag/Ag⁺) and on platinum (at -0.5 V and -1 V with a hump at -1.8 V) electrodes (Figures B3.1 and B3.2). When the potential range was increased (-3.5 V to 6 V) while using the gold electrodes, the perchlorate ions were adsorbed on the gold electrode surface which passivated the electroactive area and eventually reflected on the electrochemically inert behavior at both anodic and cathodic sides of the CV. Using platinum electrodes, when the potential window was increased, the current increased on the reduction peaks, showing that the electro-reduction of perchlorate was progressing.

The electrocatalytic reduction of perchlorate on Pt follows the mechanism in Scheme B3.1,⁹⁸ where desorption of the intermediates is negligible and platinum acts as a sacrificial anode. Perchlorate is reduced stepwise to chloride, while the platinum counter electrode is

simultaneously oxidized by the oxygen produced. The formation of PtO_2 (a dark brown solid that is soluble in aq. KOH) in the anode chamber was observed.



Scheme B3.1. Electrode reactions when reducing perchlorate on Pt electrodes.

This is, to the best of our knowledge, the first report of the electro-reduction of perchlorate from a system using ILs. In aqueous systems, the reduction of perchloric acid leads to the evolution of hydrogen which may significantly reduce the amount of perchlorate being transformed to chloride.⁹⁹ In our study, there are no acidic protons present and consequently no hydrogen evolution, allowing the electroreduction of perchlorate to proceed uninterrupted.

Based on this success, Pt was chosen as the material for the working electrode for subsequent bulk electrolysis experiments. As platinum is a very expensive material, nickel could be used as a sacrificial anode in bulk studies as shown by Rusanova *et al.*, for aqueous systems.⁹⁹

The bulk electrolysis experiment was carried out at -2 V vs. Ag/Ag^+ by chronoamperometry for 120 min on a Pt electrode at room temperature. During this bulk electrolysis of **4**, the electrochemical degradation of the perchlorate ions and their conversion into chloride ions was studied using IR and ^{35}Cl NMR. Samples were taken from the electrolytic cell periodically after 15, 30, 45, 90, and 105 min of electrolysis for analyses, and were also tested with AgNO_3 for the presence of chloride. The observed precipitation level of AgCl increased with the time of electrolysis, suggesting an increase in the chloride ion concentration in the electrolyte with time.

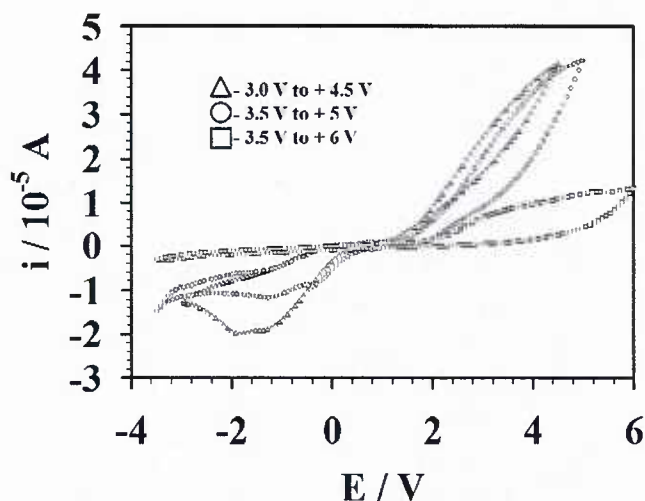


Figure B3.1. Electrochemical behavior of $[P_{66614}][ClO_4]$ on a Au electrode vs. Ag/Ag^+ at $50\text{ }^{\circ}C$ and 100 mV s^{-1} .

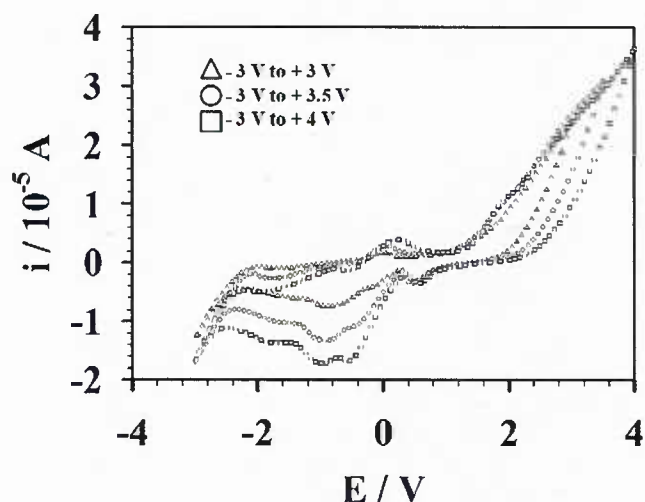


Figure B3.2. Electrochemical behaviour of $[P_{66614}][ClO_4]$ on a Pt electrode vs. Ag/Ag^+ at $50\text{ }^{\circ}C$ and 100 mV s^{-1} .

In the IR spectra (1 mM solutions of electrolyte, $[P_{66614}][ClO_4]$, in acetonitrile), the intensity of the perchlorate peak at 1081 cm^{-1} decreased with time of electrolysis, reflecting the reduction of the $[ClO_4]^-$ ions. In the ^{35}Cl NMR spectra, the peak around 1000 ppm was assigned to the $[ClO_4]^-$ anion, and the peak at 50 ppm was assigned to the Cl^- ion. As electrolysis time increased, the peak for perchlorate was diminished and the peak for chloride became prominent.

The complete disappearance of the perchlorate peak in the ^{35}Cl NMR does not, however, support that all the perchlorate anions have been converted to chloride during this short period of time. It is because the resolution of the perchlorate peak even in pure **4** was very poor when compared to that in AP, perhaps because of the rather high viscosity of the sample, or due to the lower symmetry of the phosphonium cation, compared to NH_4^+ .¹⁰⁰ However, the substantial decrease of the size of this peak in comparison to increasing size of the Cl^- peak allows us to speculate that substantial conversion is taking place.

To our knowledge we are the first to report the electrochemical degradation of perchlorate ions using an IL strategy while simultaneously recycling back the parent IL. It is conceivable

that due to the simplicity of the system and ability to recover the starting material $[P_{66614}]Cl$, that can later be reconverted back to **4**, using up further AP, the developed system could be used in a continuous fashion in the process of perchlorate removal and conversion to innocuous chloride (Figure B3.3).

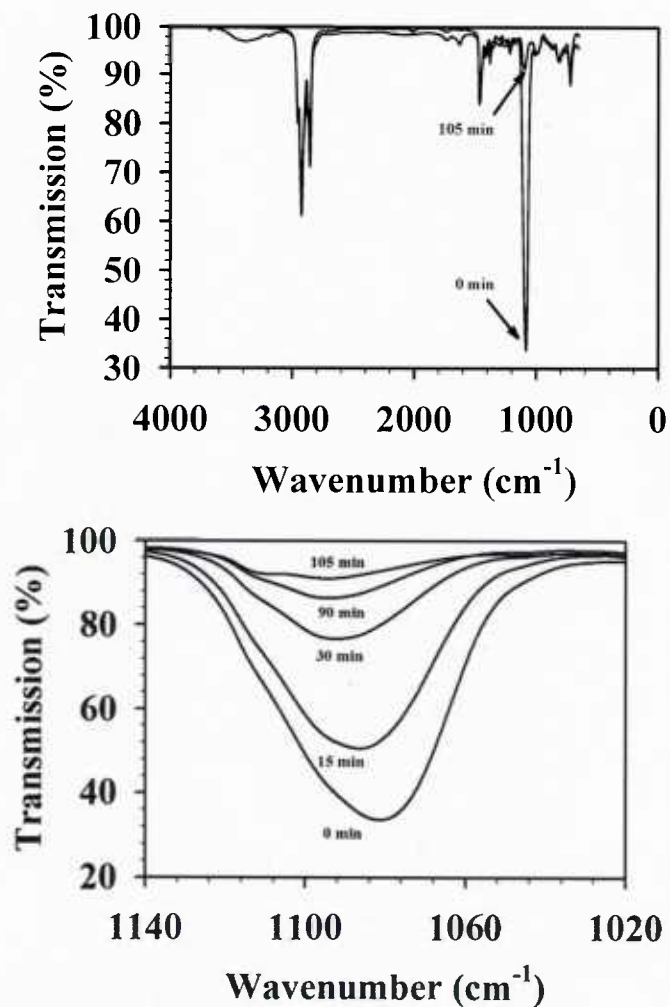


Figure B3.3. IR spectra of $[P_{66614}][ClO_4]$ in acetonitrile before (0 min) and after (105 min) electrolysis (top) and magnification of the perchlorate peak recorded during the electrolysis to monitor the degradation of perchlorate ions (bottom).

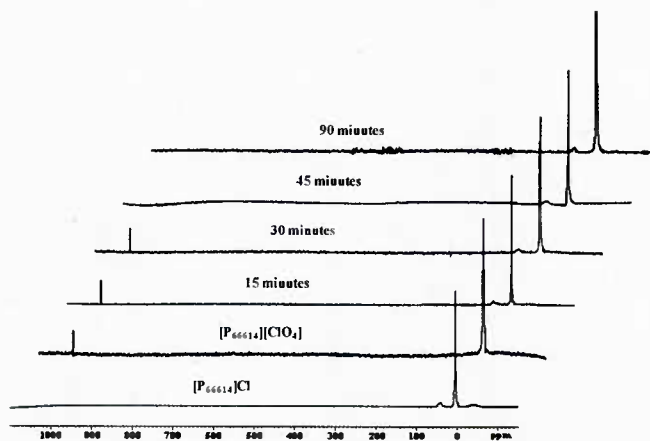


Figure B3.4. ^{35}Cl NMR spectra recorded during the electrolysis of $[\text{P}_{66614}][\text{ClO}_4]$ to determine the degradation of perchlorate ions and accumulation of chloride ions. The peak ~ 50 ppm is attributed to presence of $[\text{Cl}]^-$ anions present in the external standard (a saturated solution of 1.0 M NaCl in D_2O) and formed over time $[\text{Cl}]^-$ from the anion exchange reaction with $[\text{ClO}_4]^-$

Appendix B4

Azolium azolates from reactions of neutral azoles with 1,3-dimethylimidazolium-2-carboxylate, 1,2,3-trimethylimidazolium hydrogen carbonate, and *N,N*-dimethylpyrrolidinium hydrogen carbonate

Thermal Analyses. All synthesized compounds were thermally characterized. Melting points and decomposition temperatures were analyzed using differential scanning calorimetry (DSC) and thermogravimetric analysis (TGA) (Table B4.1). All analyzed salts exhibited thermal stabilities greater than 170 °C, with the exception of [*N,N*-diMePyr][3-NH₂-1,2,4-tri] for which T_{5%dec} (onset temperature for 5% decomposition) was recorded at 143 °C. In addition, all of the presented salts exhibited thermal stabilities higher than that of the starting IL carbonate precursors.

Table B4.1 Melting point transitions and decomposition temperature (°C) of analyzed families of [1,3-diMeIM]⁺, [1,2,3-triMeIM]⁺, and [*N,N*-diMePyr]⁺ azolate salts.

Anion/Cation	[1,3-diMeIM] ⁺		[1,2,3-triMeIM] ⁺		[<i>N,N</i> -diMePyr] ⁺	
	mp	T _{5%dec}	mp	T _{5%dec}	mp	T _{5%dec}
[4-NO ₂ -IM] ⁻	78	182 480 ^a	-- ^b	171 434 ^a	-- ^b	175
[2-Me-5-NO ₂ -IM] ⁻	112	178 485 ^a	126	182 420 ^a	128	179 391 ^a
[4,5-diNO ₂ -IM] ⁻	96	215	86	198 442 ^a	mp at T _{5%dec} (~220)	221 445 ^a
[4-NO ₂ -tri] ⁻	74	187	107	195 379 ^a	57	173 382 ^a
[3-NH ₂ -1,2,4-tri] ⁻	-- ^b	190	-- ^b	179	-- ^b	143
[5-NH ₂ -tetr] ⁻	84	206	160	202	138	178

Salts meeting the definition of ionic liquids (mp < 100 °C) are in **bold**. ^aObserved second decomposition step; ^b Due to the extremely hygroscopic character of the sample, the determination of melting point was not possible by DSC or by a visual method.

Among the 18 salts, six were classified as ILs, as they possess melting points below 100 °C. Most of the compounds generally exhibit broad melting transitions on heating and sharp crystallization transitions on cooling. Some evidence of supercooled behavior was observed, characterized by a lack of crystallization on cooling, presence of only a glass transition, followed by crystallization, and melting on heating. In five examples (two [*N,N*-diMePyr]⁺, two [1,2,3-triMeIM]⁺, and one [1,3-diMeIM]⁺) (Table B4.1), due to very high hygroscopicity of the samples, and thus difficulty in removing residual water, the melting points were not observed. For all those samples, measurements of melting points using a visual melting point apparatus were also attempted without success. Even when the samples were heated to temperatures of ~140 °C, in an attempt to remove any absorbed water, and then cooled down, no solid product was being formed. Such behavior can be associated with fast absorption of atmospheric water, or supercooled behavior of ILs. Presence of water in the sample was also confirmed by TGA analysis, where heating the samples to 100 °C in the TGA cell resulted in initial loss of mass,

and equilibration of the mass after solvent evaporation (no observed decomposition). For those samples, when the TGA cell was opened, a dramatic increase in the weight was noted indicating absorption of water from the atmosphere for a second time.

For all other salts, the melting points were able to be determined and ranged between 57 °C for $[N,N\text{-diMePyr}][4\text{-NO}_2\text{-tri}]$ and ~ 221 °C for $[N,N\text{-diMePyr}][4,5\text{-diNO}_2\text{-IM}]$, which melted at its decomposition temperature. Based on the anion structure, the lowest melting points were recorded for azolium salts with $[4,5\text{-diNO}_2\text{-IM}]^-$ and $[4\text{-NO}_2\text{-tri}]^-$ anions, with the exception of $[N,N\text{-diMePyr}][4,5\text{-diNO}_2\text{-IM}]$ (mp at $T_{5\% \text{dec}}$), which is in agreement to the results obtained for other similar salts reported previously²

The thermal stabilities of $[1,2,3\text{-triMeIM}]^+$ -based salts ranged from 171 °C for $[1,2,3\text{-triMeIM}][4\text{-NO}_2\text{-IM}]$, to 202 °C for $[1,3\text{-diMeIM}][5\text{-NH}_2\text{-tetr}]$. In case of $[1,3\text{-diMeIM}]^+$ -based salts, the thermal stabilities ranged between 178 °C for $[1,3\text{-diMeIM}][2\text{-Me-5-NO}_2\text{-IM}]$ and 215 °C $[1,3\text{-diMeIM}][4,5\text{-diNO}_2\text{-IM}]$. Similar decomposition temperatures were recorded for the $[N,N\text{-diMePyr}]^+$ -based salts with $T_{5\% \text{dec}}$ ranging between 143 °C for $[N,N\text{-diMePyr}][3\text{-NH}_2\text{-1,2,4-tri}]$ and 221 °C for $[N,N\text{-diMePyr}][4,5\text{-diNO}_2\text{-IM}]$.

Small differences between the decomposition temperatures of salts with the same anion lead to the general conclusion that it is the structure of the anion that grossly contributes to the thermal stability ranges of the formed salts. For example, when comparing the influence of the structural modification between $[4\text{-NO}_2\text{-IM}]^-$ and $[4\text{-NO}_2\text{-tri}]^-$ -based salts, a slight increase in the thermal stability was observed when shifting to the triazolate-based compound. A similar observation was made previously,² when comparing the thermal properties of other $[4\text{-NO}_2\text{-IM}]^-$ and $[4\text{-NO}_2\text{-tri}]^-$ -based salts. Along the same lines, when replacing a carbon atom in the core of $[3\text{-NH}_2\text{-1,2,4-tri}]^-$ with a nitrogen atom resulting in the structure of $[5\text{-NH}_2\text{-tetr}]^-$, an increase in decomposition temperature was observed. Also, when comparing the $T_{5\% \text{dec}}$ between $[4\text{-NO}_2\text{-IM}]^-$ and $[2\text{-Me-5-NO}_2\text{-IM}]^-$, where the only difference between analyzed anions is the presence of the methyl group on the C2 position of the heterocyclic anion in the later, it was found that the decomposition temperature did not change substantially, varying ± 10 °C. finally, it was noted that the introduction of an additional NO_2 - substituent going from $[4\text{-NO}_2\text{-IM}]^-$ to $[4,5\text{-diNO}_2\text{-IM}]^-$, caused an increase in the $T_{5\% \text{dec}}$ between 24 and 46 °C. A similar trend was observed for compounds reported earlier.²

Appendix B5

Synthesis of *N*-cyanoalkyl-substituted imidazolium halide and nitrate salts with variable *N*-alkyl and *N*-cyanoalkyl chain lengths, and the characterization of their structural and thermal properties as potential energetic ionic liquids

Melting points and thermal stability analyses.

Table B5.1. Thermal stabilities (onset to 5% decomposition) and melting/glass transitions of synthesized *N*-cyanoalkyl-functionalized imidazolium nitrate salts.

R' =	$T_{\text{onset 5\%}} (^{\circ}\text{C})$		$T_{\text{m}} / T_{\text{g}} (^{\circ}\text{C})$	
	R = Me	R = Bu	R = Me	R = Bu
-CH ₂ CN	189.0 (3a)	177.0 (3b)	-33.2 (3a)	-37.9 (3b)
-CH(CH ₃)CN	192.8 (3c)	190.0 (3d)	-43.0 (3c)	-50.9 (3d)
-(CH ₂) ₂ CN	184.0 (3e)	191.7 (3f)	-58.4 (3e)	-52.1 (3f)
-(CH ₂) ₃ CN	280.8 (3g)	273.6 (3h)	-52.0 (3g)	-55.2 (3h)
-(CH ₂) ₄ CN	279.8 (3i)	278.0 (3j)	-52.0 (3i)	-54.7 (3j)

Melting points (T_{m}) and glass transitions (T_{g}) were measured from the transition onset temperature and determined by DSC from the 2nd heating cycle at 5 °C·min⁻¹, after initial melting and cooling samples to -100 °C. Decomposition temperatures shown were determined by TGA, heating at 5 °C·min⁻¹ under dried air atmosphere and are reported as 5 wt% mass loss ($T_{\text{onset 5\%}}$).

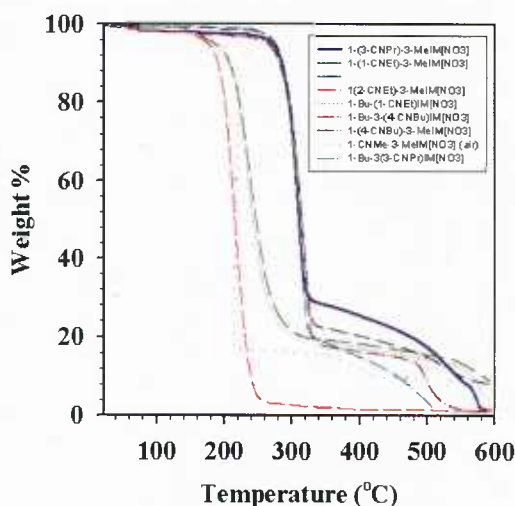


Figure B5.1. Comparative thermogravimetric analysis (TGA) plots of *N*-cyanoalkyl-functionalized imidazolium nitrate salts **3a-j**.

Comments.

- Number in parentheses, e.g. (3a), indicates the identity of the nitrate salt.
- Overall, with decreasing *N*-cyanoalkyl chain lengths, thermal stabilities of the nitrate salts were observed to decrease (Figure B5.1, $T_{\text{onset } 5\%}$), and melting points were observed to increase (Table B5.1, T_m/T_g).
- Although the thermal stabilities did not seem to differ greatly between *N*-methyl and *N*-butyl-substituted salts, the *N*-butyl salts did show a lower observed T_m/T_g in comparison with their shorter chain analogues.
- In comparing the TGA plots for all nitrate salts **3a-j** (Figure B5.1), the results indicate that most form thermally stable by-products after the initial onset of decomposition. However, the *N*-(2-cyanoalkyl)-substituted salts seem to be the exception to this trend, where near complete decomposition is observed. Possibly, the full decomposition is driven by the elimination of acrylonitrile as a leaving group in the decomposition process of *N*-(2-cyanoethyl)-functionalized salts. Considering the other salts, there is evidence reported in the literature to suggest that nitriles are capable of cyclizing or polymerizing under high heat, and these thermal products are much more stable than the starting materials.

Appendix B6

Synthesis of *N*-cyanoalkyl- and *N,N*-dicyanoalkyl-substituted imidazolium halide and dicyanamide salts with variable *N*-cyanoalkyl chain lengths, and the characterization of their structural and thermal properties as potential energetic ionic liquids

Melting points, thermal stability and impact sensitivity analyses

Table B6.1. Thermal stabilities (onset to 5% decomposition) and melting/glass transitions for synthesized *N*-cyanoalkyl- and *N,N*-dicyanoalkyl-functionalized imidazolium dicyanamide salts, **3a-k**.

Mono <i>N</i> -cyanoalkyl imidazolium dicyanamides			
R' (Compound)	T _{5%onset} (°C)	T _m (°C)	Impact (kg·cm)
-CH ₂ CN (3a)	186.6	-58.9 / 53.9	>200
--(CH ₂) ₂ CN (3b)	158.4	-66.7 / 11.9	172
--(CH ₂) ₃ CN (3c)	243.2	-79.7	170
--(CH ₂) ₄ CN (3d)	238.2	-76.4	170
--(CH ₂) ₅ CN (3e)	260.3	-78.5 / 58.4	170
--(CH ₂) ₆ CN (3f)	263.1	-77.2 / 47.5	174
<i>N,N</i> -di(cyanoalkyl)imidazolium dicyanamides			
-CH ₂ CN (3g)	144.80	-27.6 / 60.0	176
--(CH ₂) ₃ CN (3h)	161.8	-61.2 / 71.2	176
--(CH ₂) ₄ CN (3i)	167.5	-60.8 / 50.4	174
--(CH ₂) ₅ CN (3j)	162.6	-65.6 / 53.3	164
--(CH ₂) ₆ CN (3k)	154.2	-66.7 / 57.7	170

Melting points (T_m) and glass transitions (T_g) were measured from the transition onset temperature and determined by DSC from the 2nd heating cycle at 5 °C·min⁻¹, after initial melting and cooling samples to -100 °C. Decomposition temperatures shown were determined by TGA, heating at 5 °C·min⁻¹ under dried air atmosphere and are reported as 5 wt% mass loss ($T_{onset\ 5\%}$). Impact sensitivity measurements were obtained via drop-hammer test (Edwards AFB).

Comments.

- All mono-*N*-cyanoalkyl-functionalized imidazolium dca salts showed a general decrease in thermal stability with decreasing *N*-cyanoalkyl chain length (Table B6.1, $T_{onset\ 5\%}$). This drop was most dramatic when considering salts with *N*-cyanomethyl and *N*-(2-cyanoethyl)-functionalized cations (**3a** and **3b**, respectively).
- Thermal stabilities were relatively similar when comparing *N,N*-dicyanoalkyl-functionalized salts (**3g-k**), and the proximity of their $T_{onset\ 5\%}$ values to that of **3b** suggests the possibility of similar decomposition pathways (e.g., acrylonitrile elimination).
- In collaboration with Dr. Tommy Hawkins and coworkers at Edwards AFB, the impact sensitivity for dicyanamide salts **3a-k** were assessed using drop-hammer instrumental technique. The very high values obtained (last column of Table B6.1) indicate that all compounds are insensitive to mechanical impact and, in combination with their very low melting/phase transitions, might suggest successful future design options for liquids fuels.

Appendix B7

Introduction and initial demonstration of synthetic design platform for bridged multi-heterocycles with variable charge, structure, and symmetry options: Formation of 5-tetrazole-based products using a three step procedure of azole ‘click’ functionalization, ‘click’ synthesis of bi-heterocyclic precursors, and further product modification utilizing IL-based synthetic strategies

Melting points and thermal stability analyses.

Table B7.1. Thermal stabilities (onset to 5% decomposition) and melting/phase transitions of synthesized bi-heterocyclic products and their precursors, **1-4, 6, 7**.

Compound	$T_{\text{onset 5\%}}$ (°C)	T_g/T_m (°C)
1-cyanomethyl-3-methylimidazolium chloride (1)	221.1	178.7
1-(5-tetrazolidyl)methyl-3-methylimidazolium (ZnBrCl) (2)	306.9	None
1-(5-1 <i>H</i> -tetrazolyl)methyl-3-methylimidazolium chloride (3)	213.1	155.5
1-(5-tetrazolidyl)methyl-3-methylimidazolium zwitterion (4)	241.0	124.8
1-(2-cyanoethyl)-1,2,4-triazole (6)	120.4	31.43
Sodium 1-(2-(5-tetrazolidyl)ethyl)1,2,4-triazole (7)	313.7	None

Melting points (T_m) and glass transitions (T_g) were measured from the transition onset temperature and determined by DSC from the 2nd heating cycle at 5 °C·min⁻¹, after initial melting and cooling samples to -100 °C. Decomposition temperatures shown were determined by TGA, heating at 5 °C·min⁻¹ under dried air atmosphere and are reported as 5 wt% mass loss ($T_{\text{onset 5\%}}$).

Comments.

- The thermal data for all synthesized bi-heterocyclic products (**1-4** and **7**, Table B7.1) indicate that none are ILs by definition based upon melting point.
- Metal-containing compounds **2** and **7** both show very high thermal stability with virtually no phase transition. These results suggest that the material is metal coordination polymer, as similar thermal properties are noted for related compounds in the literature.

Appendix B8

Click synthesis and thermal characterization of zinc-containing, alkyl-bridged imidazolium-tetrazolates with highly variable *N*-alkyl and alkyl bridge lengths as expansion of bridged multiheterocyclic design platform

Melting points and thermal stability analyses.

Table B8.1. Thermal stabilities (onset to 5% decomposition) and melting/glass transitions of synthesized Zn-containing, alkyl-bridged imidazolium-tetrazolate zwitterions, **3a-g**.

(CH ₂) _n	<i>T</i> _{5%decomp} (°C)		<i>T</i> _m (°C)	
	R = Me	R = Bu	R = Me	R = Bu
1	307 (3a)	305 (3b)	none (3a)	none (3b)
2	266 (3c)	-----	none (3c)	-----
3	322 (3d)	321 (3e)	-52.68 (3d)	none (3e)
4	304 (3f)	306 (3g)	none (3f)	none (3g)

Melting points (*T*_m) and glass transitions (*T*_g) were measured from the transition onset temperature and determined by DSC from the 2nd heating cycle at 5 °C·min⁻¹, after initial melting and cooling samples to -100 °C. Decomposition temperatures shown were determined by TGA, heating at 5 °C·min⁻¹ under dried air atmosphere and are reported as 5 wt% mass loss (*T*_{onset 5%}).

Comments.

- All products were obtained as Zn-containing zwitterions (**3a-g**), where high thermal stabilities and no melting/glass transitions were observed (Table B8.1).

Appendix B9

Utilization of ionic liquid-based synthetic strategies for the targeting of properties via the multiheterocyclic design platform

Melting points and thermal stability analyses.

Table B9.1. Thermal stabilities (onset to 5% decomposition) and melting/glass transitions for synthesized tri-heterocyclic zwitterion, **10**, and tri-heterocyclic-based ILs **11** and **12**.

Compound	$T_{5\%onset}$ (°C)	T_{onset} (°C)	T_g/T_m (°C)
1-(2-(5-tetrazolidyl)ethyl)-3-(5-1 <i>H</i> -tetrazolyl)-methylimidazolium, (10)	237.54	247.43	49.44
1-(2-(5-1 <i>H</i> -tetrazolyl)ethyl)-3-(5-1 <i>H</i> -tetrazolyl)-methylimidazolium bis(trifluoromethanesulfonyl)amide, (11)	245.58	345.01	10.50
1,3-dimethylimidazolium 1-(2-(5-tetrazolidyl)ethyl)-3-(5-tetrazolidyl)methylimidazolium, (12)	224.37	235.69	-24.45

Melting points (T_m) and glass transitions (T_g) were measured from the transition onset temperature and determined by DSC from the 2nd heating cycle at 5 °C·min⁻¹, after initial melting and cooling samples to -100 °C. Decomposition temperatures shown were determined by TGA, heating at 5 °C·min⁻¹ under dried air atmosphere and are reported as 5 wt% mass loss ($T_{onset\ 5\%}$).

Comments.

- Upon reaction, the zwitterionic **10** was converted to both cationic and anionic components for two new room temperature ionic liquids (Table B9.1, **11** and **12**, respectively).
- All three products **10-12** are thermally stable, and the formation of ILs from the zwitterion **10** does not introduce thermal instability for the new products (thermal stability actually increases in the case of the cationic form of the tri-heterocyclic salt, **11**).

Appendix B10

Hypergolic Ionic Liquids for Monopropellant Applications

Melting points and thermal stability analyses.

Table B10.1. Summary of thermal analysis data

Compound	TGA (°C) [†]	DSC (°C) [‡]	Thermal Stability*
2-hydroxyethylhydrazine (HEH)	T _{onset} = 181.98 T _{5% dec} = 102.10 T _{dec} = 195.94	T _g = -72.11	-88.1 % weight loss
2-hydroxyethyl hydrazinium nitrate (HEHN)	T _{onset} = 214.10 T _{5% dec} = 193.63 T _{dec} = 259.67	T _g = -56.91	-23.8 % weight loss
2-hydroxyethyl hydrazinium dinitrate (HEH2N)	T _{onset} = 91.51 T _{5% dec} = 62.71 T _{dec} = 101.01	T _g = -47.89, T _m = 67 °C	-43.8% weight loss

2-Hydroxyethylhydrazinium nitrate (HEHN) and 2-hydroxyethylhydrazinium dinitrate (HEH2N) were prepared as reported by Drake. Differential Scanning Calorimetry (DSC) analysis of HEHN indicated a glass transition temperature (T_g) of $-56.9\text{ }^{\circ}\text{C}$ and no other observable transition, while HEH2N was found to have a melting point of $67\text{ }^{\circ}\text{C}$ and when supercooled a T_g of $-47.9\text{ }^{\circ}\text{C}$. HEHN was the most thermally stable with $T_{5\% \text{dec}}$ (onset to 5% decomposition) = $193\text{ }^{\circ}\text{C}$, versus $T_{5\% \text{dec}}$ for HEH2N (a solid) = $62\text{ }^{\circ}\text{C}$. Under these experimental conditions, $T_{5\% \text{dec}}$ for HEH was determined to be $102\text{ }^{\circ}\text{C}$, however, this is associated with its boiling point ($113\text{ }^{\circ}\text{C}$) rather than thermal decomposition. These data indicate substantial improvement (ca. $100\text{ }^{\circ}\text{C}$) in the temperature range of use for HEHN over HEH, while the thermal stability of HEH2N was found to be substantially lower than that of HEHN or HEH.

The longer term stability, measured by heating each sample to $75\text{ }^{\circ}\text{C}$ for 24 h (as suggested by AFOSR) decreases in the order HEHN > HEH2N > HEH. HEHN lost 24% of its mass after 24 h, with ca. 8% of this from loss of water (supported by Karl-Fisher titration). HEH2N lost 43% of its mass, of which ca. 4% was water. (It should be noted that even substantial dilution of hydrazine with water results in mixtures that function satisfactorily as rocket fuels, and the resultant systems retain the characteristics of hydrazine.¹⁰¹) By comparison, HEH lost 88% of its mass under these conditions, underscoring the anticipated improvements in lowering the volatility of HEH by converting it to its salt forms. This does also suggest that the salt forms of HEH would reduce the risk of human exposure to toxic vapors.

Appendix B11

Eutectic mixtures of Ionic Liquids

The previously reported techniques for the eutectic point analysis,¹⁰² even though using DSC instruments and samples sizes between 2 and 10 mg during each run, often require larger quantities (often > 500 mg) of each component to be milled together prior to the analysis. This introduces (i) the risk of non-homogenous mixing, (ii) the possibility of partial compound spillage, introducing error to the calculated composition, (iii) point overheating during the milling process which can cause partial decomposition, and (iv) for samples that are hygroscopic (common for many ILs), inaccurate mass calculations of the weighed mixture. All of these can result in inaccurate determination of the enthalpy of the eutectic peak necessary for precise eutectic point identification.

Our modification of the general protocol for eutectic determination^{103,104} allows for the precise eutectic point analysis of mixtures of compounds that (i) are either very difficult to obtain or expensive to purchase, (ii) have hazardous properties that restricts their usage in larger scale due to safety issues, or (iii) are sensitive (e.g., energetic compounds) which restricts the processing (e.g., milling) usually performed on samples prior to calorimetric analysis.

DSC Protocol: (1) Two separate solutions of the ILs were prepared by dissolving 1 mmol of [1,3-diMeIm][4-NO₂-Tri] or 1 mmol [1,3-diMeIm][4,5-diNO₂-Im] in water in 5 mL volumetric flasks with dry N₂ gas blown over the sample and balance. The volumetric flasks were placed under high vacuum at 50 °C for 6 h, after which time they were reweighed and water (polished to 18.1-18.2 MΩ-cm (Nanopure, Barnstead, Dubuque, IA) was added. The drying and refilling cycle allowed determination of the true mass of the salts used, since this was difficult to establish during the first weighting due to extremely high hygroscopicity of the samples.

(2) Homogenous solutions, containing various mole fractions (0.00, 0.15, 0.20, 0.25, 0.30, 0.50, 0.60, 0.625, 0.65, 0.666, 0.70, 0.75, 0.80, 0.90, 1.00) of [1,3-diMeIm][4-NO₂-Tri] and [1,3-diMeIm][4,5-diNO₂-Im] were prepared to yield a total of 50 μmol of each solution.

(3) The samples were concentrated by placement in a vacuum desiccator for 6 h at room temperature. Thereafter, concentrated solutions were transferred into pre-weighed DSC aluminum pans. The open pans were then dried under high vacuum for additional 12 h at 50 °C, after which time the pans were closed and reweighed. The final mass of the mixture of ILs was designed to be between 9 and 13 mg in each pan.

(4) The DSC protocol for determination of sample melting points involved three heating cycles and two cooling cycles. (The results of the first heating cycle were disregarded.) Each DSC cycle involved: (i) initial heating to 120 °C (heating rate 5 °C/min), (ii) isotherm at 120 °C for 20 min to allow any possible water present in the sample to evaporate, (iii) cooling to 0 °C (heating rate 10 °C/min), (iv) isotherm at 0 °C for 5 min, (v) heating to 120 °C (heating rate 2.5 °C/min), (vi) repeat steps ii-v.

(5) The results were taken from the third heating cycle, and were plotted as the molar ratio of [1,3-diMeIm][4-NO₂-Tri] to [1,3-diMeIm][4,5-diNO₂-Im] (Figure 4 and Figure 5).

(6) The melting transition peaks were integrated using PeakFit® software (Systat Software, Inc, San Jose, CA, USA). The residuals procedure used for the determination initially places peaks by finding local maxima in a smoothed data stream. Hidden peaks are then optionally added where peaks in the residuals occur.

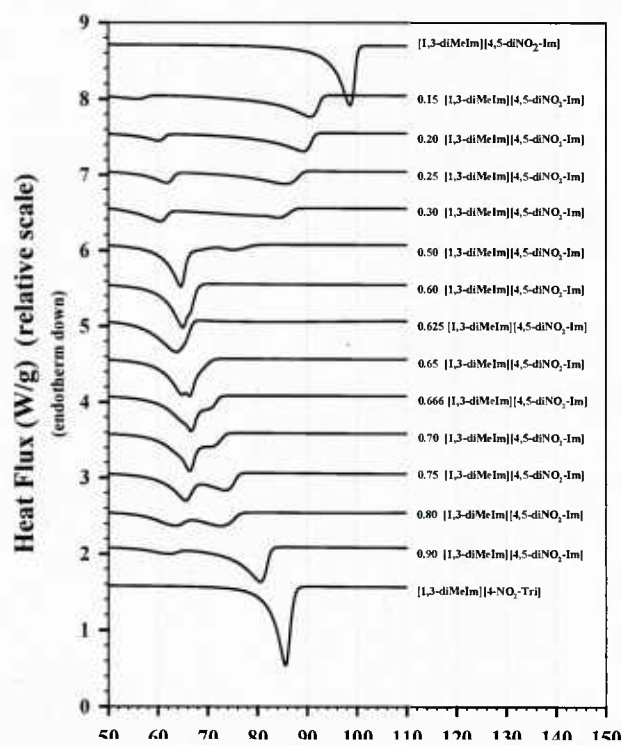


Figure B11.1. Thermal transitions of different mole fractions of mixtures of [1,3-diMeIm][4-NO₂-Tri] and [1,3-diMeIm][4,5-diNO₂-Im].

Table B11.1. Melting point maximums and enthalpy of transition for analyzed mixture of salts with varying molar ratio of components.

Mole fraction of [1,3-diMeIM][4- NO ₂ -tri]	Melting point (at maximum) of the component in excess to the eutectic composition				Melting point (at maximum) of the eutectic peak (°C)	Enthalpy of eutectic peak (J/g)
	[1,3-diMeIM][4,5-diNO ₂ -IM] mp _{max} (°C)	Enthalpy of transition (J/g)	[1,3-diMeIM][4-NO ₂ -tri] mp _{max} (°C)	Enthalpy of transition (J/g)		
0.00	98.50	91.64				0.00
0.15	95.03	68.44			55.91	13.78
0.20	90.61	63.68			60.14	21.98
0.25	89.31	51.98			61.90	34.45
0.30	85.73	55.69			60.36	35.60
0.50	84.40	9.50			64.68	65.10
0.60	75.39	11.95			64.98	73.69
0.625	66.52	2.53			63.76	81.12
0.65			66.25	30.17	64.70	78.50
0.666			70.37	10.48	66.61	71.02
0.70			70.84	15.78	66.29	72.93
0.75			73.86	33.94	65.54	58.50
0.80			74.09	24.79	63.33	39.99
0.90			80.57	80.18	62.27	21.57
1.00			85.72	101.43		0.00

Appendix C

Protocols and equipment

Appendix C1

NMR analyses. NMR spectra were obtained in DMSO-*d*₆ or D₂O with TMS or residual hydrogen signals in the deuterated solvent used as the internal standard for ¹H (360 or 500 MHz) and for ¹³C (90 or 125 MHz).

Appendix C2

TGA analysis. Thermal decomposition temperatures were measured in the dynamic heating regime using a TGA 2950 TA Instrument under helium, nitrogen, argon and air atmospheres. Samples between 2-10 mg were heated from 40–600 °C under constant heating at 5 °C min⁻¹.

Appendix C3

DSC analysis. Melting points of the isolated salts were determined by differential scanning calorimetry (DSC) using a TA Instruments model 2920 Modulated DSC (New Castle, DE) cooled with a liquid nitrogen cryostat. The calorimeter was calibrated for temperature and cell constants using indium (melting point 156.61 °C, ΔH = 28.71 J g⁻¹). Data were collected at constant atmospheric pressure, using samples between 10-40 mg in aluminum sample pans sealed using pin-hole caps. Experiments were performed heating at 5 °C min⁻¹. The DSC was adjusted so that zero heat flow was between 0 and -0.5 mW, and the baseline drift was less than 0.1 mW over the temperature range 0-180 °C. An empty sample pan was used as reference; matched sample and reference pans (within ± 0.20 mg) were used.

Appendix C4

PXRD analysis (powder X-ray diffraction). Bulk sample compositions were investigated using a Rigaku Powder Diffractometer (Woodlands, TX) at 25 °C with Cu/Kα radiation (λ = 1.5418 Å) in the 2θ range 10-50 °. Step intervals were taken at 0.1 ° steps at 1.2 ° min⁻¹. Peaks were normalized in each scan to the highest peak in the spectrum. Then each spectrum was overlaid, offset, and combined to a single graph.

XRD analysis (single crystal X-ray diffraction). Data for all single crystal structural determinations were collected on a Bruker CCD area detector-equipped diffractometer with graphite monochromated Mo/Kα radiation (λ = 0.71073 Å) and structures solved using SHELXTL. Absorption corrections were made with SADABS. All non-hydrogen atoms were readily located and refined anisotropically. The structures were refined by full-matrix least squares on *F*². In cases of disorder, alternate positions were found and refined with alternating least-squares cycles. All hydrogen atoms were found from a difference Fourier map unless otherwise stated.

Appendix C5

FT-IR analysis. Infrared (IR) analyses were obtained by direct measurement of the neat samples at room temperature by utilizing a Perkin-Elmer 100 FT-IR instrument featuring an ATR force gauge, and spectra were obtained in the range of $\nu_{\text{max}} = 650 - 4000 \text{ cm}^{-1}$.

Appendix C6

Electrochemical analysis. All electrochemistry experiments were carried out at room temperature unless stated otherwise, using a computer controlled Autolab PGSTAT (Eco Chemie B. V., The Netherlands) potentiostat. A conventional three electrode electrochemical system consisting of a platinum disc as a working electrode, platinum coil as a counter electrode, and Ag/Ag^+ as the reference electrode was used. The counter and reference electrode compartments were filled with the same electrolyte as the bulk ($[\text{P}_{66614}][\text{ClO}_4]$), but were separated from the bulk electrolyte by a glass frit. This reduces the contamination of the bulk electrolyte by the by-products from the counter electrode during electrolysis. For voltammetric measurements, working electrodes purchased from BioAnalytical Systems (Warwickshire, UK) were used. Prior to each experiment, the electrodes were polished on soft lapping pads with alumina slurry of size 1 and $0.3 \mu\text{m}$ and then washed with distilled water and dried by compressed air. All samples were degassed with Ar prior to measurement.

References

- Huddleston, J. G.; Visser, A. E.; Reichert, W. R.; Willauer, H. D.; Broker, G. A.; Rogers, R. D. *Green Chem.*, **2001**, *3*, 156.
- Smiglak, M.; Hines, C. C.; Wilson, T. B.; Singh, S.; Vincek, A. S.; Kirichenko, K.; Katritzky, A. R.; Rogers, R. D. "Ionic Liquids Based on Azolate Anions," *Chem. Eur. J.* **2009**, *16*, 1572–1584. (accepted as VIP paper).
- Drab, D. M.; Smiglak, M.; Hines, C. C.; Rogers, R. D., "Synthesis and thermal characterization of homologous *N*-cyanoalkyl-functionalized imidazolium nitrate salts as dual-functional energetic ionic liquids," **2010**, *in preparation*.
- Drab, D. M.; Smiglak, M.; Shamshina, J. L.; Schneider, S.; Hawkins, T. W.; Rogers, R. D., "Synthesis and determination of thermal characteristics for a new, homologous series of *N*-cyanoalkyl and *N,N*-dicyanoalkyl-functionalized imidazolium dicyanamide ionic liquid salts," **2010**, *in preparation*.
- Smiglak, M.; Hines, C. C.; Rogers, R. D., "Azolium azolates from reactions of neutral azoles with 1,3-dimethylimidazolium-2-carboxylate, 1,2,3-trimethylimidazolium hydrogen carbonate, and *N,N*-dimethylpyrrolidinium hydrogen carbonate," **2010**, *in preparation*.
- Smiglak, M.; Hines, C. C.; Rogers, R. D. "New Hydrogen Carbonate Precursors for Efficient and Byproduct-Free Syntheses of Ionic Liquids Based on 1,2,3-Trimethylimidazolium and *N,N*-Dimethylpyrrolidinium Cores," *Green Chem.* **2009**, *accepted*.
- Bridges, N. J.; Hines, C. C.; Smiglak, M.; Rogers, R. D. "An intermediate for the clean synthesis of ionic liquids: Isolation and crystal structure of 1,3-dimethylimidazolium hydrogen carbonate monohydrate," *Chem. Eur. J.* **2007**, *13*, 5207.
- Cordes, D. B.; Smiglak, M.; Hines, C. C.; Bridges, N. J.; Dilip, M.; Srinivasan, G.; Metlen, A.; Rogers, R. D. "Ionic Liquid-Based Routes to Conversion or Reuse of Recycled Ammonium Perchlorate," *Chem. Eur. J.* **2009**, *Early View*, DOI: 10.1002/chem.200901217.
- Drab, D. M.; Shamshina, J. L.; Smiglak, M.; Hines, C. C.; Cordes, D. B.; Rogers, R. D., "A General Design Platform for Ionic Liquid Ions Based on Bridged Multi-Heterocycles with Flexible Symmetry and Charge," *Chem. Commun.* *submitted*.
- Drab, D. M.; Smiglak, M.; Shamshina, J. L.; Rogers, R. D., "Click synthesis and thermal characterization of zinc-containing, alkyl-bridged imidazolium-tetrazolates," **2010**, *in preparation*.
- Shamshina, J. L.; Smiglak, M.; Drab, D. M.; Dykes, Jr., W. H.; Reich, A. J.; Rogers, R. D., "Hypergolic Ionic Liquids for Monopropellant Applications," **2010**, *in preparation*.
- Smiglak, M.; Bridges, N. J.; Dilip, M.; Rogers, R. D. "Direct, Atom Efficient, and Halide Free Syntheses of Azolium Azolate Energetic Ionic Liquids and Their Eutectic Mixtures, and Method for Determining Eutectic Composition," *Chem. Eur. J.* **2008**, *36*, 11314.
- Smiglak, M.; Metlen, A.; Rogers, R. D. "The Second Evolution of Ionic Liquids - From Solvents and Separations to Advanced Materials: Energetic Examples from the Ionic Liquid Cookbook" *Acc. Chem. Res.*, **2007**, *40*, 1182.
- Drab, D. M.; Smiglak, M.; Rogers, R. D. "Ionic liquids as a unique and versatile platform for the synthesis and delivery of energetic materials," In Proceedings for 54th JANNAF Propulsion Meeting, Denver, CO, (May 14-17, 2007), 62.
- Laas, H.-J.; Halpaap, R.; Richter, F.; Kocher, J. *US Pat. App. Pub.* 20030204041, 2003.
- Stearcey, M.; Pye, P. L.; Lee, J. B. *Synth. Commun.* **1989**, *19*, 1309.
- Ogihara, W.; Yoshizawa, M.; Ohno, H. *Chem. Lett.* **2004**, *33*, 1022.
- Ohno, H.; Yoshizawa, M.; Ogiwara, W.; Ogawa, H.; Taguchi, H. *Jpn. Pat.* 2004331521, 2004.
- Xue, H.; Gao, Y.; Twamley, B.; Shreeve, J. M. *Inorg. Chem.* **2005**, *44*, 5068.
- Ye, C. F.; Xiao, J. C.; Twamley, B.; Shreeve, J. M. *Chem. Commun.* **2005**, 2750.
- Xue, H.; Twamley, B.; Shreeve, J. M. *J. Mat. Chem.* **2005**, *15*, 3459.
- Tao, G.-H.; Guo, Y.; Joo, Y.-H.; Twamley, B.; Shreeve, J. M. *J. Mater. Chem.* **2008**, *18*, 5524.
- Liotta, C. L.; Pollet, P.; Belcher, M. A.; Aronson, J. B.; Samanta, S.; Griffith, K. N. *US Pat.*, 20050269001 A1, 2005.
- Klapötke, T. M.; Sabaté, C. M.; Welch, J. M. *Dalton Trans.* **2008**, 6372.
- Katritzky, A. R.; Singh, S.; Kirichenko, K.; Smiglak, M.; Holbrey, J. D.; Reichert, W. M.; Spear, S. K.; Rogers, R. D. *Chem. Eur. J.* **2006**, *12*, 4630.

- 26 Hammerl, A.; Hiskey, M. A.; Holl, G.; Klapotke, T. M.; Polborn, K.; Stierstorfer, R.; Weigand, J. J. *Chem. Mat.* **2005**, *17*, 3784.
- 27 Hammerl, A.; Holl, G.; Klapotke, T. M.; Mayer, P.; Noth, H.; Piotrowski, H.; Warchhold, M. *Eur. J. Inorg. Chem.* **2002**, *4*, 834.
- 28 Lee, K. Y.; Ott, D. G.; Stinecipher, M. M. *Ind. Eng. Chem. Proc. Des. Dev.* **1981**, *20*, 358-360.
- 29 Lee, K. Y.; Ott, D. G. *U.S. Pat. US4236014*, 1979.
- 30 Habiger, K. W.; Clifford, J. R.; Miller, R. B.; McCullough, W. F. *Proc. IEEE Particle Accelerator Conf.* **1994**, *4*, 2622.
- 31 Yasaka, Y.; Wakai, C.; Matubayasi, N.; Nakahara, M. *Anal. Chem.* **2009**, *81*, 400.
- 32 Urbanek, M.; Varenne, A.; Gebauer, P.; Krivankova L.; Gareil, P. *Electrophoresis* **2006**, *27*, 4859.
- 33 Li, Z.; Du, Z.; Gu, Y.; Zhu, L.; Zhang X.; Deng, Y. *Electrochem. Commun.* **2006**, *8*, 1270.
- 34 Berthier, D.; Varenne, A.; Gareil, P.; Digne, M.; Lienemann, C-P.; Magna, L.; Olivier-Bourbigou, H. *Analyst* **2004**, *129*, 1257.
- 35 Urbansky, E. T. *Environ. Sci. Pollut. Res.* **2002**, *9*, 187.
- 36 An introduction to energetic materials from SNPE Matériaux Energétiques website.
<http://www.energetic-materials.com/en/news.shtml> (last accessed February 27, 2009).
- 37 (a) Katritzky, A. R.; Yang, H.; Zhang, D.; Kirichenko, K.; Smiglak, M.; Holbrey, J. D.; Reichert, W. M.; Rogers, R. D. *New J. Chem.* **2006**, *3*, 349; (b) Katritzky, A. R.; Singh, S.; Kirichenko, K.; Smiglak, M.; Holbrey, J. D.; Reichert, W. M.; Spear, S. K.; Rogers, R. D. *Chem. Eur. J.* **2006**, *12*, 4630; (c) Singh, R. P.; Verma, R. D.; Meshri, D. T.; Shreeve, J. M.; *Angew. Chem. Int. Ed.* **2006**, *45*, 3584; (d) Ye, C.; Xiao, J.-C.; Twamley, B.; Shreeve, J. M. *Chem. Commun.* **2005**, 2750; (e) Hammerl, A.; Hiskey, M. A.; Holl, G.; Klapötke, T. M.; Polborn, K.; Stierstorfer, J.; Weigand, J. J. *Chem. Mater.* **2005**, *17*, 3784; (f) Xue, H.; Gao, Y.; Twamley, B.; Shreeve, J. M. *Inorg. Chem.* **2005**, *44*, 5068; (g) Astakhov, A. M.; Vasiliev, A. D.; Molokeev, M. S.; Sirotinin, A. M.; Kruglyakova, L. A.; Stepanov, R. S. *J. Struct. Chem.* **2004**, *45*, 175; (h) Katritzky, A. R.; Singh, S.; Kirichenko, K.; Holbrey, J. D.; Smiglak, M.; Reichert, W. M.; Rogers, R. D. *Chem. Commun.* **2005**, 868; (i) Hammerl, A.; Holl, G.; Kaiser, M.; Klapötke, T. M.; Kranzle, R.; Vogt, M. Z. *Anorg. Allg. Chem.* **2002**, *628*, 322.
- 38 (a) Hawkins, T.; Hall, L.; Tollison, K.; Brand, A.; McKay, M.; Drake, G. W. *Propellants, Explos., Pyrotech.* **2006**, *31*, 196; (b) Gao, Y.; Ye, C.; Twamley, B.; Shreeve J. M. *Chem. Eur. J.* **2006**, *12*, 9010; (c) Xue, H.; Gao, H.; Twamley, B.; Shreeve, J. M. *Eur. J. Inorg. Chem.* **2006**, *15*, 2959; (d) Gao, Y. Arritt, S. W. Twamley, B.; Shreeve, J. M. *Inorg. Chem.* **2005**, *44*, 1704; (e) Drake, G. W.; Hawkins, T. W.; Hall, L. A.; Boatz, J. A.; Brand, A. J. *Propellants, Explos., Pyrotech.* **2005**, *30*, 329; (f) Xue, H.; Gao, Y.; Twamley, B.; Shreeve, J. M. *Chem. Mat.* **2005**, *17*, 191; (g) Xue, H.; Twamley, B.; Shreeve, J. M. *J. Mat. Chem.* **2005**, *15*, 3459; (h) Drake, G. W. Hawkins, T. W. Boatz, J. Hall, L. Vij, A. *Propellants, Explos., Pyrotech.* **2005**, *30*, 156; (i) Xue, H.; Shreeve, J. M. *Adv. Mat.* **2005**, *17*, 2142; (j) Xue, H. Arritt, S. W. Twamley, B. Shreeve, J. M. *Inorg. Chem.* **2004**, *43*, 7972; (k) Drake, G. Hawkins, T.; Brand, A.; Hall, L.; Mckay, M.; Vij, A.; Ismail, I. *Propellants, Explos., Pyrotech.* **2003**, *28*, 174.
- 39 Trumpolt, C. W.; Crain, M.; Cullison, G. D.; Flanagan, S. J. P.; Siegel, L.; Lathrop, S. *Remediation* **2005**, *16*, 65.
- 40 (a) Przesławski, J.; Czapla, Z. *J. Phys.: Condens. Matter* **2006**, *18*, 5517; (b) Pająk, Z.; Czarnecki, P.; Szafrńska, B.; Małuszyńska, H.; Fojud, Z. *J. Chem. Phys.* **2006**, *124*, 144502/1; (c) Czapla, Z.; Dacko, S.; Kosturek, B.; Waśkowska, A. *Phys. Status Solidi B* **2005**, *242*, R122.
- 41 (a) Luboš, A.; Točík, Z.; Bradková, E.; Hostomský, Z.; Pačes, V.; Smrt, J. *Collect. Czech. Chem. Commun.* **1989**, *54*, 523; (b) Dean, R. L.; Wood, J. L. *J. Mol. Struct.* **1975**, *26*, 197.
- 42 Cammarata, L.; Kazarian, S. G.; Salter, P. A.; Welton, T. *Phys. Chem. Chem. Phys.* **2001**, *3*, 5192.
- 43 (a) Nadaf, R. N.; Siddiqui, S. A.; Daniel, T.; Lahoti, R. J.; Srinivasan, K. V. *J. Mol. Catal. A: Chem.* **2004**, *214*, 155; (b) Gholap, A. R.; Venkatesan, K.; Daniel, T.; Lahoti, R. J.; Srinivasan, K. V. *Green Chem.* **2003**, *5*, 693.
- 44 Astolfi, D. L.; Mayville, F. C. Jr. *Tetrahedron Lett.* **2003**, *44*, 9223.
- 45 Mokhtarani, B.; Mojtahedi, M. M.; Mortaheb, H. R.; Mafi, M.; Yazdani, F.; Sadeghian, F. *J. Chem. Eng. Data* **2008**, *53*, 677.

- 46 (a) Smiglak, M. Holbrey, J. D. Griffin, S. T. Reichert, W. M. Swatloski, R. P. A. R. Katritzky, H. Yang, D. Zhang, K. Kirichenko, R. D. Rogers, *Green Chem.* **2007**, *9*, 90; (b) N. J. Bridges, C. C. Hines, M. Smiglak, R. D. Rogers, *Chem. Eur. J.* **2007**, *13*, 5207.
- 47 Lang, G. G.; Inzelt, G.; Vrabec, A.; Horányi, G. *J. Electroanal. Chem.* **2005**, *582*, 249.
- 48 Hammerl, A.; Hiskey, M. A.; Holl, G.; Klapotke, T. M.; Polborn, K.; Stierstorfer, R.; Weigand, J. J. *Chem. Mat.* **2005**, *17*, 3784.
- 49 Hammerl, A.; Holl, G.; Klapotke, T. M.; Mayer, P.; Noth, H.; Piotrowski, H.; Warchhold, M. *Eur. J. Inorg. Chem.* **2002**, *4*, 834.
- 50 Katritzky, A. R.; Singh, S.; Kirichenko, K.; Holbrey, J. D.; Smiglak, M.; Reichert, W. M.; Rogers, R. D. *Chem. Commun.* **2005**, 868.
- 51 Schneider, S.; Hawkins, T.; Rosander, M.; Vaghjiani, G.; Chambreau, S.; Drake, G. *Energ Fuel* **2008**, *22*, 2871.
- 52 Haixiang G.; Young-Hyuk, J.; Brendan T.; Zhiqiang Z.; Shreeve, J. M. *Angew. Chem. Int. Ed.* **2009**, *48*, 2792.
- 53 In: *Properties of Hydrazine and Its Applications as an Energy Source*. Forbes, F. *Colloq. Int.* **1975**, p. 127.
- 54 Chambreau, S. D.; Gallegos, C. J.; Vaghjiani, G. L. Abstracts of Papers, 235th ACS National Meeting, New Orleans, LA, United States, April 6-10, 2008.
- 55 Blumenthal, J.; Guth, E. U.S. Patent 3732694, issued 15 May, 1973.
- 56 Hubbuch, T. N.; Murfree, J. A., Jr.; Duncan, W. A.; Sandlin, B. J.; Nappier, H. A. U.S. Patent 3710573, issued 16 January 1973.
- 57 <http://www.calepa.ca.gov/>, last accessed 12-10-09.
- 58 Klapotke, T. M.; Rienacker, C. M.; Zewen, H. Z. *Anorg. Allg. Chem.* **2002**, *628*, 2372.
- 59 Paustian, J. E. U.S. Patent 3769389, issued 15 October, 1973.
- 60 Dendage, P. S.; Sarwade, D. B.; Mandale, A. B.; Asthana, S. N. *J. Energ. Mat.* **2003**, *21*, 167.
- 61 Jadhav, H. S.; Talawar, M. B.; Dhavale, D. D.; Asthana, S. N.; Krishnamurthy, V. N. *Ind. J. Chem. Tech.* **2005**, *12*, 187.
- 62 Welch, D. E.; Hein, R. W., US Patent 3491160; issued 1 January, 1970.
- 63 Hussain, S.; Mattie, D. R.; Frazier, J. M. CPIA Publication **2002**, 709.
- 64 Gutowski, K. E.; Gurkan, B.; Jayaraman, S.; Maginn, E. J. 236th ACS National Meeting, Philadelphia, PA, United States, August 17-21, 2008. Publisher: American Chemical Society, Washington, D. C.
- 65 Knollmueller; K. O. Manke; S. A., Migliaro; F. W.; Rothgery; E. F. U.S. Patent 5433802, issued 18 July, 1995.
- 66 Wood, S. E.; Bryant, J. T. *Ind. Eng. Chem. Prod. Res. Dev.* **1973**, *12*, 117.
- 67 Armstrong, W. E.; Ryland, L. B.; Voge, H. H. U.S. Patent 4124538, issued 7 November, 1978.
- 68 Soares T.G. *Appl. Surf. Sci.* **2005**, *240*, 355.
- 69 Izgorodina, E. I.; Forsyth, M.; MacFarlane, D. R. *Aust. J. Chem.* **2007**, *60*, 15.
- 70 Borra, E. F.; Seddiki, O.; Angel, R.; Eisenstein, D.; Hickson, P.; Seddon, K. R.; Worden, S. P. *Nature* **2007**, *447*, 979.
- 71 Carter, M. T.; Hussey, C. L.; Strubinger, S. K. D.; Osteryoung, R. A. *Inorg. Chem.* **1991**, *30*, 1149.
- 72 Swatloski, R. P.; Spear, S. K.; Holbrey, J. D.; Rogers, R. D. *J. Am. Chem. Soc.* **2002**, *124*, 4974.
- 73 Abbott, A. P.; Cullis, P. M.; Gibson, M. J.; Harris, R. C.; Raven, E. *Green Chem.*, **2007**, *9*, 868.
- 74 Domanska, U.; Casas, L. M. *J. Phys. Chem. B* **2007**, *111*, 4109.
- 75 Sifaoui, H.; Ait-Kaci, A.; Modarressi, A.; Rogalski, M. *Thermochim. Acta* **2007**, *456*, 114.
- 76 Wonga D. S. H.; Chena, J. P.; Changa, J. M.; Choub, C. H. *Fluid Phase Equilib.* **2002**, *194*, 1089.
- 77 Domanska, U.; Bakala, I.; Pernak, J. *J. Chem. Eng. Data* **2007**, *52*, 309.
- 78 Abbott, A. P.; Boothby, D.; Capper, G.; Davies, D. L.; Rasheed, R. K. *J. Am. Chem. Soc.* **2004**, *126*, 9142.
- 79 Zhu, Q.; Song, Y.; Zhu X.; Wang, X. *J. Electroanal. Chem.*, **2007**, *601*, 229.
- 80 http://research.chem.psu.edu/brpgroup/pKa_compilation.pdf, last accessed July 20, 2009.
- 81 Kortüm, G.; Vogel, W.; Andrussov, K. *Pure Appl. Chem.*, **1961**, *1*, 364.
- 82 Silverstein, R. M.; Webster, F. X. in *Spectrometric Identification of Organic Compounds*, 6th Ed.; John Wiley and Sons, New York, 1998; p 103.
- 83 Socrates, G. in *Infrared and Raman Characteristic Group Frequencies*, John Wiley and Sons, Ltd.,

- Chichester, 2001.
- 84 Holbrey, J. D.; Reichert, W. M.; Tkatchenko, I.; Bouajila, E.; Walter, O.; Tommasi, I.; Rogers, R. D. *Chem. Commun.* **2003**, 28.
 - 85 (a) Krausa, K.; Moore, G. *J. Am. Chem. Soc.*, **1953**, 75, 1460; (b) Kallmann, S.; Steele, C. G.; Chui, N. Y. *Anal. Chem.*, **1954**, 28, 230; (c) Bishay, T. Z. *Anal. Chem.*, **1972**, 44, 1087; (d) Strelow, F. W. E. *Anal. Chem.*, **1978**, 50, 1359; (e) Sweileh, J. A.; El-Nemma, E. M. *Anal. Chim. Acta* **2004**, 523, 287; (f) Archer, C.; Vance, D. J. *Anal. At. Spectrom.*, **2004**, 19, 656; (g) Borrok, D. M.; Wanty, R. B.; Ridley, W. I.; Wolf, R.; Lamothe, P. J.; Adams, M. *Chem. Geol.* **2007**, 242, 400.
 - 86 Svehla, G. Ed. *Vogel's Qualitative Inorganic Analysis*, ed. G. Svehla, Longman Scientific & Technical, Essex, U.K., 1987, p. 126.
 - 87 To each eluted volume, concentrated HNO₃ was added until pH neutral or slightly acidic to neutralize ambient OH⁻ anions that can interfere with the AgNO₃ test. Then, an equal volume of 0.1 M AgNO₃ was added to a sample of the elute fraction (1 mL to 1 mL) and observed for precipitation. At the end of 1 L of elution, the precipitation was quite faint, detecting < 10% Cl⁻ anion from the resin.
 - 88 Nomenclature for these coordination polymers constructed based upon guidelines from McCleverty, J. A.; Connolly, N. G. (Eds.) *Nomenclature of Inorganic Chemistry II: IUPAC Recommendations 2000* (2001), Royal Chemical Society Publishing: Cambridge, UK, 130 pp.
 - 89 Brand, A.; Drake, G. W. U.S. Patent 6218577, issued 17 April 2001.
 - 90 Kobler, H.; Munz, R.; Gasser G. Al.; Simchen, G. *Justus Liebigs Annalen der Chemie* **1978**, 12, 1937.
 - 91 Reppe, W. *Ann.* **1956**, 601, 128.
 - 92 Zoltewicz J. A.; O'Halloran, J. K. *J. Org. Chem.*, **1978**, 43, 1713.
 - 93 Leonard N. J.; Jann, K. *J. Am. Chem. Soc.*, **1962**, 84, 4806.
 - 94 Kiviniemi, S.; Nissinen, M.; Lämsä, M. T.; Jalonen, J.; Rissanen, K.; Pursiainen, J. *New J. Chem.* **2000**, 24, 47.
 - 95 Arnold, L.; Tocik, Z.; Bradkova, E.; Hostomsky, Z.; Paces, V.; Smrt, J. *Coll. Czech. Chem. Commun.* **1989**, 54, 523.
 - 96 Boldyrev, V. V. *Thermochim. Acta* **2006**, 443, 1.
 - 97 (a) Xiao, L.; Johnson, K. E. *J. Electrochem. Soc.* **2003**, 150, E307; (b) Santos, V. O.; Alves, M. B.; Carvalho, M. S.; Suarez, P. A. Z.; Rubim, J. C. *J. Phys. Chem. B* **2006**, 110, 20379; (c) Da Silveira Neto, B. A.; Ebeling, G.; Goncalves, R. S.; Gozzo, F. C.; Eberlin, M. N.; Dupont, J. *Synthesis* **2004**, 8, 1155.
 - 98 Lang, G. G.; Sas, N. S.; Ujvari, M.; Horányi, G. *Electrochim. Acta* **2008**, 53, 7436.
 - 99 Rusanova, M. Y.; Polskov, P.; Muzikar, M.; Fawcett, W. R. *Electrochim. Acta* **2006**, 51, 3097.
 - 100 Prisyazhnyi, V. D.; Snezhkov, V. I.; Moshchenko, I. N. *Ukr. Khim. Zh. (Russ. Ed.)* **1994**, 60, 811.
 - 101 Lum, A. F.; Tannenbaum, S. U.S. Patent 3658609, issued 25 April, 1972.
 - 102 Mettler Toledo, *Thermal Analysis UserCom Online* **1996**, 4, 5. http://us.mt.com/mt/ed/userCom/TA_UserCom4_04355823710252341.jsp last accessed July 29, 2008.
 - 103 Buechi, J.; Hasler, C. *Pharm. Acta Helv.* **1973**, 48, 639.
 - 104 Burger, A. *Pharmazie in Unserer Zeit* **1982**, 11, 177.